A theoretical investigation of an averaged-structure eddy viscosity model applied to turbulent shear flows.

By AMIR A. KHOSSOUSI.

A thesis submitted for the degree of Doctor of Philosophy in partial fulfilment of the requirements of the Council for National Academic Awards.

Mathematics Department,
Sir John Cass School of Science,
City of London Polytechnic,
100 Minories,
London EC3.

November 1987.

C O N T E N T S

ACKNOWLEDGEMENTS

The author wishes to thank ...

Dr. M.G. Smith for supervising this project and for his constant help and guidance throughout the work,

Dr. U.T. Ehrenmark for many invaluable discussions and suggestions,

The Inner London Education Authority and the City of London Polytechnic for providing the funds and the facilities,

Professor B. Spain, Dr. U.T. Ehrenmark of City of London Polytechnic and Professor R.S. Scorer of Imperial College who kindly permitted me to attend their lectures,

and finally my family whose support and encouragements made this achievement possible.

A theoretical investigation of an averaged-structure eddy viscosity model applied to turbulent shear flows.

By A.A. Khossousi.

A B S T R A C T

The project is concerned with the study of a new mathematical model in which the structure of turbulence is described by averaging the effects of the eddies of various scales over the whole volume of flow. The model assumes that the turbulent stresses can be presented in a way analogous to the laminar stresses and the correlations between the point in question with those at other locations in the flow follow a distribution which may be assumed Gaussian.

The model is initially applied to the steady incompressible turbulent Poiseuille flows between parallel flat plates and through circular pipes. The Navier-Stokes equations are simplified and solved analytically, with the aid of Integral Transform methods and asymptotic expansions. With the appropriate numerical values for the model constants, the approximate asymptotic solutions for the mean velocities are found in good agreement with the universal laws and with the experimental data.

To test the model further, the steady incompressible turbulent boundary layer flow along the surface of a solid body is studied. It is shown that under the similarity transformations the boundary-layer equations may be simplified to give, to the first approximation, ordinary differential equations of order three. These equations are similar to the Blasius and the Falkner-Skan equations except for the presence of the additional terms representing the turbulent effects.

With the usual no-slip conditions at the wall, numerical solutions to these non-linear equations are obtained for various values of the flow parameters. For the special case when the pressure gradient related parameter $\beta=-1$, it is described how an approximate analytic solution can be obtained, by extending the existing solutions of the Falkner-Skan equation.

1. INTRODUCTION

1.1 What is turbulence?

In most text books which deal with the subject of turbulence, the authors begin their description of this type of flow by referring to its complex nature, and it is generally agreed that turbulence can not be defined precisely and universally. While some theories may apply to one flow condition, they may not apply to another, hence different turbulent motions may require different treatments.

Earlier theories of turbulence were based on analogies with the kinetic theory of gases, and assumed discontinuous collisions between discrete fluid particles. Following G. I. Taylor (1935), who first proposed that the velocity of the fluid in a turbulent motion may be assumed as a random continuous function of position and time, Hinze (1959) defined turbulence as "... irregular condition of flow in which the various quantities show a random variation with time and space coordinates, so that statistically distinct average values can be discerned" [5].

This general definition however, does not describe the phenomenon adequately, for not all chaotic motions are describable in terms of random functions. Ruelle and Takens (1971), discuss various phenomena occuring in the motion of a viscous fluid when a flow parameter, such as the Reynolds number R, is increased. For sufficiently small values of R, the physical parameters describing the flow at any point are constant in time, if the system is not subjected to any external action. As R increases the motion may remain steady but change its symmetry pattern, or may become periodic in

time. If R increases further, the motion becomes very complicated, irregular and chaotic. This is referred to as turbulence. When statistical properties of a turbulent motion can not be obtained, then the chaotic solutions of the differential equations are usually sought as the explanation of turbulence.

Fortunately, in engineering and meteorological problems no detailed description of the fluctuating fluid particles is needed and only the approximate effects of turbulence on the mean motion is considered adequate. This enables the problem of turbulence to be treated mathematically.

1.2 Where the difficulties arise.

The common practice in dealing with turbulent motions mathematically, is to split up the flow properties (such as the velocity and pressure) into a mean and a fluctuating component, and time-average the differential equations governing the flow. This process which is described in more detail in chapter two, gives rise to the appearence of extra terms, formed by the (mean) products of the velocity fluctuating components, and are known as the Reynolds stresses. It is the determination of these stresses which has proved to be the major cause of difficulties. The usual method of solving this problem is to use mathematical models capable of approximating the effects of the Reynolds stresses in terms of other flow quantities. Examples of such models are presented in the next section.

Another area of difficulty is due to the fact that the governing equations are three-dimensional. Although some problems of interest seem to be two-dimensional, turbulent

fluctuations are essentially three-dimensional in character. Any method of describing a turbulent field therefore, should be able to take this into account.

If solid boundaries are present, as in the channel and boundary layer flows, further complications develop, for a turbulent field experiences gradients. It is these types of flows we shall be investigating with the aid of our model in this report.

1.3 Various turbulence models.

The contents of this section is not intended as a review of the subject. We shall briefly discuss various approaches to the problem of turbulence, in particular the eddy-viscosity approach, as our aim is to identify and hence improve on some of the shortcomings and deficiencies associated with these models.

The energy tensor of turbulent fluctuations τ^*_{ij} $(=-\rho\overline{u_i' u_j'})$ arise from statistical correlation between streamwise and cross-stream velocity fluctuating components, u_i' and u_j'. They are known as the Reynolds or turbulent stresses and represent the exchange of momentum between adjacent layers of fluid by the fluctuating fluid velocities.

In order to be able to solve the governing equations (2.9) for any type of turbulent flow, the Reynolds stresses must be known. Since, no direct ways of finding these stresses are known at present (except in cases such as isotropic turbulence formed behind grids [1, ch.VII]), it is necessary to replace them by mathematical models to represent their effects in terms of quantities which can be determined.

This kind of approach to the problem of turbulence was originated by Boussinesq in 1877. He suggested that the Reynolds stresses can be presented in a form analogous to the laminar stresses, by the product of the mean velocity gradient $\partial\bar{u}/\partial y$, and a turbulent or eddy viscosity μ_t, which is a property of the local state of turbulence.

However, experiments have shown that μ_t is not a property that can be determined locally. It is influenced by effects of the eddying motion at other locations in the flow and depends largely on the structure of turbulence at the point in question.

Among the well-known mathematical models, put forward to express μ_t in terms of calculable quantities (like the mean velocity $\bar{u}$), are

(i) Prandtl's (1925) mixing length hypothesis (MLH),

$$\mu_t = \rho \ell_m^2 \left|\frac{\partial \bar{u}}{\partial y}\right|,$$

where ℓ_m is the mixing length. This model is quite attractive to users for its simplicity, and is capable of producing a fairly good but not accurate picture of turbulence in two-dimensional flows. The difficulty with this model is the mixing length, which has to be prescribed, and its size varies according to the distance from the boundary.

(ii) Von Kármán's similarity hypothesis (1930).

This model avoids the difficulty of specifying the mixing length, by assuming

$$\ell_m \propto \left|\frac{\partial \bar{u}}{\partial y} \Big/ \frac{\partial^2 \bar{u}}{\partial y^2}\right|.$$

Since the mixing length is determined by the local

properties of the mean flow alone, the predictions made by this model, have been found to deviate from experiments, except in the regions close to a wall.

(iii) Eddy-viscosity formulae.

These models have the general form

$$\mu_t = \rho u_o y_o f(y),$$

where u_o and y_o are characteristic global velocity and length scales, respectively. The term f(y), refers to some function of position in the flow, and its form varies according to the type of flow under consideration. These models are not very attractive, for they have a limited degree of universality. [18].

Simple models such as those listed above, determine the eddy viscosity locally, and lack the facility to capture the structural effects of turbulence. Furthermore, since the eddy viscosity is directly related to the mean velocity gradient (as in the MLH), it vanishes when the mean velocity is zero or has its maximum value, as at the centre of a pipe, where the Reynolds stresses are not only non-zero, but may in fact be quite large.

Another class of models, capable of taking account of the non-local character of turbulence are the differential models. They determine turbulence properties from the convective transport differential equations.

In his 1945 model, Prandtl proposed that the velocity scale, which in his earlier model was given by $\ell_m |\partial \bar{u}/\partial y|$, should instead be presented by the square root of the turbulence kinetic energy k ($=1/2\ \overline{u_i' u_i'}$), which may be found

from the solutions of a differential transport equation for k. The length scale still remained to be prescribed algebraically. Following this proposal and with the availability of high speed computers, various forms of differential models have since been introduced. A number of such models prior to 1972, are examined, compared and developed by Launder and Spalding [18]. The authors overall conclusions were: "In most circumstances, one-equation energy models are only marginally superior to Prandtl's mixing length model, for the transport effects on the turbulence length scale are not accounted for". They added that the more complex Two-equation models in which the turbulence length scale is also determined from the transport equation, appears to be necessary, if a more accurate prediction of turbulence is desired.

One of the most popular of the two-equation models, is the (linear) $k-\varepsilon$, in which the length scale appears in the form of a turbulence energy dissipation rate ε, where

$$\varepsilon \propto k^{3/2} \ell^{-1},$$

and the eddy viscosity is represented by

$$\mu_t = c k^2 \varepsilon^{-1},$$

where c is an empirically determined constant.

The $k-\varepsilon$ model is currently one of the standard models in use in engineering applications. Its performance in channel flows has been tested by Henry, Reynolds and El Telbany (1981, 1984), and others. The model was found capable of predicting the velocity profiles (sufficiently away from the walls), with good agreement with measured data, but the turbulence energy and hence eddy viscosity were not well predicted. The model can not be applied in the

near wall regions, as the parameters become highly sensitive there. Consequently, the model equations are usually matched to an empirically determined equation, such as the 'law of the wall', near the boundary.

With rapid advances in the computer technology, most of the research efforts in recent years have been directed towards the 'second-order' closure models, in which every component of the Reynold stress tensor is determined from the transport equations [19, 21, 22], and 'large-eddy' simulation, in which detailed computation of the time evolution of the three dimensional turbulent field is performed directly [20].

The difficulty with second-order models is the modelling of higher order turbulence correlations, required in deriving the transport equations for the Reynold stresses. As for the large-eddy simulation, finite computer capacity, prevents a direct numerical solution of eddies of small scales. This approach therefore, does not avoid the difficulty of modelling the turbulence in the near wall regions. The 'subgrid' models, which are usually used to simulate the small eddies in the vicinity of a wall, have been tested in channel flows by Kaneda and Leslie (1983). They examined the models of Schumann (1975) and Moin and Kim (1982), and found that they were in need of substantial improvements.

In addition to the difficulties outlined above, there is another disadvantage with these approaches, namely the enormous amount of computer time and memory they require. These models are therefore not very practical in simpler engineering problems, unless the necessity of using such

expensive models can be justified.

Speziale (1987), noting the shortcomings of the $k-\varepsilon$ model and the disadvantages of the alternative direct simulation and the second-order models, developed a nonlinear $k-\varepsilon$ model, which appears to have improved the predictions of the normal Reynolds stresses in channel flows. This model, as well as suffering the same kind of complications as the linear $k-\varepsilon$ mentiond earlier, requires the introduction of an additional model constant, which further complicates the calculations of a turbulent field.

1.4 The aim of the project.

In view of the great number of turbulence models which are available, scientists and engineers are often faced with the problem of choosing the most suitable, to serve their purposes. They have to decide on whether to employ a complex model to achieve a greater accuracy, or settle for a crude estimate and use a simple model. Considering those factors such as simplicity, time and costs, it is not surprising to find that many users favour simpler models, for a complex one can not always be guaranteed to produce a very accurate result after all.

The non-local effects of turbulence, as mentioned earlier, play an important role in determining the structure of a turbulent flow. As far as taking account of these effects are concerned, it appears that a user is forced to resort to one of the complex models (such as the $k-\varepsilon$), or alternatively, disregard the non-local effects completely and choose a simple model (such as the MLH).

This apparent gap in turbulence models, can be regarded

as the main inspiration of the work presented in this report. The aim is to develope a relatively simple mathematical model of turbulence in which the effects of the eddies of various scales, originating at some distance away from the point in question, are averaged over the whole volume of flow. Such a model should therefore be able to describe the 'average-structure' of a turbulent field. In addition, the three-dimensional character of turbulence is also presented, through the averaging process.

The model is introduced in chapter two, along with the basic equations which will be used in the subsequent chapters. As the preleminary test, it is applied to the simple problem of fully developed Poiseuille flow between parallel flat plates, for which an approximate analytic solution is obtained. The method of solving the equations of motion with the aid of the integral transform method and asymptotic expansions are described in chapter three. The behaviour of the velocity curves, for different values of the model constants and the Reynolds number are presented in the form of graphs.

In chapter four, the application of the model to the fully developed Poiseuille flow through circular pipes is examined. This flow is slightly more complicated than the channel flows. But once the equations are transformed into cylindrical polar coordinates, the method of approaching the problem is basically similar to that discussed in chapter three. Based on the approximate asymptotic solution presented for the mean velocity, an expression for the coefficient of resistance in smooth pipe is also presented. The results produced by this expression are compared with those given by

the Prandtl formula, deduced from the logarithmic profiles.

Chapter five belongs to the boundary layer theory, which is the final problem to be investigated with the aid of the model. This flow is of great practical importance and is more complex in comparison with the Poiseuille channel and pipe flows. Following a short introduction, the method of approximating the governing equations to obtain the boundary layer equations is described. It is shown how these non-linear partial differential equations may be transformed through similarity variables, to give (to the first approximation) an ordinary differential equation, similar to the well-known Falkner-Skan equation. It will be seen that when the pressure gradient is absent, this equation reduces to a Blasius type equation, applicable to turbulent flows. These equations are solved numerically, by using a Nag library routine. For the special case $\beta = -1$, it is shown how an approximate analytic solution may be obtained, by extending the laminar solution of the Falkner-Skan equation. In all cases, the no-slip boundary conditions at the walls are adopted.

All turbulent shear flows investigated in this report are assumed steady and incompressible, for simplicity.

The Vax 750 main frame computer at the City of London Polytechnic was used to produce the results and the graphics presented in this document. The programmes were written in Fortran and Double Precision variables were used to minimise the rounding errors and to achieve greater accuracy.

2. THE GOVERNING EQUATIONS, ASSUMPTIONS AND DEFINITIONS.

Throughout this chapter, unless otherwise stated, all equations are written in the Cartesian coordinate system, in which u, v and w are the respective components of the velocity vector $\underset{\sim}{V}$ in the x, y and z directions.

2.1 The Navier-Stokes (N-S) equations.

The mathematical equations governing the motion of a viscous Newtonian fluid are known as the Navier-Stokes equations. They consist of three equations of motion or the momentum equations and the continuity or conservation of mass equation. In this section we shall briefly discuss these equations and outline some of their important properties.

Assuming the fluid as a continuous medium, the equations of motion can be derived by applying Newton's second law of motion to a small rectangular box of fluid contained within the flow and moving with it. That is to say the product of the mass and acceleration must balance the sum of the forces acting on this box of fluid. In laminar flows, the forces responsible for the motion of fluid are the body forces such as the gravity force and the surface forces or stresses which depend (linearly in Newtonian fluids) on the rate at which the fluid is strained by the velocity.

The stresses acting on a cube of fluid form the components of the stress tensor, τ_{ij} (i,j=1,2,3). The second subscript indicates the coordinate along which the stress is acting and the first refers to the direction normal to this coordinate. The stress tensor is symmetric and thus $\tau_{ij} = \tau_{ji}$. They are known as the shear stresses if $i \neq j$ and normal

stresses if i=j. For a fluid at rest $\tau_{ij} = -P$ (i=j=1,2,3), where P is the pressure.

The stresses can be regarded as a measure of fluid resistance to deformation through the action of velocity. The rate of deformation in Cartesian tensor notation is defined by

$$\sigma_{ij} = \tfrac{1}{2}\left({}^{\partial u_i}/_{\partial x_j} + {}^{\partial u_j}/_{\partial x_i} \right), \tag{2.1}$$

which is known as the strain rate tensor and has the components

$$\sigma_{xx} = {}^{\partial u}/_{\partial x} \quad , \quad \sigma_{yy} = {}^{\partial v}/_{\partial y} \quad , \quad \sigma_{zz} = {}^{\partial w}/_{\partial z} \, , \tag{2.2}$$

and

$$\begin{aligned} \sigma_{xy} = \sigma_{yx} &= \tfrac{1}{2}\left({}^{\partial u}/_{\partial y} + {}^{\partial v}/_{\partial x} \right), \\ \sigma_{yz} = \sigma_{zy} &= \tfrac{1}{2}\left({}^{\partial v}/_{\partial z} + {}^{\partial w}/_{\partial y} \right), \\ \sigma_{xz} = \sigma_{zx} &= \tfrac{1}{2}\left({}^{\partial u}/_{\partial z} + {}^{\partial w}/_{\partial x} \right). \end{aligned} \tag{2.3}$$

The stress-strain rate relationship for a Newtonian incompressible fluid in motion can be presented by

$$\begin{aligned} \tau_{ij} &= -P\,\delta_{ij} + \mu\,\sigma_{ij} \\ &= -P\,\delta_{ij} + \tfrac{1}{2}\left({}^{\partial u_i}/_{\partial x_j} + {}^{\partial u_j}/_{\partial x_i} \right), \end{aligned} \tag{2.4}$$

where

$$\begin{aligned} \delta_{ij} &= 0 \text{ if } i \neq j \\ &= 1 \text{ if } i = j, \end{aligned}$$

and μ is the molecular viscosity [9].

In stating the above relationship, it should be noted that the fluid is assumed isotropic, so that the relation between the components of the stress and the rate of strain is the same in all directions.

By considering the net balance of stresses acting in the direction i, on an elemental cube, (in the limit as the

sides of the cube tend to zero) and applying Newton's second law, the momentum equations can be obtained, which in Cartesian tensor notation are

$$\rho\left(\partial u_i/\partial t + u_j\,\partial u_i/\partial x_j\right) = \partial \sigma_{ij}/\partial x_j + B_i\ , \qquad (2.5)$$

where the fluid is assumed incompressible (i.e. ρ = constant) and B_i represents the body forces acting in tne direction i. The terms within the brackets on the left hand side of (2.5) are the acceleration terms which include the so called convective acceleration, $u_j\,\partial u_i/\partial x_j$.

Combining (2.4) and (2.5) yields the momentum equations (2.6a), which together with the continuity equation (2.6b), form the Navier-Stokes equations for an incompressible laminar flow with constant viscosity.

$$\rho\left(\frac{\partial u_i}{\partial t} + u_j\frac{\partial u_i}{\partial x_j}\right) = -\frac{\partial p}{\partial x_i} + \mu\frac{\partial^2 u_i}{\partial x_j\,\partial x_j} + B_i\ , \qquad (2.6a)$$

and

$$\partial u_i/\partial x_1 = 0. \qquad (2.6b)$$

Detailed derivation of the momentum and continuity equations are given in references [9] and [17].

2.2 The governing equations for turbulent flows.

The N-S equations (2.6) appears to be applicable to incompressible turbulent flows in which the effects of the chaotic motion at molecular scale is negligible compared to the smallest possible eddies which may be present in the flow.

As mentioned in the previous chapter, various turbulent quantities may be expressed as having a mean and a fluctuating component. In turbulent flows, the dependent

variables vary as functions of time, regardless of whether the flow is steady or not. It is therefore convenient to take the time-average to represent the mean part of a turbulent quantity.

For an instantaneous variable ϕ, define the time-average quantity $\bar{\phi}$, at a fixed point in space, by

$$\bar{\phi}(t) = \frac{1}{T_1} \int_{T_0 - \frac{1}{2}T_1}^{T_0 + \frac{1}{2}T_1} \phi(t)\, dt \; ; \quad T_0 \ll t \ll T_1 , \tag{2.7}$$

where T_1 is the averaging time. The fluctuations are assumed to be very rapid, allowing a long enough averaging period, during which a significant mean to be formed and yet so short that there would be negligible variation in the mean in that period. A quantity averaged over such a scale can be regarded as instantaneous in the macroscopic scale.

We can then write $\phi = \bar{\phi} + \phi'$, where $\bar{\phi}$ is the time-average and ϕ' the fluctuating components. In taking time-averages the following rules apply.

For any two variables a and b and a constant c,

if $a = \bar{a} + a'$ and $b = \bar{b} + b'$,

$$\begin{aligned}
&\text{then} \quad \overline{a + b} = \bar{a} + \bar{b} , && \bar{a}' = \bar{b}' = 0 , \\
&\overline{a.b} = \bar{a}.\bar{b} + \overline{a'.b'} , && \overline{\partial a/\partial x} = \partial \bar{a}/\partial x \qquad (2.8) \\
&\bar{\bar{a}} = \bar{a} , && \overline{\int a\, dx} = \int \bar{a}\, dx , \\
&\text{and} \quad \overline{c.a} = c.\bar{a} .
\end{aligned}$$

By putting $u_j = \bar{u}_j + u'_j$ and $P = \bar{P} + P'$ in (2.6) and taking time-averages of both sides of the equations in accordance with (2.7) and (2.8), we can obtain after simplifying and rearranging, the momentum and continuity equations for incompressible turbulent flows, as

$$\rho\left(\frac{\partial \bar{u}_i}{\partial t}+\bar{u}_j\frac{\partial \bar{u}_i}{\partial x_j}\right)=-\frac{\partial \bar{p}}{\partial x_i}+\mu\frac{\partial^2 \bar{u}_i}{\partial x_j\,\partial x_j}+\frac{\partial}{\partial x_j}\left(-\rho\,\overline{u_i' u_j'}\right)+\bar{B}_i, \quad (2.9a)$$

and

$$\partial \bar{u}_i / \partial x_i = 0, \quad [9]. \quad (2.9b)$$

The above equations are similar to the laminar flow equations (2.6), except for the presence of the terms involving the Reynolds stresses τ_{ij}^{*} $(= -\rho\,\overline{u_i' . u_j'})$. These terms reflect the turbulence effects on the mean motion and as mentioned before, represent the rate at which the momentum is exchanged between layers of fluid through fluctuations.

Various methods of determiningthe Reynolds stresses, were outlined in chapter one, where the disadvantages of some of the popular turbulence models were briefly noted. Let us now introduce a model, in which the Reynolds stresses are determined by averaging the structure of turbulence over the neighbouring points.

2.3 An 'averaged-structure' turbulence model.

The model we are about to introduce is based on the Boussinesq assumption that the Reynolds stresses may be presented in a form analogous to the laminar stresses. Hence, by analogy to (2.4), we propose a form for the the Reynolds stresses which at any point $\underset{\sim}{X}$, with the mean velocity $\underset{\sim}{\bar{V}}$ and at time t, is represented by

$$\tau_{ij}^{*}(\underset{\sim}{X},t) = -\rho\,\overline{u_i' u_j'}$$

$$= -\rho\,P_t(\underset{\sim}{X},t)\,\delta_{ij} + \rho\int_{vol} F(\underset{\sim}{X},t,\underset{\sim}{X}-\underset{\sim}{X}')\,\sigma_{ij}(\underset{\sim}{X}',t)\,d\underset{\sim}{X}', \quad (2.10)$$

where

$-\rho\,P_t(\underset{\sim}{X},t)\,\delta_{ij}$ are Reynolds normal stresses,

and

$\rho\,F.\,\sigma_{ij}(\underset{\sim}{X}',t) = \frac{1}{2}\rho\,F.\left(\frac{\partial \bar{u}_i}{\partial x_j'}+\frac{\partial \bar{u}_j}{\partial x_i'}\right)$ are Reynolds shear stresses.

The weighting function F, which varies with space, time and position, represents the correlation between $\underset{\sim}{X}$ and $\underset{\sim}{X}'$, where $\underset{\sim}{X}'$ is any point within the flow. The effects of the eddies formed at the points $\underset{\sim}{X}'$ on the point $\underset{\sim}{X}$, are averaged by means of a volume integral, which is taken over the whole volume of flow.

We may choose F to be given by the products of a 'shape function', F_1, and a 'position function', F_2. In steady flows for example, we might have

$$F(\underset{\sim}{X}, \underset{\sim}{X}-\underset{\sim}{X}') = c_o F_1(\underset{\sim}{X}).F_2(|\underset{\sim}{X}-\underset{\sim}{X}'|), \qquad (2.11)$$

where c_o is a constant.

The shape function is required to represent the rate at which large-scale turbulent motions, draw free-stream fluid into a boundary layer. In addition, since near a wall viscous friction predominates, we might choose a form for F_1 which would vanish at the walls and varies with the space coordinate normal to the direction of mean motion alone. Another property that a shape function needs to possess, is to have a diminishing variation with the distance away from the boundaries, so that it would behave like a constant in the free-stream region of a flow. The exact form of the shape function varies according to the problem under consideration. The equations (3.6), (4.5) and (5.40) are examples of the shape functions, satisfying the requirements noted above.

For the dependence on $|\underset{\sim}{X}-\underset{\sim}{X}'|$, we choose an isotropic variation of rapid decay, like the Gaussian distribution function

$$F_2(|\underset{\sim}{X}-\underset{\sim}{X}'|) = \exp\{-\tfrac{1}{2\sigma^2}(\underset{\sim}{X} - \underset{\sim}{X}')^2\}. \qquad (2.12)$$

The standard deviation parameter σ, is a measure of

spread of the points $\underset{\sim}{X}'$ with respect to the point $\underset{\sim}{X}$, so that the smaller this parameter is, the closer the points $\underset{\sim}{X}'$ are located to $\underset{\sim}{X}$ and hence a greater influence is exerted on the body of fluid at $\underset{\sim}{X}$, by the eddies of small scales. If on the other hand, the effects of the eddies formed at some distance away from the point in question is considered, then σ would be of larger magnitude.

In the following chapters, the model is examined by applying it to some of the standard problems of fluid dynamics.

3. FULLY DEVELOPED STEADY POISEUILLE FLOW BETWEEN PARALLEL FLAT PLATES.

In this chapter the application of the model to the relatively simple and well-known problem of incompressible steady turbulent Poiseuille flow between two stationary parallel flat plates, at a distance 2h apart, is examined. The governing equations for this particular problem and an approximate analytical solution for the mean velocity is presented in the following sections. The method of solving the equations with the aid of the integral transform method and asymptotic expansions is described in considerable detail. With the appropriate numerical values for the model constants, the predicted mean velocity profiles are compared with the results produced by some of the similar models and the experiments.

3.1 Equations of motion.

Let the x axis be parallel to the direction of mean motion and $\bar{u}$, $\bar{v}$ and $\bar{w}$ denote the respective components of the mean velocity vector $\underset{\sim}{\bar{V}}$ in the x, y and z directions. The main characteristic feature of the Poiseuille channel flows is that the components of the mean velocity vector $\underset{\sim}{\bar{V}}$, may be assumed independent of the space coordinates x and z and the only non-zero component is the one along the direction of mean motion [15]. Hence, we can write

$$\underset{\sim}{\bar{V}} = \{\bar{u}(y) \ , \ 0 \ , \ 0\}, \qquad (3.1)$$

and the time-average momentum equations (2.9a) reduce to

$$\frac{1}{\rho} \partial \bar{P}/\partial x_i = \nu \, \partial^2 \bar{u}_i/\partial x_j \partial x_j + \frac{1}{\rho} \partial \tau^*_{ij}/\partial x_j \ , \qquad (3.2)$$

assuming steady flow with negligible body forces, and $\nu (= \mu/\rho)$ is the kinematic viscosity.

Combining (3.2) and (2.10), and dropping the bars above

the mean quantities for convenience, yields

$$\frac{1}{\rho}\frac{\partial P}{\partial x_j} = \nu\frac{\partial^2 u_i}{\partial x_j\,\partial x_j} + \frac{\partial}{\partial x_j}\left\{-P_t\,\delta_{ij} + \tfrac{1}{2}\int_{vol} F.\left(\frac{\partial u_i}{\partial x'_j} + \frac{\partial u_j}{\partial x'_i}\right) d\underset{\sim}{x'}\right\} \quad (3.3)$$

which can be written as

$$\frac{\partial}{\partial x}(P/\rho + P_t) = \nu\frac{\partial^2 u}{\partial y^2} + \tfrac{1}{2}\frac{\partial}{\partial y}\int_{vol} F.\frac{\partial u}{\partial y'}\,d\underset{\sim}{x'},$$

$$\frac{\partial}{\partial y}(P/\rho + P_t) = \tfrac{1}{2}\frac{\partial}{\partial x}\int_{vol} F.\frac{\partial u}{\partial y'}\,d\underset{\sim}{x'}, \quad (3.4)$$

and $\frac{\partial}{\partial z}(P/\rho + P_t) = 0,$

where

$$F = c_o\,F_1(y)\,F_2(|\underset{\sim}{x} - \underset{\sim}{x'}|),$$

and $F_2 = \exp\left\{-\frac{1}{2\sigma^2}(\underset{\sim}{x} - \underset{\sim}{x'})^2\right\}$ [see (2.12)], (3.5)

Bearing in mind the purposes which the shape function F_1 is required to serve (as discussed in previous chapter), the following form for the function $F_1(y)$ is proposed.

$$F_1(y) = e^{-h/\lambda}\left\{\cosh(h/\lambda) - \cosh(y/\lambda)\right\}, \quad (3.6)$$

which is an even function of y due to the parabolic nature of the velocity profile. Here, h is the distance of a wall from the centre line (y=0), λ is a characteristic length scale, and the parameter c_o is to be determined experimentally.

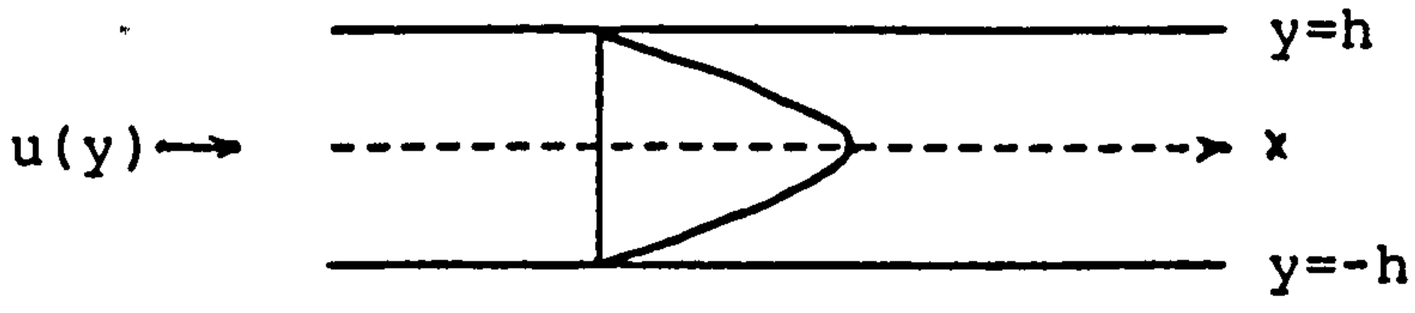

Schematic illustration of flow.

The boundary conditions to supplement the system (3.4) are

$$u = F = 0 \quad \text{at } y = \pm h. \quad (3.7)$$

The volume integral in (3.4) may be presented in a simpler form, as shown below.

$$\int_{vol} F.\frac{du(y')}{dy'}\,d\underset{\sim}{x'} = c_o\,F_1(y)\int_{vol} F_2(|\underset{\sim}{x} - \underset{\sim}{x'}|)\frac{du}{dy'}\,d\underset{\sim}{x'}$$

$$= c_o\,F_1\int_{-\infty}^{\infty}\int_{-\infty}^{\infty}\int_{-h}^{h}\exp\left\{-\frac{1}{2\sigma^2}\left[(x-x')^2 + (y-y')^2 + (z-z')^2\right]\right\}\frac{du}{dy'}\,dx'dz'dy'$$

$$= 2\pi\sigma^2 c_o\,F_1\int_{-h}^{h}\exp\left\{-(y-y')^2/2\sigma^2\right\}\frac{du}{dy'}\,dy'.$$

It can be seen that the volume integral depends on y only and from the second and third of the equations (3.4) we can write

$$\frac{\partial}{\partial y}\left(P/\rho + P_t\right) = \frac{\partial}{\partial z}\left(P/\rho + P_t\right) = 0,$$

and therefore $(P/\rho + P_t)$ varies with x alone. Hence the equations (3.4) reduce to (remember u depends on y only)

$$\frac{d}{dx}\left(P/\rho + P_t\right) = \nu \frac{d^2u}{dy^2} + \pi\sigma^2 c_0 \frac{d}{dy} F_1 \int_{-h}^{h} \exp\{-\tfrac{1}{2\sigma^2}(y-y')^2\} \frac{du}{dy'}\, dy' = K,$$

where K is a constant.

Integrating once with respect to y, yields

$$\nu \frac{du}{dy} + \pi\sigma^2 c_0 F_1 \int_{-h}^{h} \exp\{-\tfrac{1}{2\sigma^2}(y-y')^2\} \frac{du}{dy'}\, dy' = ky + k_0, \tag{3.8}$$

where K_0 is a constant.

The second term on the l.h.s. of (3.8) can be simplified by integrating by parts.

$$\int_{-h}^{h} \exp\{-\tfrac{1}{2\sigma^2}(y-y')^2\} \frac{du}{dy'}\, dy' = -\int_{-h}^{h} \frac{\partial}{\partial y'} \exp\{-\tfrac{1}{2\sigma^2}(y-y')^2\} u(y')\, dy'$$

$$= \frac{d}{dy} \int_{-h}^{h} \exp\{-\tfrac{1}{2\sigma^2}(y-y')^2\}\, u(y')\, dy',$$

since

$$\frac{\partial}{\partial y'} \exp\{-\tfrac{1}{2\sigma^2}(y-y')^2\} = -\frac{\partial}{\partial y} \exp\{-\tfrac{1}{2\sigma^2}(y-y')^2\}.$$

Hence, the equation (3.8) reduces to

$$\nu \frac{du}{dy} + \pi\sigma^2 c_0 F_1 \frac{d\phi}{dy} = ky + k_0, \tag{3.9}$$

where

$$\phi(y) = \int_{-h}^{h} u(y') \exp\{-\tfrac{1}{2\sigma^2}(y-y')^2\}\, dy'.$$

As $u(h) = u(-h)$, then u and therefore ϕ are even functions of y. Since F_1 is even, then the l.h.s. of (3.9) is odd, and hence the r.h.s. must also be odd, which implies $K_0 = 0$.

Before attempting to solve the equation (3.9), it must be made dimensionless by the usual scaling method.

3.2 Equation of motion in non-dimensional form.

Define the dimensionless variables $\hat{u}, \eta, \eta'$, a, b and c by

$$u = u_* \hat{u}(\eta), \quad y = h\eta, \quad y' = h\eta',$$

$$h = a\lambda, \quad \sigma = bh, \quad k = -u_*^2/h,$$

$$R = u_* h/\nu \quad \text{and} \quad c = \pi c_* h^2/u_*, \tag{3.10}$$

where u_* is the friction velocity defined by $u_* = \sqrt{(\tau_*/\rho)}$; $\tau_* = \mu \left.\frac{du}{dy}\right|_{y=0}$ and R is the Reynolds number.

Combining (3.9) and (3.10), gives the dimensionless equation of motion

$$\frac{1}{R}\frac{d\hat{u}}{d\eta} + c\,b^2 \hat{F}_1(\eta)\frac{d\hat{\phi}(\eta)}{d\eta} = -\eta, \tag{3.11}$$

where

$$\hat{F}_1(\eta) = e^{-a}(\cosh a - \cosh a\eta), \tag{3.12}$$

and

$$\hat{\phi}(\eta) = \int_{-1}^{1} \hat{u}(\eta') \exp\{-\tfrac{1}{2b^2}(\eta-\eta')^2\}\, d\eta'. \tag{3.13}$$

The circumflexes, indicate dimensionless quantities. The boundary conditions (3.7), become

$$\hat{u}(\eta) = \hat{F}_1(\eta) = 0 \quad \text{at } \eta = \pm 1. \tag{3.14}$$

3.3 An approximate analytical solution.

In solving the implicit equation (3.11) for $\hat{u}$, we seek an approximate series expansion in powers of η to represent the product of $\hat{F}_1(\eta)$ and $d\hat{\phi}(\eta)/d\eta$, which would then enable us to evaluate the mean velocity by simply integrating (3.11) across the channel.

For reasons which will become apparent, it is convenient to multiply throughout (3.11) by $\exp\{-\frac{1}{2b^2}(J-\eta)^2\}$ and integrate from -1 to 1. The circumflexes are dropped for convenience.

$$\frac{1}{R}\int_{-1}^{1}\frac{du}{d\eta}\exp\{-\tfrac{1}{2b^2}(\xi-\eta)^2\}\,d\eta + cb^2\int_{-1}^{1}F_1\exp\{-\tfrac{1}{2b^2}(\xi-\eta)^2\}\frac{d\phi}{d\eta}\,d\eta$$
$$= -\int_{-1}^{1}\eta\exp\{-\tfrac{1}{2b^2}(\xi-\eta)^2\}\,d\eta.$$

But

$$\int_{-1}^{1}\frac{du}{d\eta}\exp\{-\tfrac{1}{2b^2}(\xi-\eta)^2\}\,d\eta = -\int_{-1}^{1}u\frac{d}{d\eta}\exp\{-\tfrac{1}{2b^2}(\xi-\eta)^2\}\,d\eta$$
$$= d\phi(\xi)/d\xi.$$

So if we put

$$\psi(\xi) = d\phi(\xi)/d\xi, \tag{3.15}$$

and

$$g(\xi) = \int_{-1}^{1}\eta\exp\{-\tfrac{1}{2b^2}(\xi-\eta)^2\}\,d\eta, \tag{3.16}$$

then

$$\psi(\xi) + \varepsilon\int_{-1}^{1}F_1(\eta)\exp\{-\tfrac{1}{2b^2}(\xi-\eta)^2\}\psi(\eta)\,d\eta = -Rg(\xi), \tag{3.17}$$

where

$$\varepsilon = RCb^2. \tag{3.18}$$

This equation is now to be solved for $\psi(\xi)$.

Two possibilities need be considered in solving (3.17).

(i)- if ε is smaller than the lowest eigenvalue in which case (3.17) could be solved as a Neumann series, by assuming a solution of the form

$$\psi(\xi) = \sum_{n=0}^{\infty}\varepsilon^n\psi_n(\xi). \tag{3.19}$$

(ii)- if ε is not sufficiently small to ensure the convergence of the above series, then a direct solution of the equation seems desirable.

Here we shall briefly discuss the first case and just indicate, without actually solving the equation, how a solution may be arrived at. The second case, which is more complicated and of more interest (at least from a mathematical point of view), is studied in depth.

CASE (i)-

Substituting (3.19) into (3.17), we obtain

$$\sum_{n=0}^{\infty} \varepsilon^n \varphi_n(\xi) + \sum_{n=0}^{\infty} \varepsilon^{n+1} \int_{-1}^{1} k(\xi,\eta)\, \varphi_n(\eta)\, d\eta = -R\, g(\xi),$$

where

$$k(\xi,\eta) = \exp\{-\tfrac{1}{2b^2}(\xi-\eta)^2\}\, F_1(\eta).$$

Equating the coefficients of equal powers of ε yields

$$\varphi_0 = -R g,$$

$$\varphi_1 + \int_{-1}^{1} k(\xi,\eta)\, \varphi_0\, d\eta = 0,$$

$$\varphi_2 + \int_{-1}^{1} k(\xi,\eta)\, \varphi_1\, d\eta = 0,$$

$$\vdots$$

$$\varphi_n + \int_{-1}^{1} k(\xi,\eta)\, \varphi_{n-1}\, d\eta = 0,$$

or

$$\varphi_n = (-1)^n \int_{-1}^{1} k_n(\xi,\eta)\, \varphi_0(\eta)\, d\eta \;;\; n = 1, 2, \ldots.$$

To find the reccurence relation for k, we write

$$\int_{-1}^{1} k_n(\xi,\eta)\varphi_0(\eta)d\eta = \int_{-1}^{1} d\eta\, k(\xi,\eta) \int_{-1}^{1} k_{n-1}(\eta,\zeta)\, \varphi_0(\zeta)\, d\zeta$$

$$= \int_{-1}^{1} d\zeta\, \varphi_0(\zeta) \int_{-1}^{1} k(\xi,\eta)\, k_{n-1}(\eta,\zeta)\, d\eta$$

$$= \int_{-1}^{1} d\eta\, \varphi_0(\eta) \int_{-1}^{1} k(\xi,\zeta)\, k_{n-1}(\zeta,\eta)\, d\zeta.$$

Therefore

$$k_n(\xi,\eta) = \int_{-1}^{1} k(\xi,\zeta)\, k_{n-1}(\zeta,\eta)\, d\zeta. \qquad (3.20)$$

Since we are interested in u, the integration can in fact be performed on (3.11) directly. Combining (3.11), (3.15) and (3.18) gives

$$du/d\eta = -R\eta - F_1(\eta) \sum_{n=0}^{\infty} \varepsilon^{n+1} \varphi_n(\eta).$$

Integrating once w.r.t. η gives the solution in the form

$$u = \tfrac{1}{2} R(1-\eta^2) - \sum_{n=0}^{\infty} \varepsilon^{n+1} \int_{-1}^{1} F_1(\eta')\, \varphi_n(\eta')\, d\eta', \qquad (3.21)$$

where

$$\varphi_n(\eta') = (-1)^n \int_{-1}^{1} k_n(\eta',\zeta)\, \varphi_0(\zeta)\, d\zeta \;;\; n = 1, 2, \ldots.$$

The first term on the r.h.s. of (3.21) reflects the laminar profile, while the remaining terms represent the effects associated with turbulence.

CASE (ii)-

The situation in which ε is large is of more interest, mainly because a straight forward series solution does not appear to be possible, and on the other hand, since the parameter ε is directly proportional to the Reynolds number (according to 3.18), it seems reasonable to expect ε to have large values in turbulent flows.

An alternative approach to the problem in this case would be to work with the transformed version of the equations and seek a solution in the form of an asymptotic series.

Let $\bar{f}(s)$ denote the Fourier Transform of $f(\eta)$, defined by

$$\mathcal{F}\{f(\eta)\} = \bar{f}(s) = \int_{-\infty}^{\infty} e^{is\eta} f(\eta)\, d\eta, \qquad (3.22a)$$

and

$$\mathcal{F}^{-1}\{\bar{f}(s)\} = f(\eta) = \frac{1}{2\pi}\int_{-\infty}^{\infty} e^{-is\eta} \bar{f}(s)\, ds, \quad [23]. \qquad (3.22b)$$

If we extend the definition of $F_1(\eta)$ to the whole real line and put

$$F_1(\eta) = 0 \quad \text{for} \quad |\eta| \geq 1,$$

then (3.17) gives a continuation of ψ to the whole real line and transforms to

$$\bar{\psi}(s) + \varepsilon \int_{-\infty}^{\infty} d\xi\, e^{is\xi} \int_{-\infty}^{\infty} F_1(\eta) \exp\left\{-\frac{1}{2b^2}(\xi-\eta)^2\right\} \psi(\eta)\, d\eta$$

$$= -R\,\bar{g}(s). \qquad (3.23)$$

The double integral in above can be simplified by making use of the Convolution theory [23].

Let

$$T = \int_{-\infty}^{\infty} d\xi\, e^{isx} \int_{-\infty}^{\infty} K_1(\xi-\eta)\, K_2(\eta)\, d\eta\,, \tag{3.24}$$

where

$$K_1(\xi-\eta) = \exp\{-\tfrac{1}{2b^2}(\xi-\eta)^2\}\,, \tag{3.25}$$

and

$$K_2(\eta) = F_1(\eta)\,\varphi(\eta). \tag{3.26}$$

The inner integral in (3.24) represents the convolution of K_1 and K_2, and we can write

$$T = \int_{-\infty}^{\infty} d\xi\, e^{isx}\,[K_1(\xi) * K_2(\xi)] = \bar{K}_1(s)\,\bar{K}_2(s)\,, \tag{3.27}$$

where

$$\begin{aligned}\bar{K}_1(s) &= \int_{-\infty}^{\infty} e^{isx} \exp\{-\tfrac{1}{2b^2}x^2\}\,dx \\ &= \sqrt{(2\pi)}\,b\,\exp\{-\tfrac{1}{2}b^2s^2\}\,.\end{aligned} \tag{3.28}$$

and

$$\begin{aligned}\bar{K}_2(s) &= \int_{-\infty}^{\infty} e^{isx} F_1(x)\,\varphi(x)\,dx \\ &= \tfrac{1}{2\pi}\,\bar{F}_1(s) * \bar{\varphi}(s).\end{aligned} \tag{3.29}$$

Hence (3.27) becomes

$$\begin{aligned}T &= b\sqrt{(2\pi)}\exp\{-\tfrac{1}{2}b^2s^2\}\,\bar{F}_1(s) * \bar{\varphi}(s) \\ &= b\sqrt{(2\pi)}\exp\{-\tfrac{1}{2}b^2s^2\}\int_{-\infty}^{\infty}\bar{F}_1(s-t)\,\bar{\varphi}(t)\,dt,\end{aligned} \tag{3.30}$$

where

$$\bar{F}_1(s) = \frac{2a\,e^{-a}}{s(s^2+a^2)}\{a\cosh a\sin s - s\sinh a\cos s\}. \tag{3.31}$$

[see appendix A1].

Having simplified the double integral, the equation (3.23) becomes

$$\bar{\varphi}(s) = -R\,\bar{g}(s) - e^{-\frac{1}{2}b^2s^2}\,\Psi(s); \tag{3.32}$$

where

$$\Psi(s) = 1/\sqrt{(2\pi)}\;\varepsilon\, b\int_{-\infty}^{\infty}\bar{F}_1(s-t)\,\bar{\varphi}(t)\,dt. \tag{3.33}$$

Substituting $\bar{\varphi}(t)$ in the above, by (3.32), yields

$$\begin{aligned}\Psi(s) = -\frac{1}{\sqrt{(2\pi)}}\,\varepsilon\, b\Big[R\int_{-\infty}^{\infty}\bar{F}_1(s-t)\,\bar{g}(t)\,dt \\ + \int_{-\infty}^{\infty}\bar{F}_1(s-t)\,e^{-\frac{1}{2}b^2t^2}\,\Psi(t)\,dt\Big].\end{aligned}$$

It is convenient to write

$$\Psi(s) = \bar{f}(s) + \bar{J}(s) , \tag{3.34}$$

where

$$\bar{f}(s) = -\frac{1}{\sqrt{(2\pi)}} \varepsilon b R \int_{-\infty}^{\infty} \bar{F}_1(s-t)\, \bar{g}(t)\, dt , \tag{3.35}$$

and

$$\bar{J}(s) = -\frac{1}{\sqrt{(2\pi)}} \varepsilon b \int_{-\infty}^{\infty} \bar{F}_1(s-t)\, e^{-\frac{1}{2}b^2t^2}\, \Psi(t)\, dt. \tag{3.36}$$

To solve (3.34), we make the assumption that b>>1 and look for an asymptotic series solution of the form

$$\Psi(s) \sim b^{\rho} \sum_{j=0}^{\infty} b^{-j}\, \Psi_j(s) , \tag{3.37}$$

where the exponent ρ is a constant to be determined in the process.

Physically, large b implies that the neighbouring points $\underset{\sim}{X}'$, whose effects on the point in question we are averaging, are more widely spread. This in effect means that the eddies of larger scale, which may have been formed at some distance away from the lump of fluid under consideration, will show their effect.

Let us now turn our attention to the integrals involved in (3.34), namely $\bar{f}(s)$ and $\bar{J}(s)$, and see how they may be presented in asymptotic forms.

First consider $\bar{f}(s)$, as given by (3.35). The integrand in this equation contains $\bar{g}(t)$, the method of evaluating which is described below.

$$\bar{g}(t) = \int_{-\infty}^{\infty} e^{it\xi}\, g(\xi)\, d\xi , \tag{3.38}$$

where

$$g(\xi) = \int_{-1}^{1} \eta \exp\{-\tfrac{1}{2b^2}(\xi-\eta)^2\}\, d\eta .$$

If we put

$$\xi = \tfrac{1}{2} b x \qquad \text{and} \qquad \eta = \tfrac{1}{2} b y ,$$

so that

$$d\xi = \tfrac{1}{2} b\, dx \qquad \text{and} \qquad d\eta = \tfrac{1}{2} b\, dy ,$$

then

$$g(\sqrt{2}\,b\,x) = \int_{-1/\sqrt{2}\,b}^{1/\sqrt{2}\,b} 2\,b^2 y\, \exp\{-(x-y)^2\}\, dy$$

$$= 2\,b^2 e^{-x^2} \int_{-1/\sqrt{2}\,b}^{1/\sqrt{2}\,b} y\, \exp\{2xy - y^2\}\, dy$$

$$= 2\,b^2 e^{-x^2} \sum_{n=0}^{\infty} \frac{1}{n!} H_n(x) \int_{-1/\sqrt{2}\,b}^{1/\sqrt{2}\,b} y^{n+1}\, dy\,, \qquad (3.39)$$

where $H_n(x)$ is the Hermite polynomial , defined by

$$H_n(x) = \left[\frac{d^n}{dy^n}\left\{e^{2xy-y^2}\right\}\right]_{y=0} = (-1)^n e^{x^2} \frac{d^n}{dx^n}\, e^{-x^2}\,,$$

with the generating function

$$\exp\{2xy - y^2\} = \sum_{n=0}^{\infty} y^n H_n(x)/n!\,, \qquad [31].$$

The integral in (3.39) vanishes if n is an even integer and hence

$$g(\sqrt{2}\,b\,x) = \frac{\sqrt{2}}{b}\, e^{-x^2} \sum_{m=0}^{\infty} \frac{H_{2m+1}(x)}{(2m+3)(2m+1)!} \left(\frac{1}{2b^2}\right)^m\,, \qquad (3.40)$$

where

$$H_{2m+1}(x) = -e^{x^2} \frac{d^{2m+1}}{dx^{2m+1}}\, e^{-x^2} \quad ; \quad n = 2m+1.$$

The convergence of the series in (3.40) is proved in appendix A2.

Replacing the series expansion given by (3.40) for g, in (3.38) gives

$$\bar{g}(t) = -2 \sum_{m=0}^{\infty} \frac{(1/2b^2)^m}{(2m+3)(2m+1)!} \int_{-\infty}^{\infty} e^{i\sqrt{2}\,b\,t\,x} \frac{d^{2m+1}}{dx^{2m+1}}\, e^{-x^2}\, dx.$$

To evaluate the above integral, let

$$I_{2m+1} = \int_{-\infty}^{\infty} e^{i\sqrt{2}\,b\,t\,x} \frac{d^{2m+1}}{dx^{2m+1}}\, e^{-x^2}\, dx.$$

Successive integration by parts, yields

$$I_{2m+1} = -2\,b^2 t^2\, I_{2m-1} \quad ; \quad m \geq 1\,,$$

from which one can deduce

$$I_{2m+1} = (-2\,b^2 t^2)^m\, I_1\,,$$

where

$$I_1 = \int_{-\infty}^{\infty} e^{i\sqrt{2}bt\,x}\,\frac{de^{-x^2}}{dx}\,dx = -i\sqrt{(2\pi)}\,bt\,e^{-\frac{1}{2}b^2t^2}.$$

Hence, the expansion for $\bar{g}(t)$ reduces to

$$\bar{g}(t) = 2\sqrt{(2\pi)}\,bi\sum_{m=0}^{\infty}\frac{(-1)^m}{(2m+3)(2m+1)!}\,t^{2m+1}\,e^{-\frac{1}{2}b^2t^2}. \qquad (3.41)$$

Combining the above equation with (3.35) gives

$$\bar{f}(s) = -2\varepsilon bR\int_{-\infty}^{\infty}\left\{\sum_{m=0}^{\infty}\frac{(-1)^m}{(2m+3)(2m+1)!}\,t^{2m+1}\right\}\bar{F}_1(s-t)\,e^{-\frac{1}{2}b^2t^2}\,dt,$$

which after splitting the integral can be presented in the form

$$\bar{f}(s) = -2\varepsilon bR\int_{0}^{\infty}\left\{\sum_{m=0}^{\infty}\frac{(-1)^m}{(2m+3)(2m+1)!}\,t^{2m+1}\right\}\left\{\bar{F}_1(s-t)-\bar{F}_1(s+t)\right\}e^{-\frac{1}{2}b^2t^2}\,dt.$$

The above integral is of the Laplace type, and since b is assumed large, the major contribution to the integral arises from the region close to the origin within which t is small. In this region we can write, using Taylor's theorem,

$$\bar{F}_1(s-t)-\bar{F}_1(s+t) = -2\sum_{k=0}^{\infty}\bar{F}_1^{(2k+1)}(s)\,t^{2k+1}/(2k+1)!\ , \qquad (3.42)$$

(the exponent whithin brackets denotes repeated differentiation). Hence

$$\bar{f}(s) = 4\varepsilon bR\int_{0}^{\infty}t^2\left\{\sum_{m=0}^{\infty}\frac{(-1)^m}{(2m+3)(2m+1)!}\,t^{2m}\right\}\left\{\sum_{k=0}^{\infty}\frac{\bar{F}_1^{(2k+1)}(s)}{(2k+1)!}\,t^{2k}\right\}e^{-\frac{1}{2}b^2t^2}\,dt,$$

$$= 4\varepsilon bR\int_{0}^{\infty}t^2\sum_{k=0}^{\infty}\left\{\sum_{m=0}^{k}\frac{(-1)^m}{(2m+3)(2m+1)!}\,\frac{\bar{F}_1^{(2k-2m+1)}(s)}{(2k-2m+1)!}\right\}t^{2k}\cdot e^{-\frac{1}{2}b^2t^2}\,dt.$$

We can write for convenience

$$\bar{f}(s) = 4\varepsilon bR\int_{0}^{\infty}\sum_{k=0}^{\infty}A_k(s)\,t^{2k+2}\cdot e^{-\frac{1}{2}b^2t^2}\,dt, \qquad (3.43)$$

where

$$A_k(s) = \sum_{m=0}^{k}\frac{(-1)^m}{(2m+3)(2m+1)!}\,\frac{\bar{F}_1^{(2k-2m+1)}(s)}{(2k-2m+1)!}\,. \qquad (3.44)$$

To estimate the integral in (3.43) for large b, Watson's lemma is employed to give

$$\bar{f}(s) \sim 2\varepsilon i R/b \sum_{k=0}^{\infty} A_k(s)\, 2^{k+3/2}\, \Gamma(k+\tfrac{3}{2})\, b^{-2k}, \text{[6 ,p.48]}. \quad (3.45)$$

Since

$$\varepsilon = R c b^2,$$

then $$f(s) = O(\varepsilon/b) = O(b).$$

A similar method, as described above, can be used to represent $\bar{J}(s)$ in an asymptotic form. So once again, splitting the integral in (3.36) gives

$$\bar{J}(s) = -\frac{\varepsilon b}{\sqrt{(2\pi)}} \int_0^{\infty} e^{-\frac{1}{2}b^2t^2}\, \Psi(t)\{\bar{F}_1(s-t) - \bar{F}_1(s+t)\}\, dt. \quad (3.46)$$

Since $\Psi(t)$ is an odd function, then for small values of t, it has the Taylor expansion

$$\Psi(t) = \sum_{i=0}^{\infty} \frac{\Psi^{(2i+1)}(0)\, t^{2i+1}}{(2i+1)!}, \quad (3.47)$$

which together with (3.42), gives

$$\bar{J}(s) = \frac{2\varepsilon b}{\sqrt{(2\pi)}} \int_0^{\infty} \sum_{m=0}^{\infty} B_m(s)\, t^{2m+2}\, .e^{-\frac{1}{2}b^2t^2}\, dt, \quad (3.48)$$

where

$$B_m(s) = \sum_{i=0}^{m} \frac{\bar{F}_1^{(2m-2i+1)}(s)\, \Psi^{(2i+1)}(0)}{(2m-2i+1)!\,(2i+1)!}, \quad (3.49)$$

and from (3.37)

$$\Psi^{(2i+1)}(0) \sim b^{\rho} \sum_{j=0}^{\infty} b^{-j}\, \Psi_j^{(2i+1)}(0).$$

Watson's lemma is again used here to give

$$\bar{J}(s) \sim \frac{2\varepsilon b}{\sqrt{(2\pi)}} \sum_{m=0}^{\infty} \frac{1}{2} B_m(s)\, \Gamma\left(\frac{2m+3}{2}\right) 2^{m+3/2} b^{-(2m+3)}. \quad (3.50)$$

Since

$$B_m(s) = O(b^{\rho}) \quad \text{and} \quad \varepsilon = O(b^2),$$

it follows that $\bar{J}(s) = O(b^{\rho})$.

Returning to the equation (3.34), since Ψ and $\bar{J}$ are both $O(b^{\rho})$ and $\bar{f}$ is $O(b)$, then choosing $\rho = 1$ would make all the terms of equal order and of the forms (each term is written in full. i.e. ξ is replaced by Rcb^2 and $A_j(s)$, $B_m(s)$ and $\Psi^{(2i+1)}(0)$ by their respective expansions)

$$\Psi(s) \sim b \sum_{j=0}^{\infty} b^{-j} \Psi_j(s),$$

$$\bar{f}(s) \sim 4 l_2 i R^2 c b \sum_{k=0}^{\infty} \sum_{m=0}^{k} \frac{(-1)^m 2^k \Gamma(k+3/2)}{(2m+3)(2m+1)!(2k-2m+1)!} \bar{F}_1^{(2k-2m+1)}(s) b^{-2k},$$

and

$$\bar{J}(s) \sim \frac{2}{\sqrt{\pi}} Rcb \sum_{m=0}^{\infty} \sum_{i=0}^{m} \sum_{j=0}^{\infty} \frac{2^m \Gamma(m+3/2)}{(2m-2i+1)!(2i+1)!} \bar{F}_1^{(2m-2i+1)}(s) \Psi_j^{(2i+1)}(0) b^{-2}$$

Having established the above asymptotic forms, we can now determine $\Psi_j(s)$; $j = 0,1,2,\ldots$, by collecting and equating terms of equal order from either side of (3.34). Since $b>>1$, we shall retain terms of $O(1/b^4)$ in the solution and ignore terms of $O(1/b^5)$ and smaller. Our solution will thus have the form

$$\Psi(s) \sim b\,\Psi_0(s) + \Psi_1(s) + \frac{1}{b}\Psi_2(s) + \frac{1}{b^2}\Psi_3(s)$$

$$+ \frac{1}{b^3}\Psi_4(s) + \frac{1}{b^4}\Psi_5(s) + O(1/b^5). \qquad (3.51)$$

The reason for taking so many terms in the series, is that we found unless $\psi(\eta)$ contains some terms of $O(1/b^4)$, the final solution for u would be independent of b. In order to be consistent, if such terms are to be retained in $\psi(\eta)$, they must also be included in $\Psi(s)$.

If we take terms of $O(b)$ we have

$$\Psi_0(s) = \frac{2}{3}\sqrt{(2\pi)}\, i R^2 C \bar{F}_1^{(1)}(s) + Rc \bar{F}_1^{(1)}(s) \Psi_0^{(1)}(0). \qquad (3.52)$$

Differentiating once w.r.t. s yields

$$\Psi_0^{(1)}(s) = \frac{2}{3}\sqrt{(2\pi)}\, i R^2 c \bar{F}_1^{(2)}(s) + Rc \bar{F}_1^{(2)}(s) \Psi_0^{(1)}(0).$$

Putting $s = 0$ and rearranging leads to

$$\Psi_0^{(1)}(0) = \frac{2}{3}\sqrt{(2\pi)} \frac{i R^2 c \bar{F}_1^{(2)}(0)}{1 - Rc \bar{F}_1^{(2)}(0)},$$

and if substituted back in (3.52) and rearranged gives

$$\Psi_0(s) = \frac{2}{3}\sqrt{(2\pi)}\,\frac{iR^2c\,\bar{F}_1^{(1)}(s)}{1-RC\,\bar{F}_1^{(2)}(0)}\,. \qquad (3.53)$$

Terms of O(1), yields

$$\Psi_1(s) = RC\,\bar{F}_1^{(1)}(s)\,\Psi_1^{(1)}(0),$$

which by differentiating once and putting s = 0, one can deduce

$$\Psi_1(s) = 0\,. \qquad (3.54)$$

Similarly, by taking terms of $O(1/b^2)$ and $(1/b^4)$, we find

$$\Psi_3(s) = 0 \qquad \text{and} \qquad \Psi_5(s) = 0,$$

respectively.

Taking terms of O(1/b) and following the same procedure as above, we get

$$\Psi_2(s) = \sqrt{(2\pi)}\,iR^2c\left\{\frac{1}{3}\bar{F}_1^{(3)}(s) - \frac{1}{5}\bar{F}^{(1)}(s)\right\} + \sqrt{(2\pi)}\,\frac{iR^3c^2}{1-RC\,\bar{F}_1^{(2)}(0)}$$
$$\cdot\left\{\left[\frac{1}{3}\bar{F}_1^{(4)}(0) - \frac{1}{5}\bar{F}_1^{(2)}(0)\right]\bar{F}_1^{(1)}(s) + \frac{2}{3}\,\frac{RC\,\bar{F}_1^{(2)}(0)\,\bar{F}_1^{(4)}(0)}{1-RC\,\bar{F}_1^{(2)}(0)}\,\bar{F}_1^{(1)}(s)\right.$$
$$\left. + \frac{1}{3}\left[\bar{F}_1^{(2)}(0)\,\bar{F}_1^{(3)}(s) + \bar{F}_1^{(4)}(0)\,\bar{F}_1^{(1)}(s)\right]\right\}. \qquad (3.55)$$

Finally, terms of $O(1/b^3)$, gives

$$\Psi_4(s) = \sqrt{(2\pi)}\,iR^2c\left\{\frac{1}{30}\bar{F}_1^{(5)}(s) - \frac{1}{15}\bar{F}_1^{(3)}(s) + \frac{1}{70}\bar{F}_1^{(1)}(s)\right\}$$
$$+ RC\left\{\bar{F}_1^{(1)}(s)\,\Psi_4^{(1)}(0) + \frac{1}{2}\bar{F}_1^{(3)}(s)\,\Psi_2^{(1)}(0) + \frac{1}{2}\bar{F}_1^{(1)}(s)\,\Psi_2^{(3)}(0)\right.$$
$$\left. + \frac{1}{8}\bar{F}_1^{(5)}(s)\,\Psi_0^{(1)}(0) + \frac{5}{12}\bar{F}_1^{(3)}(s)\Psi_0^{(3)}(0) + \frac{1}{9}\bar{F}_1^{(1)}(s)\,\Psi_0^{(5)}(0)\right\}. \qquad (3.56)$$

By differentiating the above once and putting s = 0, we can find $\Psi_4^{(1)}(0)$. The derivatives of Ψ_0 and Ψ_2 at s = 0, which also appear in (3.56) can be found from (3.53) and (3.55). Considering the number of terms these substitutions generate, the expression for $\Psi_4(s)$ would be hopelessly complicated. Fortunately, as will be seen later, the

contribution from the terms in (3.56) to the solution will be $O(1/b^6)$. The exact expression for $\Psi_4(s)$ therefore, does not appear to be necessary, as we are neglecting terms of $O(1/b^5)$ and smaller.

The above expressions for $\Psi_j(s)$; j = 0, 2 and 4, contain the derivatives of $\bar{F}_1(s)$ up to and including the sixth order. Obviously, differentiating $\bar{F}_1(s)$, as given by (3.31), to this order, does not seem practical, and we shall use the more efficient technique of expanding $\bar{F}_1(s)$ in the powers of s before performing the differentiation. From (3.31)

$$\bar{F}_1(s) = \frac{2\,a\,e^{-a}}{s\,(s^2+a^2)}\,(\,a\cosh a \sin s - s \sinh a \cos s)$$

$$= 2\,a\,e^{-a}\Big\{\frac{1}{a^2}\sum_{j=0}^{\infty}(-1)^j\left(\frac{s}{a}\right)^{2j}\Big\}\Big\{\sum_{k=0}^{\infty}(-1)^k\Big[\frac{a\cosh a}{(2k+1)!}-\frac{\sinh a}{(2k)!}\Big]s^{2k}\Big\},$$

which can be written as

$$\bar{F}_1(s) = 2\,e^{-a}\sum_{j=0}^{\infty}\gamma_j\,s^{2j},$$

where

$$\gamma_j = \sum_{k=0}^{j}(-1)^j\,a^{2k-2j-1}\Big\{\frac{a\cosh a}{(2k+1)!}-\frac{\sinh a}{(2k)!}\Big\}. \qquad (3.57)$$

Repeated differentiation yields

$$\bar{F}_1^{(m)} = 2\,e^{-a}\sum_{j=0}^{\infty}(2j)(2j-1)\cdots(2j-m+1)\,\gamma_j\,s^{2j-m}\;;\; m\geq 1. \qquad (3.58)$$

Since $\bar{F}_1(s)$ is an even function, then all its odd derivatives vanish at s = 0 and the even ones reduce to

$$\bar{F}_1^{(2)}(0) = 4e^{-a}\gamma_1\quad,\quad \bar{F}_1^{(4)}(0) = 48\,e^{-a}\gamma_2\,,$$

and (3.59)

$$\bar{F}_1^{(6)}(0) = 2.(5!)\,e^{-a}\gamma_3\,,$$

where

$$\gamma_1 = -\left(\frac{1}{a}\right)^3\Big\{a\cosh a - \sinh a\Big\} - \frac{1}{a}\Big\{\frac{1}{3!}\,a\cosh a - \frac{1}{2!}\sinh a\Big\}, \qquad (3.60)$$

and

$$\gamma_2 = \left(\frac{1}{a}\right)^5\Big\{a\cosh a - \sinh a\Big\} + \left(\frac{1}{a}\right)^3\Big\{\frac{1}{3!}\,a\cosh a - \frac{1}{2!}\sinh a\Big\}$$

$$+\;\frac{1}{a}\Big\{\frac{1}{5!}\,a\cosh a - \frac{1}{4!}\sinh a\Big\}. \qquad (3.61)$$

The expression for Υ_3 will not be required.

Substituting the equations (3.58) and (3.59) into (3.53) and (3.55) and simplifying, gives

$$\Psi_0(s) = i\alpha_0 \sum_{j=0}^{\infty} j\,\gamma_j\, s^{2j-1}, \tag{3.62}$$

and

$$\Psi_1(s) = i\alpha_1 \sum_{j=0}^{\infty} j\,\gamma_j\, s^{2j-1} + i\alpha_0 \sum_{j=0}^{\infty} j(2j-1)(j-1)\gamma_j\, s^{2j-3}, \tag{3.63}$$

where

$$\alpha_0 = \frac{8\sqrt{(2\pi)}R^2 c\, e^{-a}}{3(1-4Rc\,e^{-a}\gamma_1)}, \tag{3.64}$$

and

$$\alpha_1 = \frac{4\sqrt{(2\pi)}R^2 c\, e^{-a}}{(1-4Rc\,e^{-a}\gamma_1)^2}\left[32Rc\,e^{-a}\gamma_2 - \tfrac{1}{5}(1-4Rc\,e^{-a}\gamma_1)\right]. \tag{3.65}$$

With similar substitutions, (3.56) will have a form, like

$$\Psi_4(s) = \left\{ i\alpha_2 \sum_{j=0}^{\infty} j\gamma_j\, s^{2j-1} + i\alpha_3 \sum_{j=0}^{\infty} j(2j-1)(j-1)\gamma_j\, s^{2j-3} + i\alpha_4 \sum_{j=0}^{\infty} j(2j-1)(j-1)(2j-3)(j-2)\gamma_j\, s^{2j-5} \right\},$$

where α_2, α_3 and α_4 are some constants, containing R, a, c and γ_3. Hence, the asymptotic solution (3.51) of the equation (3.34), becomes

$$\begin{aligned}\Psi(s) \sim b\left\{ i\alpha_0 \sum_{j=0}^{\infty} j\,\gamma_j\, s^{2j-1} \right\} &+ \frac{1}{b}\left\{ i\alpha_1 \sum_{j=0}^{\infty} j\,\gamma_j\, s^{2j-1} + i\alpha_0 \sum_{j=0}^{\infty} j(2j-1)(j-1)\gamma_j\, s^{2j-3} \right\} \\ &+ \frac{1}{b^3}\left\{ i\alpha_2 \sum_{j=0}^{\infty} j\,\gamma_j\, s^{2j-1} + i\alpha_3 \sum_{j=0}^{\infty} j(2j-1)(j-1)\gamma_j\, s^{2j-3} + i\alpha_4 \sum_{j=0}^{\infty} j(2j-1)(j-1)(2j-3)(j-2)\right. \\ &\left. \cdot\,\gamma_j\, s^{2j-5} \right\} + O(1/b^5).\end{aligned}$$

Returning to the equation (3.32) and combining it with (3.41) and the above series, we find

$$\begin{aligned}\bar{\chi}(s) \sim -e^{-\frac{1}{2}b^2s^2}\Big\{ & 2\sqrt{(2\pi)}\,iRb \sum_{m=0}^{\infty} \frac{(-1)^m}{(2m+3)(2m+1)!}\, s^{2m+1} \\ & + i(\alpha_0 b + \alpha_1/b + \alpha_2/b^3) \sum_{j=0}^{\infty} j\,\gamma_j\, s^{2j-1} \\ & + i(\alpha_0/b + \alpha_3/b^3) \sum_{j=0}^{\infty} j(2j-1)(j-1)\gamma_j\, s^{2j-3} \\ & + i\,\alpha_4/b^3 \sum_{j=0}^{\infty} j(2j-1)(j-1)(2j-3)(j-2)\gamma_j\, s^{2j-5} \\ & + O(1/b^5)\Big\}.\end{aligned} \tag{3.66}$$

This series is the Fourier Transform of the function of interest, namely ψ, which can now be evaluated by taking the Inverse Fourier Transform, according to

$$\psi(\zeta) = \frac{1}{2\pi} \int_{-\infty}^{\infty} \bar{\psi}(s)\, e^{-i\zeta s}\, ds.$$

Substituting (3.66) in the above and integrating term by term, gives (method of integration is presented in the appendix A3)

$$\begin{aligned}\psi(\zeta) \sim & -\sqrt{(2/\pi)}\, Rb \sum_{n=0}^{\infty} A_n(\zeta)\, \Gamma(n+3/2)\,(\sqrt{2}/b)^{2n+3} \\ & - \frac{1}{2\pi}(\alpha_0 b + \alpha_1/b - \alpha_2/b^3) \sum_{k=0}^{\infty} B_k(\zeta)\, \Gamma(k+1/2)\,(\sqrt{2}/b)^{2k+1} \\ & - \frac{1}{4\pi}(\alpha_0/b + \alpha_3/b^3) \sum_{l=0}^{\infty} D_l(\zeta)\, \Gamma(l-1/2)\,(\sqrt{2}/b)^{2l-1} \\ & - \frac{1}{2\pi}(\alpha_4/b^3) \sum_{r=0}^{\infty} E_r(\zeta)\, \Gamma(r-3/2)\,(\sqrt{2}/b)^{2r-3}, \end{aligned} \tag{3.67}$$

where

$$A_n = \sum_{m=0}^{n} \frac{(-1)^n\, \zeta^{2n-2m+1}}{(2n-2m+1)!\,(2m+1)!\,(2m+3)},$$

$$B_k = \sum_{j=0}^{k} \frac{(-1)^{k-j}\, \zeta^{2k-2j+1}}{(2k-2j+1)!}\, j\, \gamma_j,$$

$$D_l = \sum_{j=0}^{l} \frac{(-1)^{l-j}\, \zeta^{2l-2j+1}}{(2l-2j+1)!}\, j(2j-1)(2j-2)\, \gamma_j,$$

and

$$E_r = \sum_{j=0}^{r} \frac{(-1)^{r-j}\, \zeta^{2r-2j+1}}{(2r-2j+1)!}\, j(2j-1)(j-1)(2j-3)(j-2)\, \gamma_j,$$

$$B_0 = D_0 = D_1 = E_0 = E_1 = E_2 = 0.$$

Since $\bar{\psi}(s)$ has an error of $O(1/b^5)$, then $\psi(\zeta)$ will be accurate up to $O(1/b^4)$. We may therefore neglect terms of $O(1/b^5)$ and smaller in (3.67). Hence

$$\begin{aligned}\psi(\zeta) \sim & -2R\left[A_0(\zeta)/b^2 + 3A_1(\zeta)/b^4\right] - \frac{1}{\sqrt{(2\pi)}}\left[\alpha_0 B_1(\zeta)/b^2 + \alpha_1 B_1(\zeta)/b^4\right. \\ & \left. + 3\alpha_0 B_2(\zeta)/b^4 + \tfrac{3}{2}\alpha_0 D_2(\zeta)/b^4\right] + O(1/b^5), \end{aligned} \tag{3.68}$$

where

$$A_0 = \tfrac{1}{3}\zeta \quad , \quad A_1 = -\frac{1}{3!}\left(\frac{\zeta^3}{3} + \frac{\zeta}{5}\right),$$

$$B_1 = \gamma_1 \zeta \quad , \quad B_2 = -\frac{\gamma_1}{3!}\zeta^3 + 2\gamma_2 \zeta,$$

and $D_2 = 12\,\gamma_2\,\zeta$. (3.69)

Having found ψ, we return to the equation of motion (3.11), which combined with (3.15), can be written as

$$dU/d\eta = -R\eta - Rcb^2 F_1(\eta)\psi(\eta). \tag{3.70}$$

It now remains to replace ψ in (3.70), by its asymptotic expansion (3.68), and integrate it once to obtain an expression for the mean velocity profile.

Combining equations (3.70), (3.68), (3.69), (3.64) and (3.65) together with (3.12), simplifying and rearranging yields

$$dU/d\eta = -R\eta - (\cosh a - \cosh a\eta)(\alpha\eta+\beta\eta^3), \tag{3.71}$$

where

$$\alpha = \frac{R(1-\lambda)}{4\gamma_1\lambda}\left[-\frac{2}{3} + \frac{1}{5b^2} - \frac{8\gamma_2(1-\lambda)}{\lambda b^2\gamma_1}\right], \tag{3.72}$$

$$\beta = \frac{R(1-\lambda)}{12\,b^2\gamma_1\lambda}, \tag{3.73}$$

and

$$\lambda = 1 - 4Rce^{-a}\gamma_1. \tag{3.74}$$

To find the mean velocity u, at a distance η from the wall ($\eta'=-1$), the equation (3.71) must now be integrated. Thus

$$U = \int_{-1}^{\eta}\{-R\eta' - (\cosh a - \cosh a\eta')(\alpha\eta' + \beta\eta'^3)\}\,d\eta',$$

where η' is a dummy variable.

Integrating the above equation by parts, gives the final expression for the mean velocity profile for this particular problem, in the form

$$\begin{aligned} U = {} & \tfrac{1}{2}R(1-\eta^2) + \alpha\left\{\tfrac{1}{2}(1-\eta^2)\cosh a + \frac{1}{a}(\eta\sinh a\eta - \sinh a)\right. \\ & \left. - \frac{1}{a^2}(\cosh a\eta - \cosh a)\right\} + \beta\left\{\tfrac{1}{4}(1-\eta^4)\cosh a\right. \\ & + \frac{1}{a}(\eta^3\sinh a\eta - \sinh a) - \frac{3}{a^2}(\eta^2\cosh a\eta - \cosh a) \\ & \left. + \frac{6}{a^3}(\eta\sinh a\eta - \sinh a) - \frac{6}{a^4}(\cosh a\eta - \cosh a)\right\}. \end{aligned} \tag{3.75}$$

The first term on the r.h.s. of the equation (3.75), corresponds to the laminar solution, while the remaining terms represent the turbulent effects.

In a fully developed turbulent channel flow, it is known that the effect of turbulence on the velocity distribution is to slow down the flow in the middle parts of the channel [29]. In the sketch below therefore, if curve (1) represents a typical laminar velocity profile, then curve (2) is an indication of the type of velocity distribution one could expect if the flow was turbulent.

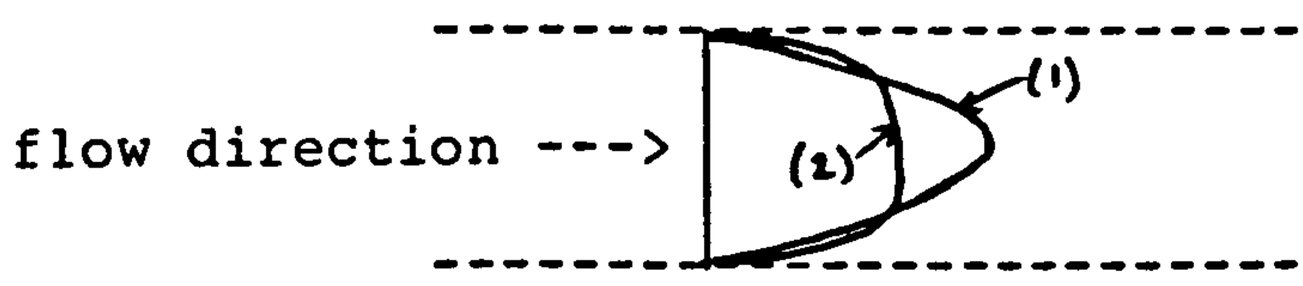

The extent to which the curve is flattened, is dependent on the level of turbulence present in the flow.

The terms representing the turbulent effects in (3.75), are expected to illustrate such changes in the velocity curves. The model constants a, b and c, and the Reynolds number R, can be varied to allow us to examine and observe the flow patterns under different conditions and varying turbulence level. The determination of the model constants and their effects on the flow, is the subject of the following sections.

3.4 Determination of the model constants.

To fit a set of numerical values to the model constants a, b and c, in order to obtain the desirable mean velocity profiles, we shall use the method called the 'overall-prediction' by Launder and Spalding [18]. The technique would be to guess some initial values for the constants, and then improve them gradually in the process of comparing the results with the experimental data. There are however, disadvantages with this technique, namely that it is time consuming, expensive on the computer, and it does not usually lead to a unique set of values. But it is useful in the sense that it can at least, provide a range of values within which the constants may vary, and it allows us to observe the behaviour of the velocity curves during the process.

To choose the initial values, it is usually possible to do better than a wild guess. As for instance, we know in our problem that all the constants are positive and that b is assumed large compared with unity. Although what is meant by large, still remains a question.

It may also be possible to establish some approximate upper or lower bound values for some of the constants, by studying the equation (3.75) in the limits, as these constants tend to their extreme values in different combinations.

Taking c as unity for simplicity, the possible cases which could arise, as far as the constants a and b are concerned, are examined below.

Case 1- small a, large b :

Letting $b \longrightarrow \infty$, we have

$$\alpha \longrightarrow \frac{R(\lambda-1)}{6\gamma_1\lambda} \quad \text{and} \quad \beta \longrightarrow 0,$$

and (3.75) reduces to

$$U \approx \frac{R}{2}(1-\eta^2) + \alpha S, \tag{3.76}$$

where

$$S = \frac{1}{2}(1-\eta^2)\cosh a + \frac{1}{a}(\eta \sinh a\eta - \sinh a) \tag{3.77}$$
$$- \frac{1}{a^2}(\cosh a\eta - \cosh a).$$

Since a is assumed to be small, the hyperbolic functions in S and γ_1 may be replaced by the first few terms of their Taylor series, namely

$$\sinh a = a + \frac{a^3}{3!} + \cdots,$$

and

$$\cosh a = 1 + \frac{a^2}{2!} + \cdots.$$

This would simplify the expressions for S and γ_1 as

$$S \approx \frac{a^2}{8}(1-\eta^2) + O(a^4), \tag{3.78}$$

and

$$\gamma_1 \approx -\frac{4}{5!}a^2 + O(a^4). \tag{3.79}$$

Also for small a, the expression for α can further be simplified as shown below.

$$\alpha \approx \frac{R(\lambda-1)}{6\gamma_1\lambda},$$

where

$$\lambda = 1 - 4Re^{-a}\gamma_1$$
$$= 1 - 4R\left(1 - a + \frac{a^2}{2!} - \ldots\right)\left(-\frac{4}{5!}a^2\right).$$

Hence

$$\lambda \approx 1 + \frac{16}{5!}Ra^2 + o(a^3). \tag{3.80}$$

Replacing λ and γ_1 by their respective series in the above, yields

$$\alpha \approx -\frac{5!}{24}\,\frac{16/5!\;R^2a^2}{1 + 16/5!\;Ra^2}.$$

But

$$(1 + 16/5!\;Ra^2)^{-1} = 1 - \frac{16}{5!}Ra^2 + \cdots,$$

by the Binomial series, provided $16/5!\,Ra^2 < 1$ or $a^2 < 15/2R$.

Thus

$$\alpha \approx R^2\left(-\frac{2}{3} + \frac{4}{45}a^2R\right) + O(a^4). \tag{3.81}$$

Hence

$$\alpha S \approx -\frac{R^2a^2}{12}(1-\eta^2)^2 + O(a^4).$$

Finally, combining (3.76) with the above, we obtain

$$u \approx \frac{R}{2}(1-\eta^2) - \frac{R^2a^2}{12}(1-\eta^2)^2 + O(a^4). \tag{3.82}$$

Since $u \geqslant 0$ and $0 \leqslant \eta^2 \leqslant 1$, the following (approximate) relationship can be deduced from (3.82).

$$0 < a \leqslant \sqrt{(6/R)}. \tag{3.83}$$

Case 2- small a, moderate b.

Here the assumption is that b is not very large, and therefore the contribution from the third term in (3.75) is significant. Thus

$$U = \frac{R}{2}(1-\eta^2) + \alpha S + \beta T, \tag{3.84}$$

where S is given by (3.77), and

$$\begin{aligned} T = {} & \frac{1}{4}(1-\eta^4)\cosh a + \frac{1}{a}(\eta^3 \sinh a\eta - \sinh a) \\ & - \frac{3}{a^2}(\eta^2\cosh a\eta - \cosh a) + \frac{6}{a^3}(\eta \sinh a\eta - \sinh a) \\ & - \frac{6}{a^4}(\cosh a\eta - \cosh a). \end{aligned} \tag{3.85}$$

Once again, since a is small, the expressions for S and γ_1 may be simplified as in the previous case [see (3.78) and (3.79)], and by applying the same technique, i.e. using the Taylor's and the Binomial series, we can approximate the expressions for T, γ_2, α and β as follows.

$$T \approx \frac{a^2}{24}(2\eta^6 - 3\eta^4 + 1) + O(a^4),$$

$$\gamma_2 \approx \frac{6}{7!}a^2 + O(a^4),$$

$$\alpha \approx R^2\left(-\frac{2}{3} + \frac{1}{5b^2} + \frac{4}{45}Ra^2 + \frac{2}{175}\frac{Ra^2}{b^2}\right) + O(a^4),$$

and

$$\beta \approx \frac{R^2}{3b^2}\left(1 - \frac{2}{15}Ra^2\right) + O(a^3).$$

The condition of convergence of the series for α and β is

$$a^2 < 15/2R.$$

Forming the products $\alpha\delta$ and βT from the above equations and substituting them in (3.84), leads to

$$u \approx \frac{R}{2}(1-\eta^2) - \frac{R^2a^2}{12}(1-\eta^2)^2\left(1-\frac{3}{10b^2}\right) + \frac{R^2a^2}{72b^2}(2\eta^6-3\eta^4+1) + O(a^4). \qquad (3.86)$$

Since $u \geqslant 0$, then

$$\frac{R}{2}(1-\eta^2) - \frac{R^2a^2}{12}(1-\eta^2)^2\left(1-\frac{3}{10b^2}\right) + \frac{R^2a^2}{72b^2}(2\eta^6-3\eta^4+1) \geqslant 0.$$

As $R > 0$, $b > 1$ and $0 \leqslant \eta^2 \leqslant 1$, then every term in the above is positive, and we require this inequality to hold even when the second term (the one with negative factor), has its largest value, i.e. when $\eta = 0$. Thus

$$\frac{R}{2} - \frac{R^2a^2}{12}\left(1-\frac{3}{10b^2}\right) + \frac{R^2a^2}{72b^2} \geqslant 0,$$

or

$$a^2\left(1+\frac{7}{15b^2}\right) \leqslant \frac{6}{R} \quad \text{, approximately.} \qquad (3.87)$$

The situations in which a is large have little physical significance and do not give much information as far as the equation (3.75) is concerned, as in such cases, the presence of the negative exponentials in a, reduce this equation to the laminar flow problem.

The approximate relationships (3.83) and (3.87) obtained above for the special cases, can be used as a guide in choosing the initial values for the constants. As for instance, they provide the information as to how large or how small the constants can be for a given Reynolds number.

Once we have a set of initial values, the equation (3.75) can be fed into the computer, which on inputting R, a, b and c, would enable us to plot the mean velocity curves across the channel.

The computer results and the behaviour of the curves

when the constants are varied are presented and discussed in the following section.

3.5 RESULTS AND DISCUSSION.

We examined the solution (3.75), with many different values of the model constants and the Reynolds number. It appears that although b can take any value greater than unity, the parameter a can only take small values. The relationships (3.83) and (3.87) seem to support this statement. It was found that for Reynolds numbers up to 10^7, we can expect a to be of $O(10^{-3})$, approximately. As far as the parameter c is concerned, it seems that the mean velocities depart from their parabolic profiles for large values of c.

Figure 3.1 is typical of the many profiles we obtained for various values of a, b and c. It shows the variation of the mean velocity with the Reynolds number, for a=0.005, b=10 and c=0.01. It is noted that when $R=10^3$, the solution describes the laminar profile. Beyond some critical Reynolds number which is of $O(10^3)$, we know that turbulence sets in and the profiles become fuller in the middle parts of the channel. This effect is clearly visible in figure 3.1 as R is increased from 10^3 to 10^7.

The effects of the parameters a, b and c on the mean velocity, are illustrated by figures 3.2, 3.3 and 3.4, respectively. The solution appears to be very sensitive to small changes in a, whose limiting value (in this example) was found to be about a=0.01, i.e. for values less than 0.01 all profiles can be presented by the same curve. Such limiting value for b in the example shown by figure 3.3, was found at about b=10 .

The variation of the mean velocity with c is examined in figure 3.4, and the departure from the parabolic profiles in this example appeared for values of $c<2.5$.

In figure 3.5, a velocity profile, given by the equation (3.75), is compared with the universal velocity distribution laws for turbulent channel flow (equation 3.88), deduced from Von Kármán's similarity hypothesis, and equation (3.89) deduced from Prandtl's theory:

$$\frac{u_{max}-u}{u_*} = -\frac{1}{\chi}\left\{\ln\left[1-\sqrt{(1-\eta/h)}\right]+\sqrt{(1-\eta/h)}\right\}, \tag{3.88}$$

$$\frac{u_{max}-u}{u_*} = \frac{1}{\chi}\ln\frac{h}{y}, \tag{3.89}$$

where y is the distance from the wall, u_* is the frictional velocity and the dimensionless constant χ is determined from experiment. The maximum velocity u_{max} is the velocity at the centre of the channel, [29, pp. 553-555].

It can be seen that the velocity profile produced by the equation (3.75) is in good agreement with those given by the above universal laws. It is also noted that unlike the universal laws which show indefinite values for the velocity at the wall, our prediction shows a finite value there.

In plotting the equations (3.88) and (3.89), we have replaced y/h $(=\eta)$ by $1-y/h$, so that y measures the distance from the centre line.

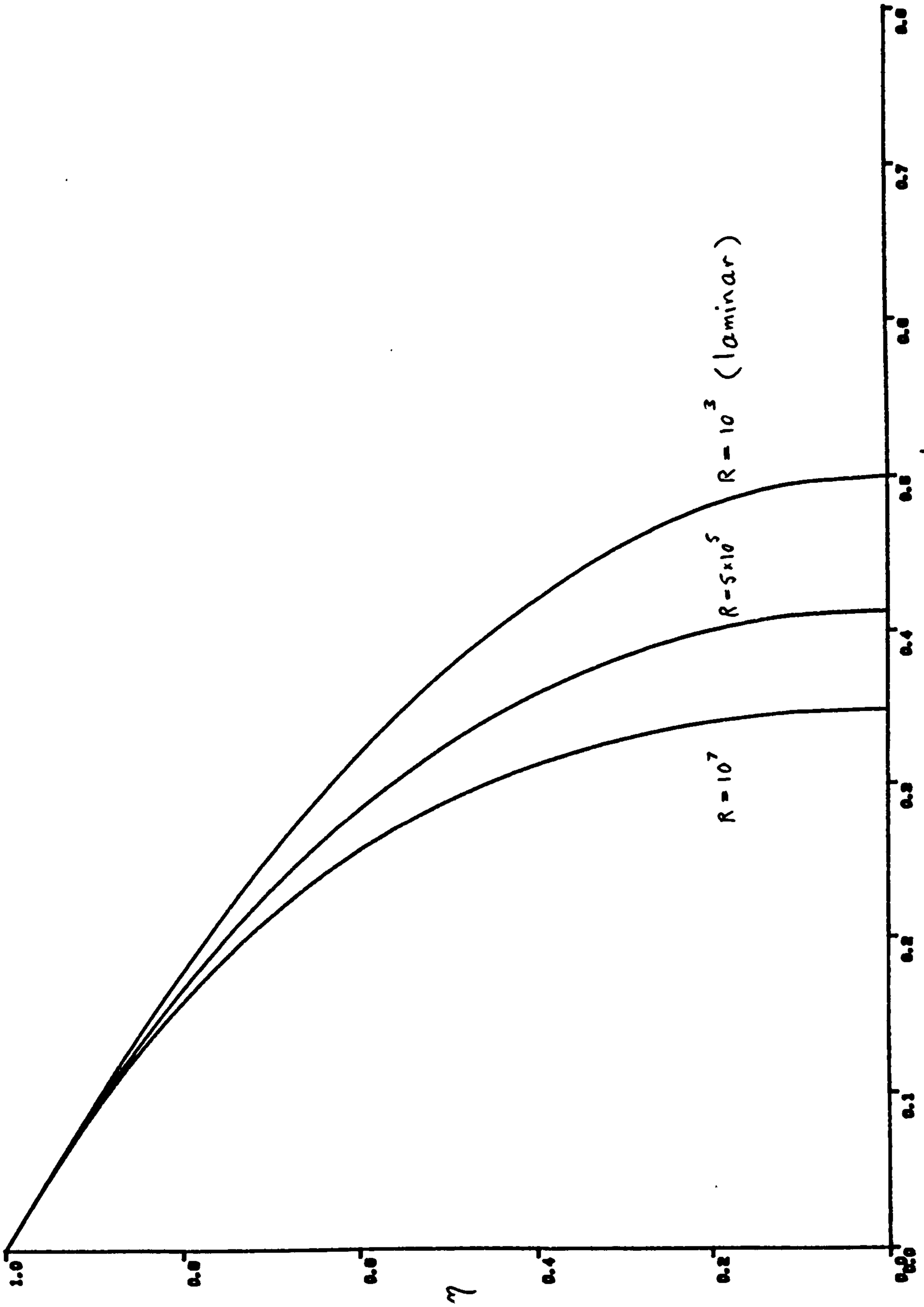

Fig. 3.1 Variation of the mean velocity (eqn. 3.75) with R, for a=0.005, b=10 and c=0.01 .

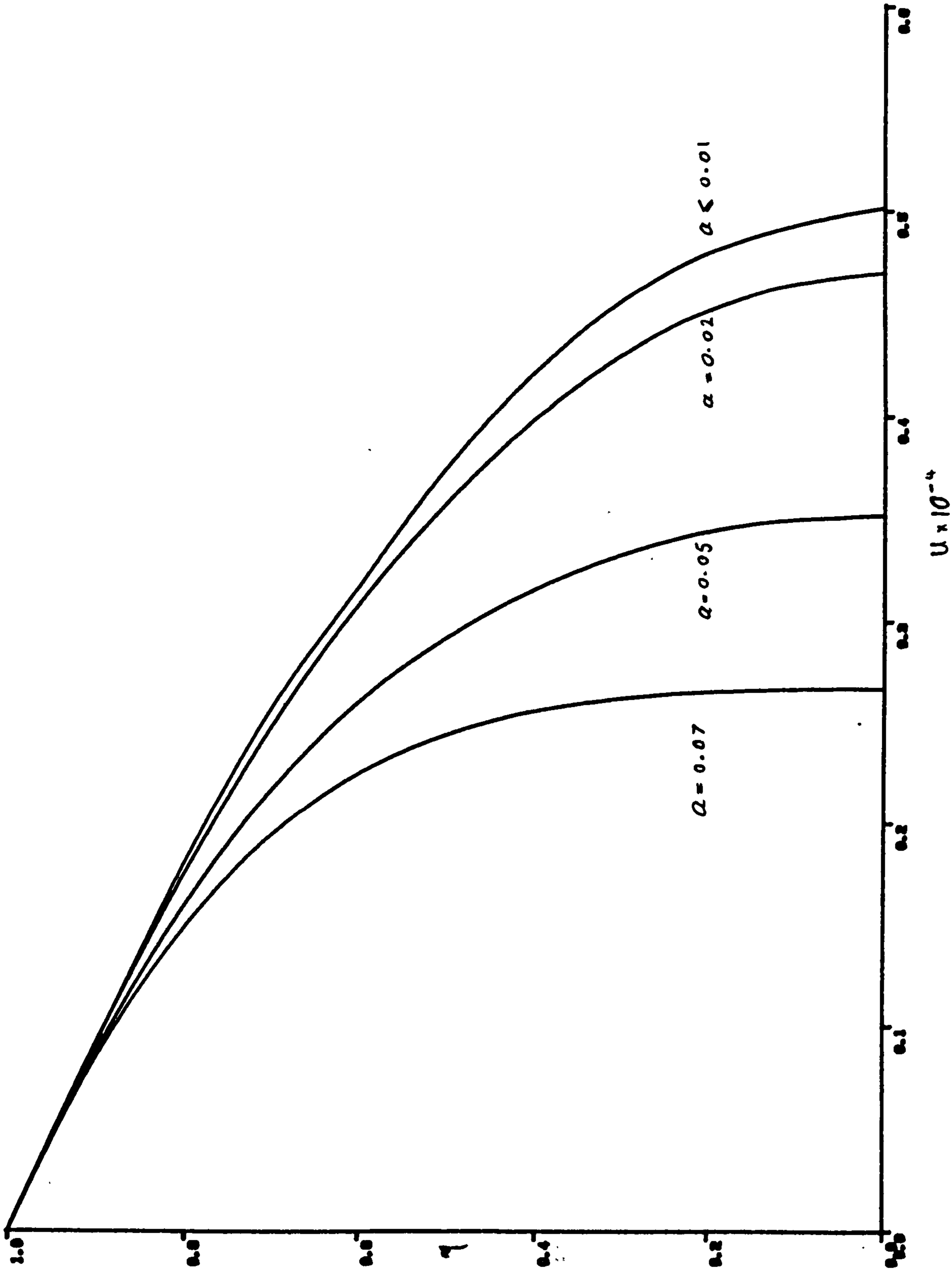

Fig. 3.2 Variation of the mean velocity (eqn. 3.75) with a, for $R=10^4$, $b=5$ and $c=0.1$.

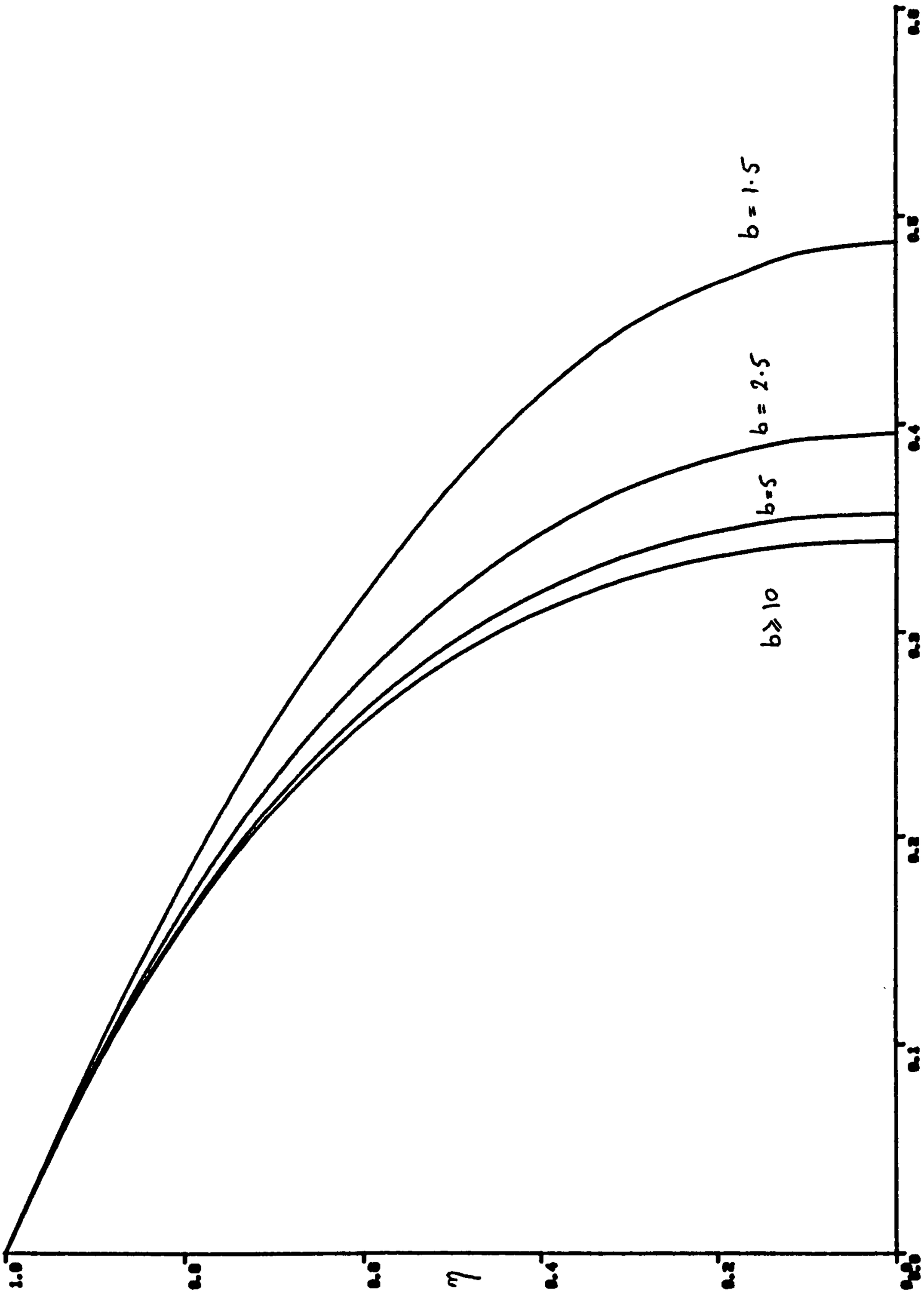

Fig. 3.3 Variation of the mean velocity (eqn. 3.75) with b, for $R=10^5$, $a=0.005$ and $c=1$.

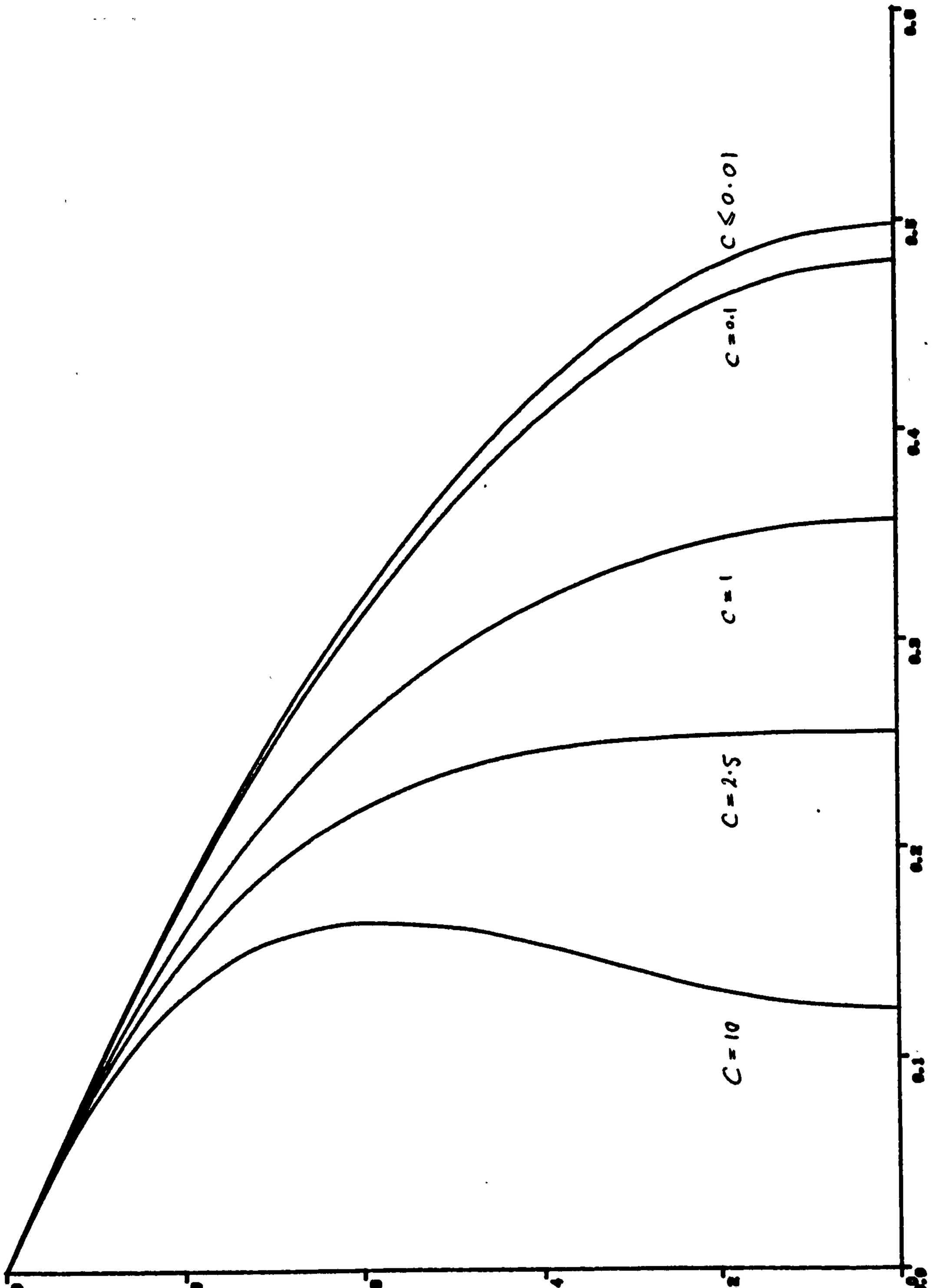

Fig. 3.4 Variation of the mean velocity (eqn. 3.75) with c, for $R=10^5$, $a=0.005$ and $b=5$.

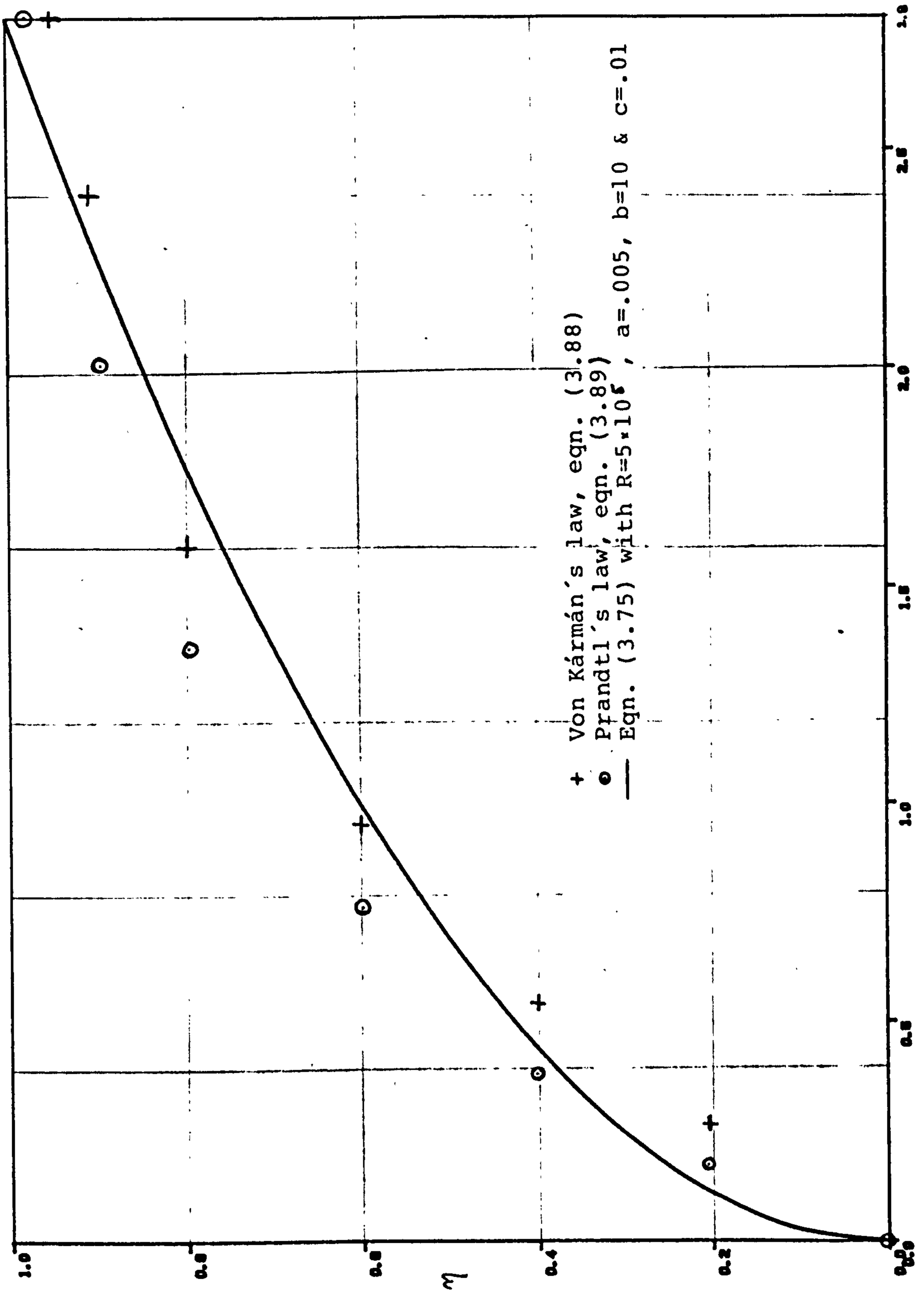

Fig. 3.5 Comparison of eqn. (3.75) with Von Kármán's and Prandtl's velocity distribution laws.

4. FULLY DEVELOPED STEADY POISEUILLE FLOW THROUGH CIRCULAR PIPES.

This type of flow is chosen to examine the model further, for its great practical importance and the many experimental results that are available for comparison.

The governing equations are transformed into cylindrical polar coordinates, and an approximate analytical solution is presented in this chapter.

The method of solving the equations with the aid of the integral transform method and asymptotic expansions is described in detail.

With the appropriate numerical values for the model constants, the predicted mean velocity profiles and the skin friction coefficients, are compared with the results produced by similar models and experiments.

The governing equations and the method of solving the equation of motion for this problem are basically similar to the one discussed in the preceding chapter. Therefore, unless otherwise stated, the definitions and the assumptions made in the previous chapters, remain valid here.

4.1 The governing equations in cylindrical polar coordinates

Let r, θ and z denote the radial, azimuthal and axial coordinates, and u_r, u_θ and u_z denote the components of the mean velocity vector $\underset{\sim}{V}$, in the respective directions.

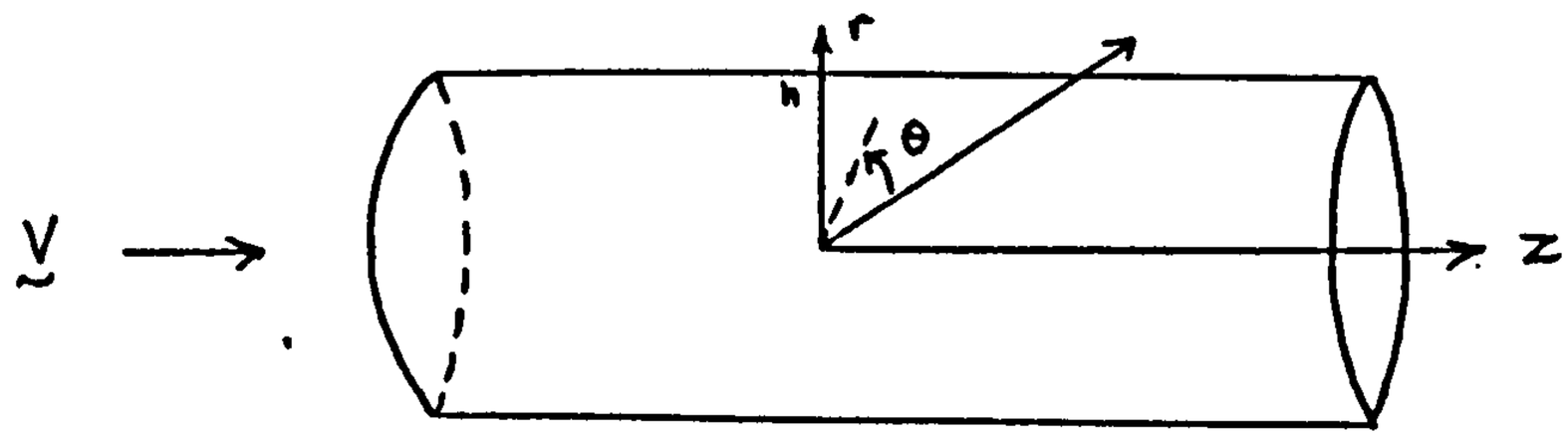

Since, in the Poiseuille flows, the only non-zero velocity component is assumed in the directin of the mean motion and depends on the distance from the wall [see ch.3], we have

$$\underset{\sim}{V} = \{0,0,u(r)\}, \qquad (4.1)$$

where

$$u(r) = u_z(r),$$

and the time-average momentum equation (3.3) can again be used here.

Transforming this equation into cylindrical polar coordinates r, θ and z, by means of the following transformations,

$$x = r\cos\theta\,, \quad y = r\sin\theta\,, \quad z = z,$$

$$x' = r'\cos\theta'\,, \quad y' = r'\sin\theta'\,, \quad z' = z', \qquad (4.2)$$

and $$dx'dy'dz' = r'dr'd\theta'dz',$$

together with (4.1), we obtain

$$\frac{\partial}{\partial r}\left(P/\rho + P_t\right) = 0,$$

$$\frac{1}{r}\frac{\partial}{\partial \theta}\left(P/\rho + P_t\right) = 0,$$

and

$$\frac{\partial}{\partial z}\left(P/\rho + P_t\right) = \nu\left(\frac{\partial^2 u}{\partial r^2} + \frac{1}{r}\frac{\partial u}{\partial r}\right) + \frac{1}{r}\frac{\partial}{\partial r}\left\{\frac{r}{2}\int_{vol} F(\underset{\sim}{r}, \underset{\sim}{r}-\underset{\sim}{r}')\frac{du}{dr'}\, r'dr'd\theta'dz'\right\}. \qquad (4.3)$$

Once again, the weighting function F, represents the correlation between the point $\underset{\sim}{r}$ and any other point $\underset{\sim}{r}'$ within the flow, and may be presented as the product of a shape function F_1 and a position function F_2 [see ch. 2], i.e.

$$F = c_o\, r/r'\, F_1(r)F_2(|\underset{\sim}{r}-\underset{\sim}{r}'|), \qquad (4.4)$$

The shape function varies with r alone, and to meet our requirements, as outlined in chapter two, the following form for F_1 is introduced.

$$F_1(r) = \left[1 - e^{-(h-r)/\lambda} - \frac{h-r}{\lambda} e^{-h/\lambda} \right], \qquad (4.5)$$

where h is the radius of the pipe, λ is a characteristic length scale, and c_o is to be determined experimentally.

The position function is again presented by the Gaussian distribution function (2.12), which in the cylindrical polar coordinates has the form

$$F_2(|\underline{r} - \underline{r}'|) = \exp\left\{ -\frac{1}{2\sigma^2} \left[r^2 + r'^2 - 2rr'\cos(\theta - \theta') + (z - z')^2 \right] \right\}. \qquad (4.6)$$

The reason for introducing the ratio r/r' in the model is that if we have a small volume of fluid at a point A with the coordinates (r', θ', z') and another at point B, at some distance away, with the coordinates (r, θ, z), then the eddies responsible for turbulence at point A would affect the volume of flow at point B, and the correlation between these points is in fact presented by F. Since we are trying to correlate the effects at a distance r with those at r', and if r' is of moderate size and r is small, we are 'packing' the effects in. The 'crowding' is thus in the ratio of the rings, i.e. $2\pi r / 2\pi r'$ or r/r'. This ratio would remove the singularity at r=0, which is the result of the focusing effects of the eddies originating at a radius r' around the centre of the pipe.

The equation (4.3), combined with (4.4), yields

$$\frac{\partial}{\partial z}\left(P/\rho + P_t \right) = \nu\left(\frac{\partial^2 u}{\partial r^2} + \frac{1}{r}\frac{\partial u}{\partial r} \right) + \frac{c_o}{2r}\frac{\partial}{\partial r}\left\{ r^2 F_1(r) \int_{vol} F_2(|\underline{r} - \underline{r}'|) \frac{du}{dr'} dr' d\theta' dz' \right\}. \qquad (4.7)$$

Consider the volume integral on the r.h.s. of the above and denote it by Ω. Then substituting for F_2 from (4.6), we can write

$$\Omega = \int_0^h \exp\left\{ -\frac{1}{2\sigma^2}(r^2 + r'^2) \right\} \frac{du}{dr'} dr' \int_{-\pi}^{\pi} \exp\left\{ \frac{1}{\sigma^2} rr'\cos(\theta - \theta') \right\} d\theta' \cdot \int_{-\infty}^{\infty} \exp\left\{ -\frac{1}{2\sigma^2}(z - z')^2 \right\} dz'. \qquad (4.8)$$

The third integral in the above can easily be evaluated to give

$$\int_{-\infty}^{\infty} \exp\{-\tfrac{1}{2\sigma^2}(z-z')^2\}\, dz' = \sigma\sqrt{(2\pi)}\,. \qquad (4.9)$$

The second integral is more complicated and the method of evaluating it, using the Bessel functions, is described below.

Let $\Omega_2 = \int_{-\pi}^{\pi} \exp\{\tfrac{1}{\sigma^2} rr'\cos(\theta-\theta')\}\, d\theta'$.

If we put $\gamma = rr'/\sigma^2$, then the integrand can be written as

$$\exp\{\gamma\cos(\theta-\theta')\},$$

which is equivalent to

$$\exp\{i[-i\gamma\cos(\theta-\theta')]\}.$$

This can be expressed as a series of Bessel coefficients of order n, $J_n(z)$, using the result

$$e^{iz\cos\phi} = J_0(z) + 2i\cos\phi\, J_1(z) + 2i^2\cos(2\phi)\, J_2(z) + \cdots,$$

[35, P.351]. Thus

$$\exp\{i[-i\gamma\cos(\theta-\theta')] = J_0(-i\gamma) + 2i\cos(\theta-\theta')\, J_1(-i\gamma) + 2i^2\cos[2(\theta-\theta')]\, J_2(-i\gamma) + \cdots.$$

Since the above Bessel coefficients have purely imaginary argument, it is convenient to replace them by the Modified Bessel functions, $I_n(z)$, defined by

$$I_n(z) = i^{-n} J_n(iz) = \sum_{k=0}^{\infty} \frac{(\frac{1}{2}z)^{n+2k}}{k!\,(n+k)!}\,, \qquad (4.10)$$

[35, p. 366]. Thus

$$\exp\{i[-i\gamma\cos(\theta-\theta')]\}$$

$$= I_0(-\gamma) + 2i\cos(\theta-\theta')\, i\, I_1(-\gamma) + 2i^2\cos[2(\theta-\theta')]\, i^2 I_2(-\gamma) + \cdots$$

$$= I_0(-\gamma) + 2\sum_{n=1}^{\infty} i^{2n}\cos[n(\theta-\theta')]\, I_n(-\gamma).$$

Hence

$$\Omega_2 = \int_{-\pi}^{\pi} \{I_0(-\gamma) + 2\sum_{n=1}^{\infty} i^{2n} I_n(-\gamma)\cos[n(\theta-\theta')]\}\, d\theta'.$$

Using the identity

$$\cos[n(\theta-\theta')] \equiv \cos(n\theta)\cos(n\theta') + \sin(n\theta)\sin(n\theta'),$$

we can write

$$\Omega_2 = I_0(-\gamma)\int_{-\pi}^{\pi} d\theta' + 2\sum_{n=1}^{\infty} \epsilon^{2n} I_n(-\gamma)\{\cos(n\theta)\int_{-\pi}^{\pi}\cos(n\theta')\,d\theta' + \sin(n\theta)\int_{-\pi}^{\pi}\sin(n\theta')\,d\theta'\}.$$

But

$$\int_{-\pi}^{\pi}\cos(n\theta')\,d\theta' = 0 \qquad \text{for } n \geq 1,$$

and

$$\int_{-\pi}^{\pi}\sin(n\theta')\,d\theta' = 0 \qquad \text{for all } n.$$

Hence, the second integral reduces to

$$\Omega_2 = 2\pi I_0(-\gamma),$$

where, from (4.10)

$$I_0(-\gamma) = I_0(+\gamma),$$

and

$$\gamma = rr'/\sigma^2.$$

Therefore

$$\Omega_2 = 2\pi I_0(rr'/\sigma^2), \tag{4.11}$$

where

$$I_0(rr'/\sigma^2) = \sum_{k=0}^{\infty}\frac{(rr'/2\sigma^2)^{2k}}{k!^2}. \tag{4.12}$$

Combining (4.9) and (4.11) with (4.8), reduces the volume integral to

$$\Omega = (2\pi)^{3/2}\sigma\int_0^h \exp\{-\tfrac{1}{2\sigma^2}(r^2+r'^2)\}I_0(\tfrac{rr'}{\sigma^2})\frac{du}{dr'}\,dr'. \tag{4.13}$$

Recalling the equation (4.7), since the volume integral is a function of r, then the r.h.s. of this equation is a function of r only, whereas the l.h.s. varies with z alone. So we can write

$$\frac{\partial}{\partial z}(P/\rho + P_t) =$$

$$\nu(\frac{d^2u}{dr^2}+\frac{1}{r}\frac{du}{dr}) + \sqrt{2}\,\pi^{3/2}C_0\sigma\frac{1}{r}\frac{d}{dr}\{r^2F_1(r)\phi(r)\} = K, \tag{4.14}$$

where K is a constant, and

$$\phi(r) = \int_0^h \exp\{-\tfrac{1}{2\sigma^2}(r^2+r'^2)\}I_0(\tfrac{rr'}{\sigma^2})\frac{du}{dr'}\,dr'. \tag{4.15}$$

Note that the partial derivatives have been replaced by total derivatives in (4.14), since u is a function of r

alone.

Multiplying throughout (4.14) by r and integrating once w.r.t. r, yields

$$\nu r\, du/dr + \sqrt{2}\,\pi^{3/2} c_0\, \sigma\, r^2 F_1(r)\, \phi(r) = \tfrac{1}{2} k r^2 + K_0 ,$$

where K_0 is a constant.

Putting r=0 in the above, implies that $K_0=0$, and we can divide throughout this equation by r, to find

$$\nu\, du/dr + \sqrt{2}\,\pi^{3/2} c_0\, \sigma\, r F_1(r)\, \phi(r) = \tfrac{1}{2} k r. \qquad (4.16)$$

This is the equation of motion for the steady Poiseuille turbulent flows through circular pipes, the dimensionless version of which is presented in the following section.

4.2 Equation of motion in non-dimensional form.

Define the dimensionless variables $\hat{u}, \eta, \eta'$, a, b and c, by

$$u = u_0 \hat{u}(\eta), \quad r = h\eta, \quad r' = h\eta',$$
$$h = a\lambda, \quad \sigma = bh, \quad R = u_0 h/\nu, \qquad (4.17)$$
$$K = -2u_0^2/h \quad \text{and} \quad c = \sqrt{2}\,\pi^{3/2} c_0 h^2/u_0,$$

where u_0 is the friction velocity (as defined in chapter 3) and R is the Reynolds number.

If we combine (4.16) with (4.17), we find the dimensionless equation of motion in the form

$$\frac{1}{R}\, d\hat{u}/d\eta + c b \eta\, \hat{F}_1(\eta)\, \hat{\phi}(\eta) = -\eta, \qquad (4.18)$$

where

$$\hat{\phi}(\eta) = \int_0^1 \exp\{-\tfrac{1}{2b^2}(\eta^2+\eta'^2)\}\, I_0(\tfrac{\eta\eta'}{b^2})\, \frac{d\hat{u}}{d\eta'}\, d\eta', \qquad (4.19)$$

and

$$\hat{F}_1(\eta) = 1 - e^{-a(1-\eta)} - a\, e^{-a}.(1-\eta). \qquad (4.20)$$

The boundary conditions for (4.18) are

$$\hat{u}(\eta) = \hat{F}_1(\eta) = 0 \quad \text{at } \eta = 1. \qquad (4.21)$$

4.3 An approximate analytical solution.

To solve the equation (4.18), a similar method as that discussed in section 3.3 may be used here to approximate the products of $\hat{F}_1(\eta)$ and $\hat{\phi}(\eta)$ by a series expansion in powers of η, before performing the integration. Removing the circumflexes for convenience, we multiply throughout (4.18) by

$$R\left[\exp\left\{-\frac{1}{2b^2}(\xi^2+\eta^2)\right\} I_0(\xi\eta/b^2)\, d\eta\right],$$

and integrate from 0 to 1. Thus

$$\phi(\xi) + \varepsilon \int_0^1 \eta\, F_1(\eta)\, \phi(\eta) \exp\left\{-\frac{1}{2b^2}(\xi^2+\eta^2)\right\} I_0(\xi\eta/b^2)\, d\eta$$
$$= -\frac{R}{2}\, g(\xi)\,, \qquad (4.22)$$

where

$$\phi(\xi) = \int_0^1 \exp\left\{-\frac{1}{2b^2}(\xi^2+\eta^2)\right\} I_0(\xi\eta/b^2)\, \frac{du}{d\eta}\, d\eta\,, \qquad (4.23)$$

$$g(\xi) = \int_0^1 \eta \exp\left\{-\frac{1}{2b^2}(\xi^2+\eta^2)\right\} I_0(\xi\eta/b^2)\, d\eta\,. \qquad (4.24)$$

and

$$\varepsilon = Rcb. \qquad (4.25)$$

The equation (4.22) is equivalent to the (3.17) of the preceding chapter, and the chosen method of solving this equation, is again dependent on the size of ε.

The situation in which ε is smaller than the lowest eigen value, may be approached by a similar method we discussed for (3.17), and we shall not go into it any further here. Instead, we shall again concentrate on the more interesting case when ε is large and seek a solution in the form of an asymptotic series.

The Hankel transform, as opposed to the Fourier which was used in the previous case, seems more appropriate for this problem.

Define the Hankel transform pair $\bar{f}_\nu(s)$ and $f_\nu(x)$ by

$$\bar{f}_\nu(s) = \int_0^\infty f_\nu(x)\, J_\nu(xs)\, x\, dx, \qquad (4.26a)$$

and

$$f_\nu(x) = \int_0^\infty \bar{f}_\nu(s)\, J_\nu(xs)\, s\, ds, \quad [23]. \qquad (4.26b)$$

If we extend the definition of $F_1(\eta)$ to the positive real line and put

$$F_1(\eta) = 0 \quad \text{for} \quad \eta \geq 1,$$

then transforming (4.22) in accordance with (4.26a), yields

$$\bar{\phi}(s) + \varepsilon \int_0^\infty d\xi\, J_\nu(\xi s)\, \xi \int_0^\infty \eta\, F_1(\eta)\, \phi(\eta) \exp\{-\tfrac{1}{2b^2}(\xi^2+\eta^2)\} \cdot I_0(\xi\eta/b^2)\, d\eta = -\tfrac{R}{2}\, \bar{g}(s), \qquad (4.27)$$

where

$$\bar{\phi}(s) = \int_0^\infty d\xi\, J_\nu(\xi s)\, \xi \int_0^1 \exp\{-\tfrac{1}{2b^2}(\xi^2+\eta^2) I_0(\tfrac{\xi\eta}{b^2}) \tfrac{du}{d\eta} d\eta, \qquad (4.28)$$

and

$$\bar{g}(s) = \int_0^\infty d\xi\, J_\nu(\xi s)\, \xi \int_0^1 \eta \exp\{-\tfrac{1}{2b^2}(\xi^2+\eta^2) I_0(\tfrac{\xi\eta}{b^2})\, d\eta. \qquad (4.29)$$

The expression for $\bar{g}(s)$ can be presented in a simpler form by using the following result

$$\int_0^\infty e^{-\rho^2 t^2} J_\nu(at)\, J_\nu(bt)\, t\, dt = \tfrac{1}{2\rho^2} \exp\{-\tfrac{1}{4\rho^2}(a^2+b^2)\} I_\nu(ab/2\rho^2), \qquad (4.30)$$

where $\mathrm{Re}(\nu) > -1$ and $|\arg p| < \pi/4$, [34 , p.395].

To apply the above result to the equation (4.29), we need to rewrite it as

$$\bar{g}(s) = \int_0^1 d\eta\, e^{-\eta^2/2b^2} \cdot \eta \int_0^\infty e^{-\xi^2/2b^2} J_\nu(\xi s)\, I_0(\xi\eta/b^2)\, \xi\, d\xi.$$

By putting $\nu = 0$, and using (4.10), the second integral in the above becomes

$$\int_0^\infty e^{-\xi^2/2b^2} J_0(\xi s)\, J_0(i\xi\eta/b^2)\, \xi\, d\xi,$$

and by comparing it to (4.30), can be written as

$$b^2 \exp\{-\tfrac{1}{2} b^2 (s^2 - \tfrac{\eta^2}{b^4})\}\, I_0(is\eta),$$

which is equivalent to

$$b^2 e^{-\frac{1}{2} b^2 s^2} \cdot e^{\eta^2/2b^2}\, J_0(s\eta).$$

Hence

$$\bar{g}(s) = b^2 e^{-\frac{1}{2}b^2 s^2} \int_0^1 \eta J_0(s\eta)\, d\eta.$$

Replacing $J_0(s\eta)$ by its expansion, using

$$J_n(z) = \sum_{k=0}^{\infty} \frac{(-1)^k (\frac{1}{2}z)^{n+2k}}{k!\,(n+k)!} \qquad \text{[35 , p.350],} \quad (4.31)$$

and integrating, we find

$$\bar{g}(s) = \frac{1}{s} b^2 e^{-\frac{1}{2}b^2 s^2} \sum_{k=0}^{\infty} \frac{(-1)^k (\frac{1}{2}s)^{2k+1}}{k!\,(k+1)!}$$

$$= \frac{1}{s} b^2 e^{-\frac{1}{2}b^2 s^2} J_1(s). \qquad (4.32)$$

The second term on the l.h.s. of (4.27) may also be simplified in a similar fashion, by putting $\nu = 0$ and making use of (4.10) and (4.30), to find

$$\varepsilon b^2 e^{-\frac{1}{2}b^2 s^2} \int_0^{\infty} \eta F_1(\eta) \phi(\eta) J_0(s\eta)\, d\eta,$$

or if we put

$$\psi = F_1(\eta)\, \phi(\eta), \qquad (4.33)$$

we have

$$\varepsilon b^2 e^{-\frac{1}{2}b^2 s^2} \bar{\psi}(s), \qquad (4.34)$$

where $\bar{\psi}(s)$ is the Hankel transform of $\psi(\eta)$, according to (4.26a). Hence, the equation (4.27) becomes

$$\bar{\phi}(s) = -\tfrac{1}{2} R\, \bar{g}(s) - \varepsilon b^2 e^{-\frac{1}{2}b^2 s^2} \bar{\psi}(s). \qquad (4.35)$$

To find $\bar{\psi}(s)$, where

$$\bar{\psi}(s) = \int_0^{\infty} \eta J_0(s\eta) F_1(\eta) \phi(\eta)\, d\eta,$$

we use (4.26b) to replace $\phi(\eta)$ by

$$\phi(\eta) = \int_0^{\infty} \bar{\phi}(\sigma) J_0(\eta\sigma)\, \sigma\, d\sigma,$$

so that

$$\bar{\psi}(s) = \int_0^{\infty} d\eta\, \eta\, J_0(s\eta) F_1(\eta) \int_0^{\infty} \bar{\phi}(\sigma) J_0(\eta\sigma)\, \sigma\, d\sigma.$$

If we replace $\bar{\phi}(\sigma)$ in the above by (4.35), we find

$$\bar{\psi}(s) = \int_0^{\infty} d\eta\, \eta\, J_0(s\eta) F_1(\eta) \int_0^{\infty} \left\{ -\tfrac{1}{2} R\, \bar{g}(\sigma) - \varepsilon b^2 e^{-\frac{1}{2}b^2\sigma^2} \bar{\psi}(\sigma) \right\} J_0(\eta\sigma)\, \sigma\, d\sigma.$$

It is convenient to write the above as

$$\bar{\pi}(s) = \bar{f}(s) + \bar{P}(s), \tag{4.36}$$

where

$$\bar{f}(s) = -\frac{R}{2}\int_0^\infty d\eta\, \eta\, J_0(s\eta) F_1(\eta) \int_0^\infty \bar{g}(\sigma) J_0(\eta\sigma)\sigma\, d\sigma, \tag{4.37}$$

and

$$\bar{P}(s) = -\varepsilon b^2 \int_0^\infty d\eta\, \eta\, J_0(s\eta) F_1(\eta) \int_0^\infty e^{-\frac{b^2 s^2}{2}} \bar{\pi}(\sigma) J_0(\eta\sigma)\sigma\, d\sigma. \tag{4.38}$$

To solve (4.36), we once again make the assumption that $b \gg 1$ and look for an asymptotic solution of the form

$$\bar{\pi}(s) \sim b^{\rho} \sum_{t=0}^{\infty} b^{-t} \bar{\pi}_t(s), \tag{4.39}$$

where the constant ρ will be determined in the process. But first, we need to evaluate $\bar{f}(s)$ and $\bar{p}(s)$ in the forms of asymptotic series.

To find $\bar{f}(s)$:

Consider the second integral on the r.h.s. of (4.37) and denote it by I. Replacing $J_0(\eta\sigma)$ and $\bar{g}(\sigma)$ by their series expansions, given by (4.31) and (4.32), respectively, and simplifying, gives

$$\begin{aligned} I &= \int_0^\infty \bar{g}(\sigma) J_0(\eta\sigma)\sigma\, d\sigma, \\ &= b^2 \int_0^\infty \sigma\, e^{-\frac{1}{2}b^2\sigma^2} \sum_{k=0}^{\infty} \frac{(-1)^k \sigma^{2k}}{k!(k+1)!\, 2^{2k+1}} \sum_{j=0}^{\infty} \frac{(-1)^j \eta^{2j} \sigma^{2j}}{j!\, 2^{2j}}\, d\sigma, \\ &= b^2 \int_0^\infty \sigma\, e^{-\frac{1}{2}b^2\sigma^2} \sum_{j=0}^{\infty} \left\{ \sum_{k=0}^{j} \frac{(-1)^k}{k!(k+1)!\, 2^{2k+1}} \frac{(-1)^{j-k} \eta^{2j-2k}}{(j-k)!^2\, 2^{2j-2k}} \right\} \sigma^{2j}\, d\sigma. \\ &= b^2 \int_0^\infty \sum_{j=0}^{\infty} A_j(\eta)\, \sigma^{2j+1} e^{-\frac{1}{2}b^2\sigma^2}\, d\sigma, \end{aligned} \tag{4.40}$$

where

$$A_j(\eta) = \sum_{k=0}^{j} \frac{(-1)^j}{2^{2j+1} k!\,(k+1)!\,(j-k)!^2} \eta^{2j-2k}. \tag{4.41}$$

Applying Watson's Lemma [6] to estimate the above integral for large b, and simplifying, yields

$$I \sim \sum_{j=0}^{\infty} A_j(\eta)\, \Gamma(j+1)\, 2^j\, b^{-2j}.$$

Finally, substituting the above back into (4.37),

together with (4.41), gives

$$\bar{f}(s) \sim -\tfrac{1}{2} R \sum_{j=0}^{\infty} \left\{ \sum_{k=0}^{j} \frac{(-1)^j \Gamma(j+1)\, b^{-2j}}{2^{j+1}\, k!\,(k+1)!\,(j-k)!^2} \int_0^{\infty} J_0(s\eta) F(\eta)\, \eta^{2j-2k+1}\, d\eta \right\}. \tag{4.42}$$

To find $\bar{p}(s)$:

A similar method as the one described above, may be used to find $\bar{p}(s)$ in an asymptotic form.

Let L denote the second integral in (4.38), then

$$L = \int_0^{\infty} e^{-\frac{1}{2} b^2 \sigma^2}\, \bar{\psi}(\sigma)\, J_0(\eta\sigma)\, \sigma\, d\sigma. \tag{4.43}$$

Since

$$\bar{\psi}(\sigma) = \int_0^{\infty} \eta\, J_0(\sigma\eta)\, \psi(\eta)\, d\eta,$$

and

$$J_0(-\sigma\eta) = J_0(\sigma\eta),$$

then $\bar{\psi}(\sigma)$ is an even function, and its Taylor expansion is

$$\bar{\psi}(\sigma) = \sum_{m=0}^{\infty} \frac{1}{(2m)!}\, \bar{\psi}^{(2m)}(0)\, \sigma^{2m}.$$

Replacing $\bar{\psi}$ in (4.43) by the above and J_0 by its series expansion (4.31), gives

$$L = \int_0^{\infty} \sigma\, e^{-\frac{1}{2} b^2 \sigma^2} \sum_{m=0}^{\infty} \frac{\bar{\psi}^{(2m)}(0)\, \sigma^{2m}}{(2m)!} \cdot \sum_{k=0}^{\infty} \frac{(-1)^k\, \eta^{2k}\, \sigma^{2k}}{k!^2\, 2^{2k}}\, d\sigma$$

$$= \int_0^{\infty} \sigma\, e^{-\frac{1}{2} b^2 \sigma^2} \sum_{k=0}^{\infty} \left\{ \sum_{m=0}^{k} \frac{\bar{\psi}^{(2m)}(0)}{(2m)!} \frac{(-1)^{k-m}\, \eta^{2k-2m}}{(k-m)!^2\, 2^{2k-2m}} \right\} \sigma^{2k}\, d\sigma$$

$$= \int_0^{\infty} \sum_{k=0}^{\infty} B_k(\eta)\, \sigma^{2k+1}\, e^{-\frac{1}{2} b^2 \sigma^2}\, d\sigma, \tag{4.44}$$

where

$$B_k(\eta) = \sum_{m=0}^{k} \frac{\bar{\psi}^{(2m)}(0)}{(2m)!} \frac{(-1)^{k-m}}{(k-m)!^2} (\eta/2)^{2k-2m}, \tag{4.45}$$

and from (4.39),

$$\bar{\psi}^{(2m)}(0) = b^{\rho} \sum_{t=0}^{\infty} b^{-t}\, \bar{\psi}_t^{(2m)}(0). \tag{4.46}$$

Using Watson's Lemma again, the integral in (4.44) reduces to

$$L \sim \sum_{k=0}^{\infty} B_k(\eta)\, \Gamma(k+1)\, 2^k\, b^{-2k-2}.$$

Combining the above with (4.38), together with (4.45) and (4.46) an simplifying, we find

$$\bar{P}(s) \sim -\varepsilon \sum_{k=0}^{\infty} \sum_{m=0}^{k} \sum_{t=0}^{\infty} \Gamma(k+1)\, 2^{2m-k}\, b^{-\rho-t-2k}\, \frac{(-1)^{k-m}\, \bar{\psi}_t^{(2m)}(0)}{(k-m)!^2\,(2m)!} \cdot \int_0^{\infty} J_0(s\eta) F_1(\eta) \eta^{2k-2m+1}\, d\eta. \quad (4.47)$$

Having established the asymptotic forms for $\bar{f}$ and $\bar{p}$, we now compare the orders of magnitude of each term in (4.36). From the equations (4.39), (4.42) and (4.47), with $\varepsilon = Rcb$, we get

$$\bar{\psi}(s) = \bar{f}(s) + \bar{p}(s). \quad (4.48)$$

$\bar{\psi}(s)$: $O(b^{\rho})$; $\bar{f}(s)$: $O(1)$; $\bar{p}(s)$: $O(b^{\rho+1})$

Since we must at least have two terms of equal orders in this equation, we choose $\rho = -1$, and the terms in (4.48) become

$$\bar{\psi}(s) \sim b^{-1} \sum_{t=0}^{\infty} b^{-t}\, \bar{\psi}_t(s),$$

$$\bar{f}(s) \sim -R/4 \sum_{j=0}^{\infty} \sum_{k=0}^{j} \frac{(-1)^j \Gamma(j+1)\, b^{-2j}}{2^j\, k!\,(k+1)!\,(j-k)!^2}\, M_{j,k}(s),$$

and

$$\bar{p}(s) \sim -RC \sum_{k=0}^{\infty} \sum_{m=0}^{k} \sum_{t=0}^{\infty} \Gamma(k+1)\, 2^{2m-k}\, b^{-2k-t}\, \frac{(-1)^{k-m}\, \bar{\psi}_t^{(2m)}(0)}{(k-m)!^2\,(2m)!}\, M_{k,m}(s),$$

where

$$M_{m,n}(s) = \int_0^{\infty} J_0(s\eta) F_1(\eta) \eta^{2m-2n+1}\, d\eta. \quad (4.49)$$

Note that

$$M_{m,n}(s) = \bar{F}_1(s) \quad \text{if} \quad m = n. \quad (4.50)$$

The solution we seek is of the form

$$\bar{\psi}(s) \sim b^{-1} \sum_{t=0}^{\infty} b^{-t}\, \bar{\psi}_t(s),$$

and since $b \gg 1$, this can be approximated to

$$\bar{\psi}(s) \sim \frac{1}{b}\, \bar{\psi}_0(s) + \frac{1}{b^2}\, \bar{\psi}_1(s) + \frac{1}{b^3}\, \bar{\psi}_2(s) + O(1/b^4). \quad (4.51)$$

To find $\bar{\psi}_t(s)$, for t = 0 to 2, we can again use the method of successive approximations, by collecting and equating terms of equal orders from either side of (4.48).

If we take terms of O(1), then

$$0 = -\frac{R}{4} M_{0,0}(s) - RC\ \bar{\psi}_0(s) M_{0,0}(s).$$

Hence

$$\bar{\psi}_0(0) = -1/4C. \tag{4.52}$$

Terms of O(1/b), yields

$$\bar{\psi}_0(s) = -RC\ \bar{\psi}_1(0) M_{0,0}(s). \tag{4.53}$$

Putting s=0 in the above and comparing it with (4.52), we have

$$\bar{\psi}_1(0) = 1/4RC^2 M_{0,0}(0), \tag{4.54}$$

and subsequently

$$\bar{\psi}_0(s) = -M_{0,0}(s)/4C M_{0,0}(0). \tag{4.55}$$

Terms of $O(1/b^2)$, gives

$$\bar{\psi}_1(s) = R/8 \cdot M_{1,0}(s) + R/16 \cdot M_{1,1}(s) - RC\bar{\psi}_2(0) M_{0,0}(s)$$
$$+ \tfrac{1}{2} RC\bar{\psi}_0(0) M_{1,0}(s) - RC\bar{\psi}_0^{(1)}(0) M_{1,1}(s).$$

Combining the above with (4.52) and simplifying, yields

$$\bar{\psi}_1(s) = -RC\bar{\psi}_2(0) M_{0,0}(s) + \{R/16 - RC\bar{\psi}_0^{(1)}(0)\} M_{1,1}(s).$$

But from (4.50),

$$M_{0,0}(s) = M_{1,1}(s). \tag{4.56}$$

Hence

$$\bar{\psi}_1(s) = \{-RC\bar{\psi}_2(0) + R/16 - RC\bar{\psi}_0^{(1)}(0)\} M_{0,0}(s). \tag{4.57}$$

Differentiating (4.53) twice and putting s=0, gives

$$\bar{\psi}_0^{(1)}(0) = -RC\bar{\psi}_1(0) M_{0,0}^{(1)}(0).$$

Substituting the above in (4.57), together with (4.54), gives

$$\bar{\psi}_1(s) = \{-RC\bar{\psi}_2(0) + R/16 + R/4 \frac{M_{0,0}^{(1)}(0)}{M_{0,0}(0)}\} M_{0,0}(s). \tag{4.58}$$

If we now put s=0 in this equation and compare it with (4.54), we have

$$\bar{\psi}_2(0) = 1/4C \left\{ \frac{-1}{R^2C^2 M_{0,0}^2(0)} + \frac{1}{4} + \frac{M_{0,0}^{(1)}(0)}{M_{0,0}(0)} \right\}. \tag{4.59}$$

Finally, substituting the above back in (4.58) and simplifying, yields

$$\bar{\psi}_1(s) = \frac{1}{4RC^2}\,\frac{M_{0,0}(s)}{M_{0,0}^2(0)} \quad . \tag{4.60}$$

Terms of $O(1/b^3)$, yields

$$\bar{\psi}_2(s) = -RC\,\bar{\psi}_3(0)M_{0,0}(s) + \tfrac{1}{2}RC\,\bar{\psi}_1(0)M_{1,0}(s) - RC\,\bar{\psi}_1^{(2)}(0)M_{1,1}(s) \tag{4.61}$$

Combining the above with (4.54) and (4.60), together with (4.56), gives

$$\bar{\psi}_2(s) = -RC\,\bar{\psi}_3(0)M_{0,0}(s) + \frac{1}{8C}\,\frac{M_{1,0}(s)}{M_{0,0}(0)} - \frac{1}{4C}\,\frac{M_{0,0}^{(2)}(0)}{M_{0,0}^2(0)}\,M_{0,0}(s).$$

If we again put s=0 in this equation and compare it with (4.59), we get

$$-RC\,\bar{\psi}_3(0) = -\frac{1}{4R^2C^3M_{0,0}^3(0)} + \frac{1}{16C\,M_{0,0}(0)} + \frac{M_{0,0}^{(2)}(0)}{2C\,M_{0,0}^2(0)} - \frac{M_{1,0}(0)}{8C\,M_{0,0}^2(0)}.$$

Finally, combining the above with (4.61), yields

$$\bar{\psi}_2(s) = \frac{1}{4C\,M_{0,0}(0)}\left\{\frac{-1}{R^2C^2M_{0,0}^2(0)} + \frac{1}{4} - \frac{M_{1,0}(0)}{2M_{0,0}(0)} + \frac{M_{0,0}^{(2)}(0)}{M_{0,0}(0)}\right\}M_{0,0}(s) + \frac{M_{1,0}(s)}{8C\,M_{0,0}(0)}. \tag{4.62}$$

It now remains to evaluate $M_{m,n}(s)$; m,n = 0 and 1, and their derivatives, which appear in the expressions for $\bar{\psi}_t$; t=0,1 and 2.

Consider

$$M_{m,n}(s) = \int_0^\infty J_0(s\eta)\,F_1(\eta)\,\eta^{2m-2n+1}\,d\eta,$$

where

$$F_1(\eta) = 1 - e^{-a(1-\eta)} - ae^{-a}.(1-\eta).$$

From the equations (4.26a) and (4.50), we have

$$M_{0,0}(s) = M_{1,1}(s) = \bar{F}_1(s).$$

Hence

$$\bar{F}_1(s) = \int_0^\infty J_0(s\eta)\,F_1(\eta)\,\eta\,d\eta = \int_0^1 J_0(s\eta)\,F_1(\eta)\,\eta\,d\eta,$$

since $F_1(\eta) = 0$ for $\eta \geq 1$.

Substituting for $F_1(\eta)$ from the above, and for $J_0(s\eta)$ from (4.31), gives

$$\bar{F}_1(s) = \sum_{k=0}^{\infty}\frac{(-1)^k\,s^{2k}}{k!^2\,2^{2k}}\int_0^1\left\{1 - e^{-a(1-\eta)} - ae^{-a}(1-\eta)\right\}\eta^{2k+1}\,d\eta.$$

Therefore

$$\bar{F}_1(s) = M_{0,0}(s) = M_{1,1}(s) =$$

$$= \sum_{k=0}^{\infty} \frac{(-1)^k s^{2k}}{k!^2\, 2^{2k}} \left\{ \frac{1 - a e^{-a}}{2k+2} + \frac{a e^{-a}}{2k+3} - \sum_{r=0}^{2k+1} \sum_{n=0}^{\infty} \frac{(-1)^{r+n} (2k+1)!\, a^n}{(2k+1-r)!\, r!\, (n+r+1)\, n!} \right\} \quad (4.63)$$

The method of evaluation of the above integral is presented in the appendix A4.

Putting s=0 in (4.63), yields

$$M_{0,0}(0) = M_{1,1}(0) = \frac{1}{2}(1 - a e^{-a}) + \frac{1}{3} a e^{-a} - \sum_{r=0}^{1} \sum_{n=0}^{\infty} \frac{(-1)^{r+n} a^n}{(1-r)!\, r!\, (n+r+1)\, n!}$$

$$= \frac{1}{2} - \frac{1}{6} a e^{-a} - \sum_{n=0}^{\infty} \frac{(-1)^n a^n}{n!} \left[\frac{1}{n+1} - \frac{1}{n+2} \right]$$

$$= \frac{1}{2} - \frac{1}{6} a e^{-a} - \sum_{n=0}^{\infty} \frac{(-1)^n a^n}{(n+2)!} .$$

The above equation can be written as

$$M_{0,0}(0) = M_{1,1}(0) = \frac{1}{2} - \frac{1}{6} a e^{-a} - \frac{1}{a^2}(e^{-a} - 1 + a) . \quad (4.64)$$

Now consider

$$M_{1,0}(s) = \int_0^1 J_0(s\eta) F_1(\eta) \eta^3 \, d\eta .$$

A similar technique as the one used in evaluating $M_{0,0}(s)$, is again applied here, to find

$$M_{1,0}(s) = \sum_{k=0}^{\infty} \frac{(-1)^k s^{2k}}{k!^2\, 2^{2k}} \left\{ \frac{1 - a e^{-a}}{2k+4} + \frac{a e^{-a}}{2k+5} - \sum_{r=0}^{2k+3} \sum_{n=0}^{\infty} \frac{(-1)^{r+n} (2k+3)!\, a^n}{(2k+3-r)!\, r!\, (n+r+1)\, n!} \right\} \quad (4.65)$$

Putting s=0 in the above, yields

$$M_{1,0}(0) = \frac{1}{4}(1 - a e^{-a}) + \frac{1}{5} a e^{-a} - \sum_{r=0}^{3} \sum_{n=0}^{\infty} \frac{(-1)^{r+n} 3!\, a^n}{(3-r)!\, r!\, (n+r+1)\, n!} \quad (4.66)$$

$$= \frac{1}{4} - \frac{1}{20} a e^{-a} - \sum_{n=0}^{\infty} \frac{(-1)^n a^n}{n!} \left[\frac{1}{n+1} - \frac{3}{n+2} + \frac{3}{n+3} - \frac{1}{n+4} \right]$$

$$= \frac{1}{4} - \frac{1}{20} a e^{-a} - 6 \sum_{n=0}^{\infty} \frac{(-1)^n a^n}{(n+4)!} .$$

We can write the above as

$$M_{1,0} = \frac{1}{4} - \frac{1}{20} a e^{-a} - \frac{6}{a^4}\left(e^{-a} - 1 + a - \frac{1}{2!} a^2 + \frac{1}{3!} a^3\right) . \quad (4.67)$$

Finally, to find $M_{0,0}^{(2)}(0)$, we differentiate (4.63) twice and put s=0. Hence

$$M_{0,0}^{(2)}(0) = -\frac{1}{2} \left\{ \frac{1}{4}(1 - a e^{-a}) + \frac{1}{5} a e^{-a} - \sum_{r=0}^{3} \sum_{n=0}^{\infty} \frac{(-1)^{r+n} 3!\, a^n}{(3-r)!\, r!\, (n+r+1)\, n!} \right\} .$$

Comparing the above with (4.66), we can write

$$M_{0,0}^{(2)}(0) = -\tfrac{1}{2} M_{1,0}(0), \qquad (4.68)$$

and the equation (4.62) reduces to

$$\bar{\psi}_2(s) = \frac{1}{4c\, M_{0,0}(0)}\left\{\frac{-1}{R^2c^2 M_{0,0}^2(0)} + \frac{1}{4} - \frac{M_{1,0}(0)}{M_{0,0}(0)}\right\} M_{0,0}(s) + \frac{M_{1,0}(s)}{8c\, M_{0,0}(0)} .$$

At this point let us put

$$M_0 = M_{0,0}(0) \quad \text{and} \quad M_1 = M_{1,0}(0) ,$$

for convenience.

With the expressions we obtained above for $\bar{\psi}_t$; t=0,1 and 2, the equation (4.51) becomes

$$\bar{\psi}(s) \sim \left(\frac{A_0}{b} + \frac{A_1}{b^2} + \frac{A_2}{b^3}\right) M_{0,0}(s) + \frac{A_3}{b^3} M_{1,0}(s) , \qquad (4.69)$$

where

$$A_0 = \frac{-1}{4c\, M_0} , \qquad A_1 = \frac{1}{4Rc^2 M_0^2} ,$$

$$A_2 = \frac{1}{4c\, M_0}\left[\frac{-1}{R^2c^2 M_0^2} + \frac{1}{4} - \frac{M_1}{M_0}\right] , \qquad (4.70)$$

and

$$A_3 = \frac{1}{8c\, M_0} .$$

Note that $A_3 = -A_0/2$.

Returning to (4.35) and substituting (4.69) in this equation, we find

$$\bar{\phi}(s) \sim -\tfrac{1}{2} R\bar{q}(s) - \varepsilon b^2 e^{-\frac{1}{2}b^2s^2}\left\{\left(\frac{A_0}{b} + \frac{A_1}{b^2} + \frac{A_2}{b^3}\right) M_{0,0}(s) - \frac{A_0}{2b^3} M_{1,0}(s)\right\} .$$

Combining the above with (4.32), (4.63) and (4.65), together with (4.25), yields

$$\bar{\phi}(s) \sim -\tfrac{1}{2} R b^2 e^{-\frac{1}{2}b^2s^2} \sum_{j=0}^{\infty} \frac{(-1)^j s^{2j}}{2^{2j+1} j!\,(j+1)!}$$

$$- Rce^{-\frac{1}{2}b^2s^2} \sum_{k=0}^{\infty} \frac{(-1)^k s^{2k}}{k!^2\, 2^{2k}}\left\{(A_0b^2 + A_1b + A_2)E_k - \tfrac{1}{2}A_0 E_{k+1}\right\}, \qquad (4.71)$$

where

$$E_k = \frac{1-ae^{-a}}{2k+1} + \frac{ae^{-a}}{2k+3} - \sum_{r=0}^{2k+1}\sum_{n=0}^{\infty} \frac{(-1)^{r+n}(2k+1)!\, a^n}{(2k+1-r)!\, r!\,(n+r+1)\, n!} . \qquad (4.72)$$

Note that

$$E_0 = M_0 \quad \& \quad E_1 = M_1 . \qquad (4.73)$$

We can now find $\phi(\eta)$, by taking the inverse Hankel

Transform according to (4.26b). i.e.

$$\phi(\eta) = \int_0^\infty J_0(\eta s)\, \bar{\phi}(s)\, s\, ds .$$

Hence

$$\phi(\eta) = -\tfrac{1}{4} R b^2 \sum_{j=0}^{\infty} \frac{(-1)^j}{2^{2j}\, j!\,(j+1)!} \int_0^\infty J_0(\eta s)\, e^{-\frac{1}{2}b^2 s^2}\, s^{2j+1}\, ds$$

$$- Rc \sum_{k=0}^{\infty} \frac{(-1)^k}{k!^2\, 2^{2k}} \{(A_0 b^2 + A_1 b + A_2) E_k - \tfrac{1}{2} A_0 E_{k+1}\} \int_0^\infty J_0(\eta s) e^{-\frac{b^2 s^2}{2}} s^{2k+1} \, ds . \qquad (4.74)$$

To evaluate the integrals in the above, let

$$I = \int_0^\infty J_0(s\eta)\, e^{-\frac{1}{2}b^2 s^2}\, s^{2j+1}\, ds ,$$

and put $\eta s = \zeta$, so that $ds = \frac{1}{\eta} d\zeta$.

Then

$$I = \int_0^\infty J_0(\zeta)\, e^{-\frac{1}{2\eta^2} b^2 \zeta^2} \left(\frac{\zeta}{\eta}\right)^{2j+1} \frac{d\zeta}{\eta} = \frac{1}{\eta^{2j+2}} \int_0^\infty \zeta^{2j+1} J_0(\zeta)\, e^{-\frac{b^2\zeta^2}{2\eta^2}} d\zeta .$$

To evaluate this integral, the following result can be used.

$$\int_0^\infty t^{\mu-1} J_\nu(t)\, e^{-s^2 t^2} dt = \frac{\Gamma\{\frac{1}{2}(\nu+\mu)\}}{2^{\nu+1}\, s^{\mu+\nu}}\, {}_1F_1\left(\frac{\mu+\nu}{2}\,;\, \nu+1\,;\, \frac{-1}{4s^2}\right),$$

where

$$\mathrm{Re}(\mu+\nu) > 0 \quad \text{and} \quad |\arg s| < \pi/4 \qquad [31,\ p.173],$$

and ${}_1F_1$ is the confluent hypergeometric function [31, p.112].

Comparing our integral with the above, we find

$$I = \frac{2^j \Gamma(j+1)}{b^{2j+2}}\, {}_1F_1(j+1\,;\,1\,;\,-\eta^2/2b^2), \qquad (4.75)$$

where

$${}_1F_1(j+1\,;\,1\,;\,-\eta^2/2b^2) = \frac{1}{\Gamma(j+1)} \sum_{i=0}^{\infty} \frac{\Gamma(i+j+1)}{\Gamma(i+1)\, i!} (-\eta^2/2b^2)^i . \qquad (4.76)$$

Combining (4.74) and (4.75) and simplifying, yields

$$\phi(\eta) = -\frac{R}{4} \sum_{j=0}^{\infty} \frac{(-1)^j}{2^j\,(j+1)!\, b^{2j}}\, {}_1F_1(j+1\,;\,1\,;\,-\eta^2/2b^2)$$

$$- Rc \sum_{k=0}^{\infty} \frac{(-1)^k}{k!\, 2^k} \left\{\left(\frac{A_0}{b^{2k}} + \frac{A_1}{b^{2k+1}} + \frac{A_2}{b^{2k+2}}\right) E_k - \frac{A_0}{2b^{2k+2}} E_{k+1}\right\} {}_1F_1(k+1;1;-\eta^2/2b^2) \qquad (4.77)$$

To be consistent with the assumption we made at the beginning of the analysis, we shall ignore terms of $O(1/b^4)$

and smaller in the above equation and approximate it to

$$\phi(\eta) \approx -\frac{R}{4}\left\{{}_1F_1(1;1;-\eta^2/2b^2) - \frac{1}{4b^2}\,{}_1F_1(2;1;-\eta^2/2b^2)\right\}$$

$$-Rc\left\{(A_0 + A_1/b + A_2/b^2)E_0 - A_0/2b^2\,E_1\right\}{}_1F_1(1;1;-\eta^2/2b^2)$$

$$+\tfrac{1}{2}Rc\left\{(A_0/b^2 + A_1/b^3)E_1\right\}{}_1F_1(2;1;-\eta^2/2b^2) + O(1/b^4). \quad (4.78)$$

Recalling the equation (4.76), we can approximate this equation to the same order, so that

$${}_1F_1(1;1;-\eta^2/2b^2) = \sum_{i=0}^{\infty}\frac{1}{i!}(-\eta^2/2b^2)^i \approx 1 - \eta^2/2b^2 + O(1/b^4),$$

and

$${}_1F_1(2;1;-\eta^2/2b^2) = \sum_{i=0}^{\infty}\frac{\Gamma(i+2)}{\Gamma(i+1)\,i!}(-\eta^2/2b^2)^i \approx 1 - \eta^2/b^2 + O(1/b^4).$$

Combining these equations with (4.78) and simplifying, yields

$$\phi(\eta) \approx -R\left\{\frac{1}{4} - \frac{1}{16b^2} + c\left(A_0 + \frac{A_1}{b} + \frac{A_2}{b^2}\right)E_0 - c\,\frac{A_0}{b^2}E_1 - c\,\frac{A_1}{2b^3}E_1\right\}$$

$$+R\left\{\frac{1}{8b^2} + \frac{c}{2}\left(\frac{A_0}{b^2} + \frac{A_1}{b^3}\right)E_0\right\}\eta^2 + O(1/b^4). \quad (4.79)$$

where $E_0 = M_0$ and $E_1 = M_1$ [see (4.73)].

If we substitute for E_0 and E_1 from the above, and for A_0, A_1 and A_2 from (4.70), the equation (4.79) simplifies to

$$\phi(\eta) \approx -\frac{1}{4bcM_0}\left\{1 - \frac{1}{RbcM_0} - \frac{M_1}{2b^2M_0}\right\} + \frac{\eta^2}{8cb^3M_0}. \quad (4.80)$$

This equation can now be substituted back into the equation of motion (4.18), which together with (4.20) becomes

$$dU/d\eta = -R\eta + \left\{(1 - ae^{-a}) + ae^{-a}\eta - e^{-a(1-\eta)}\right\}\left\{\alpha\eta + \beta\eta^3\right\} + O(\tfrac{1}{b}), \quad (4.81)$$

where

$$\alpha = \frac{1}{4M_0}\left\{R - \frac{1}{bcM_0} - \frac{RM_1}{2b^2M_0}\right\},$$

$$\beta = -\frac{R}{8b^2M_0^2},$$

and M_0 and M_1 are given by (4.64) and (4.67), respectively.

To find the mean velocity u, we simply integrate (4.81) once w.r.t. η, to give

$$u = -\frac{R}{2}\eta^2 + \frac{1}{2}\alpha(1-ae^{-a})\eta^2 + \frac{1}{3}\alpha a e^{-a}\eta^3$$

$$-\alpha\left\{\frac{1}{a}\eta e^{-a(1-\eta)} - \frac{1}{a^2}e^{-a(1-\eta)}\right\} + \frac{1}{4}\beta(1-ae^{-a})\eta^4$$

$$+\frac{1}{5}\beta a e^{-a}\eta^5 - \beta\left\{\frac{1}{a}\eta^3 e^{-a(1-\eta)} - \frac{3}{a^2}\eta^2 e^{-a(1-\eta)} + 6\left(\frac{\eta}{a^3} - \frac{1}{a^4}\right)e^{-a(1-\eta)}\right\} + K,$$

where K is a constant of integration. To determine K, we use the boundary condition u=0 at $\eta=1$, to find

$$K = \frac{R}{2} - \frac{\alpha}{2}(1-ae^{-a}) - \frac{\alpha}{3}ae^{-a} + \alpha\left(\frac{1}{a} - \frac{1}{a^2}\right)$$

$$-\frac{\beta}{4}(1-ae^{-a}) - \frac{\beta}{5}ae^{-a} + \beta\left(\frac{1}{a} - \frac{3}{a^2} + \frac{6}{a^3} - \frac{6}{a^4}\right).$$

Hence, the final solution for the mean velocity in the steady turbulent Poiseuille flows through circular pipes, has the form

$$u = \frac{R}{2}(1-\eta^2)$$

$$-\alpha\left\{\frac{1}{2}(1-ae^{-a})(1-\eta^2) + \frac{1}{3}ae^{-a}(1-\eta^3)\right.$$

$$\left. -\frac{1}{a}[1-\eta e^{-a(1-\eta)}] + \frac{1}{a^2}[1-e^{-a(1-\eta)}]\right\}$$

$$-\beta\left\{\frac{1}{4}(1-ae^{-a})(1-\eta^4) + \frac{1}{5}ae^{-a}(1-\eta^5) - \frac{1}{a}[1-\eta^3 e^{-a(1-\eta)}]\right.$$

$$+\frac{3}{a^2}[1-\eta^2 e^{-a(1-\eta)}] - \frac{6}{a^3}[1-\eta e^{-a(1-\eta)}] \qquad (4.82)$$

where $\left. +\frac{6}{a^4}[1-e^{-a(1-\eta)}]\right\}$,

$$\alpha = \frac{1}{4M_0}\left\{R - \frac{1}{bcM_0} - \frac{RM_1}{2b^2M_0}\right\}, \qquad \beta = -\frac{R}{8b^2M_0^2},$$

$$M_0 = \frac{1}{2} - \frac{1}{6}ae^{-a} - \frac{1}{a^2}(e^{-a} - 1 + a),$$

and

$$M_1 = \frac{1}{4} - \frac{1}{20}ae^{-a} - \frac{6}{a^4}\left(e^{-a} - 1 + a - \frac{a^2}{2!} + \frac{a^3}{3!}\right).$$

The approximate analytical solution presented above, includes the laminar solution as well as the terms representing turbulence effects. The laminar profiles emerges when the tubulent effects are small, i.e. when a and b both tend to infinity in (4.82), in which case

$$\alpha \longrightarrow R/2 \quad \text{and} \quad \beta \longrightarrow 0 \quad \text{as} \quad a \text{ and } b \longrightarrow \infty \ ,$$

and hence

$$u = \frac{R}{2}(1-\eta^2) - \frac{R}{4}(1-\eta^2) = \frac{R}{4}(1-\eta^2) \ ,$$

which is the velocity distribution in the laminar Poiseuille pipe flows [29]. The remaining terms in (4.82) are expected to illustrate the effects of turbulence on the velocity profiles. These effects which were discussed in the previous chapter, depend largely on the Reynolds number and the model constants a, b and c. In the next section, we discuss how these constants may be determined.

4.4 Determination of the model constants.

The same strategy as the one described in section 3.4, may be used here to fit a set of numerical values to the model constants. So once again we need to choose some initial values for our parameters, and then by observing the plots of the velocity curves, try to arrive at the optimum values for the constants.

To assist us with choosing the initial values, the equation (4.82) was examined as a and b approached their extreme values, in order to see how they may be related to one another. But unlike the case we discussed in the chapter three [see (3.84) and (3.87)], the constants here did not appear to be dependant on each other or the Reynolds number. The reason for this is that although the equations (3.75)

and (4.82) are similar, the model constants and the Reynolds number appear in different orders in each eqution, partly due to the difference in the shape functions used in each case.

In view of this situation, it seems that the best choice for the starting values would be those which have produced satisfactory results in the previous case.

Before examining our solution with such values, let us look at the coefficient of resistance for smooth pipes and its relation to the velocity distribution in turbulent flows. Such relationship can further assist us with choosing the model constants.

4.5 The coefficient of resistance in smooth pipes.

The frictional resistance in smooth pipes has been the subject of numerous investigations, both theoretically and experimentally, since the beginning of this century. Among the first to establish an empirical formula for the dimensionless coefficient of resistance λ, in fully developed turbulent pipe flows was Blasius, who in 1911 discovered that this coefficient is related to the Reynolds number, in the form

$$\lambda = 0.3164\, R_e^{-1/4} \qquad \text{[29, p.561]}, \qquad (4.83)$$

where $R_e = \tilde{u}d/\nu$ is the Reynolds number in which $\tilde{u}$ is the mean velocity over the cross-sectional area and d is the diameter of the pipe. The experimental values obtained by Nikuradse, shows that this formula produces accurate results up to $R=10^5$.

The relationship between the coefficient of resistance and the mean velocity profile can be obtained by considering

the balance of forces due to the sum of the laminar and turbulent shearing stresses on the circumference and the pressure difference on the end faces of the pipe. This relationship is

$$\lambda = 8(u_*/\alpha)^2 \qquad \text{[29, p.573]}, \qquad (4.84)$$

where u_* is the friction velocity.

If the logarithmic mean velocity distribution law is combined with the above, we obtain the Prandtl's universal law of friction for smooth pipes as

$$1/\sqrt{\lambda} = 2\log(R_*\sqrt{\lambda}) - 0.8 , \qquad \text{[29, pp.572-575]}. \qquad (4.85)$$

We shall now try to arrive at a similar relationship by using the velocity distribution given by (4.82) instead of the logarithmic law, to see how it compares with the Prandtl and the Blasius equations.

The mean velocity of flow $\tilde{u}$, over the cross-sectional area is given by

$$\tilde{u} = \frac{1}{\pi}\int_0^1 2\pi\eta\, u\, d\eta .$$

On substituting for u in the above from (4.82), integrating and simplifying, we obtain

$$\tilde{u} = \frac{R}{4} - \alpha G_1 - \beta G_2 , \qquad (4.86)$$

where

$$G_1 = \frac{1}{4} - \frac{1}{20}a e^{-a} - \frac{1}{a} + \frac{3}{a^2} - \frac{2}{a^3} + \frac{2}{a^4}(1 - e^{-a}) ,$$

and

$$G_2 = \frac{1}{6} - \frac{1}{42}a e^{-a} - \frac{1}{a} + \frac{5}{a^2} - \frac{20}{a^3} + \frac{60}{a^4} - \frac{120}{a^5} + \frac{120}{a^6}(1 - e^{-a}).$$

The Reynolds number R, in (4.86) which is formed by the friction velocity u_*, and the pipe radius h, may be rearranged as shown below.

$$R = \frac{u_* h}{\nu} = \frac{1}{2}\frac{u_*}{\tilde{u}}\frac{\tilde{u} d}{\nu} = \frac{1}{2}\frac{u_*}{\tilde{u}} R_* ,$$

where

$$R_o = \frac{\tilde{u}\, d}{\nu} .$$

But from (4.84)

$$\frac{u_o}{\tilde{u}} = \frac{1}{2\sqrt{2}} \sqrt{\lambda} .$$

Thus

$$R = \frac{\sqrt{\lambda}}{4\sqrt{2}} R_o , \qquad (4.87)$$

and (4.86) becomes

$$\frac{2\sqrt{2}}{\sqrt{\lambda}} = \frac{R_o \sqrt{\lambda}}{16\sqrt{2}} - \alpha G_1 - \beta G_2 , \qquad (4.88)$$

where

$$\alpha = \frac{R_o \sqrt{\lambda}}{4\sqrt{2}} \left\{ \frac{1}{4M_o} - \frac{\sqrt{2}}{R_o \sqrt{\lambda}\, b c\, M_o^2} - \frac{M_1}{8 b^2 M_o^2} \right\} ,$$

and

$$\beta = - \frac{R_o \sqrt{\lambda}}{32\sqrt{2}\, b^2 M_o} .$$

Finally, combining the above expressions for α and β with (4.88), and simplifying, we find

$$\frac{1}{\sqrt{\lambda}} = \alpha_o R_o \sqrt{\lambda} + \beta_o , \qquad (4.89)$$

where

$$\alpha_o = \frac{1}{64} \left[1 - \left(\frac{1}{M_o} - \frac{M_1}{2 b^2 M_o^2} \right) G_1 - \frac{G_2}{2 b^2 M_o} \right] ,$$

and

$$\beta_o = \frac{G_1}{8\sqrt{2}\, b c M_o^2} .$$

The above relationship is compared with the Prandtl's universal law of friction (4.85), for Reynolds numbers ranging from 10^3 to 2×10^4 (Fig. 4.1a), and 5×10^5 to 10^7 (Fig. 4.1b). The agreement appears to be fairly good, considering we are comparing a logarithmic relationship with an asymptotic one.

4.6 RESULTS AND DISCUSSION

In comparing the frictional resistance (eqn. 4.89) with the Prandtl's formula, we found values of α_* and β_*, for which the best least square fit was obtained. These values are shown in figures 4.1a and 4.1b for various values of the Reynolds number. To assign numerical values to the model constants, we look for values of a, b and c, such that

$$2.582\times10^{-6} < \alpha_* < 6.925\times10^{-4} \quad \text{and} \quad 4.197 < \beta_* < 8.995 \ .$$

One set of values which satisfies the above constraints, is a=2.6315, b=8 and c=0.009, and it gives $\alpha_*=2.945\times10^{-5}$ and $\beta_*=5.525$.

In figure 4.2, the solution (4.82) is examined with such values for Reynolds numbers ranging from 10^3 to 10^7. The same effects which were observed in the study of Poiseuille channel flow in the previous chapter are also noted here: The velocity profiles become fuller with the increase in the Reynolds number.

The effects of the variations in a, b and c on the profiles are shown by figures 4.3, 4.4 and 4.5 respectively. It appears that the solution is most sensitive to small changes in these parameters when they are of small order of magnitude.

Comparison with the Von Kármán's and Prandtl's Universal velocity distributions for smooth pipes (eqns. 4.90 & 4.91) and with experimental results, is made in figure 4.6 .

The agreement appears to be fairly good in the middle parts of the pipe. But as the boundary is approached our profile seems to deviate from the universal profiles. However, we note that at the boundary where the universal laws can not describe the velocity, our profile is capable

of determining the velocity there.

$$\frac{u_{max} - u}{u_*} = -\frac{1}{\varkappa}\{\ln[1-\sqrt{(1-y/h)}] + \sqrt{(1-y/h)}\}, \qquad (4.90)$$

$$\frac{u_{max} - u}{u_*} = 5.75 \log(h/y), \qquad (4.91)$$

where y is measured from the wall, h is the radius of the pipe, u_* is the frictional velocity and the dimensionless constant $\varkappa$ is determined from experiment. The maximum velocity u_{max} is the velocity at the centre of the pipe, [29, pp.570-571].

Note that in figure 4.6, the wall distance y/h (= η), is measured from the centre of the pipe.

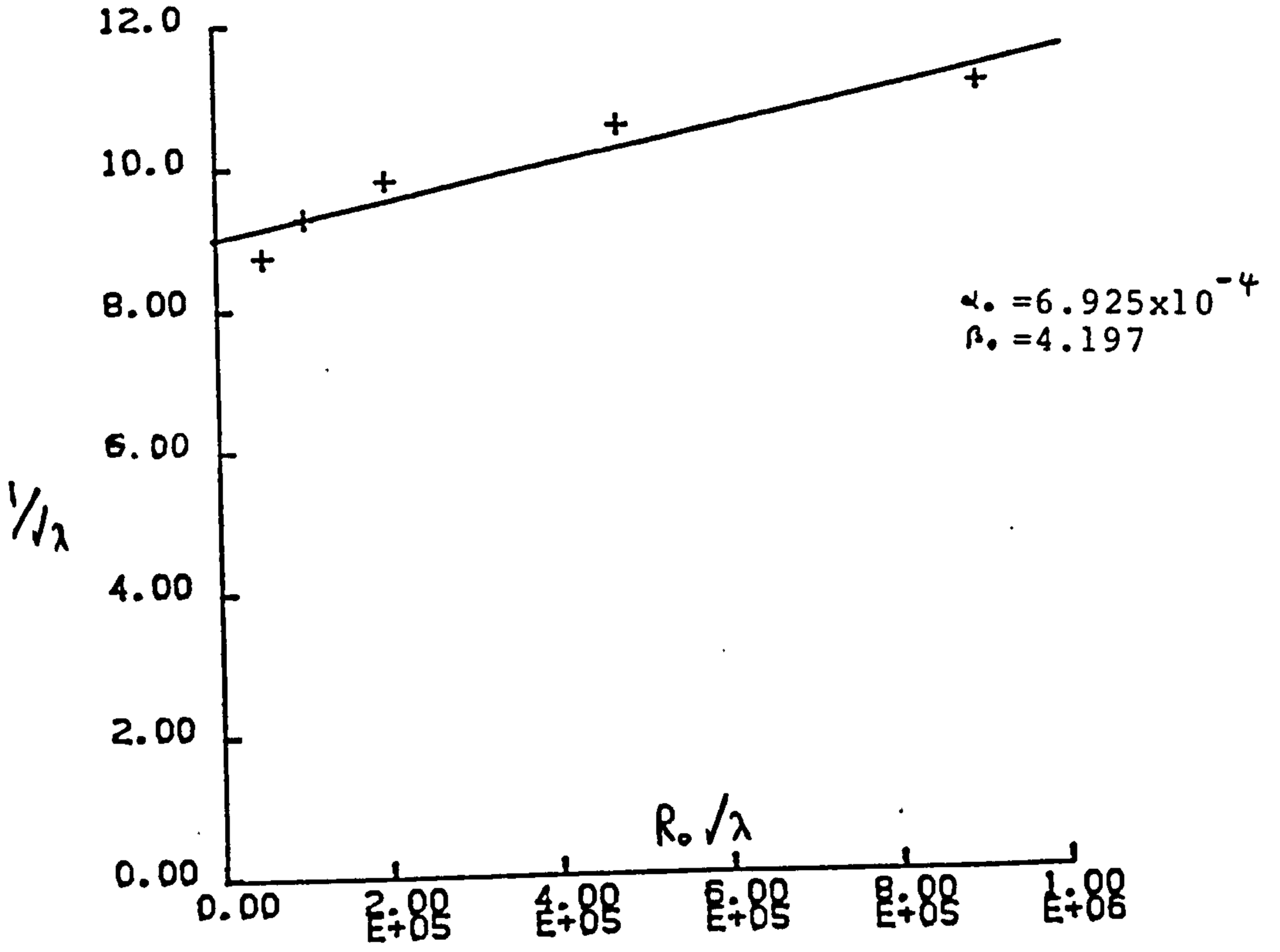

Fig. 4.1a, R_0: $10^3 \longrightarrow 2\times10^4$.

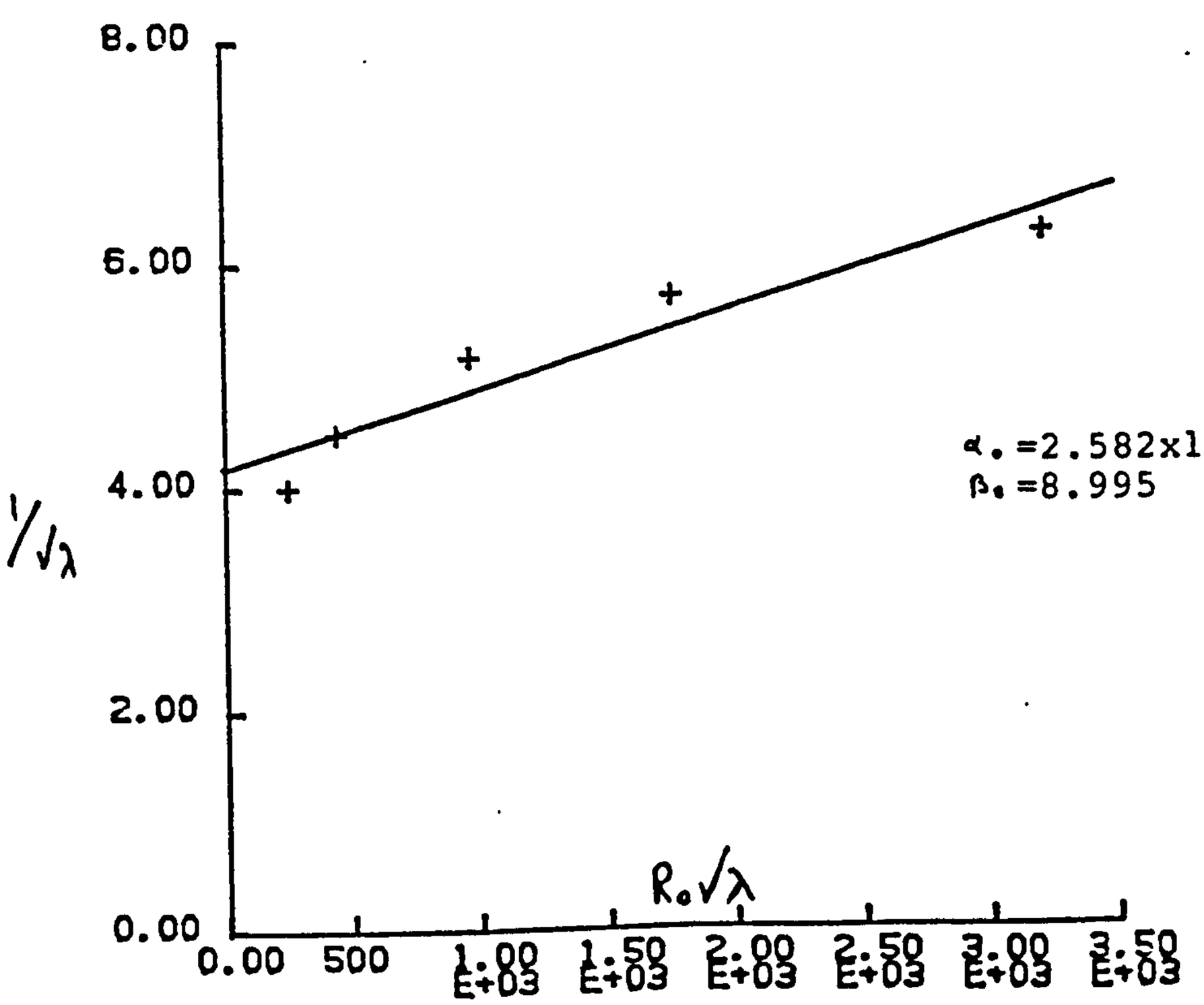

Fig. 4.1b, R_0: $5\times10^5 \longrightarrow 10^7$.

Frictional resistance in smooth pipes.

+: Prandtl formula (4.85), ——— :Equation (4.89).

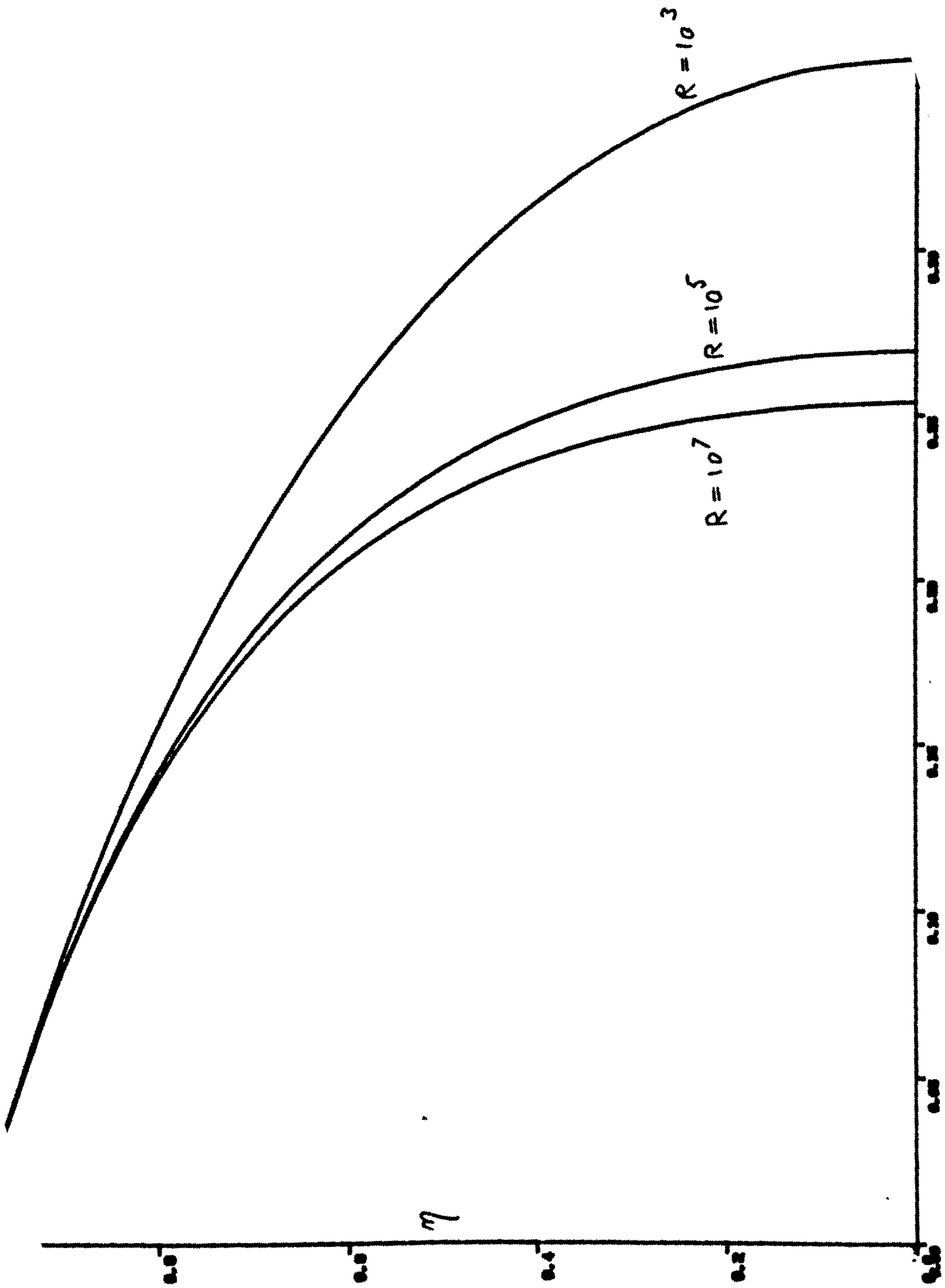

Fig. 4.2 Variation of the mean velocity (eqn. 4.82) with R, for a=2.6315, b=8 and c=0.009 .

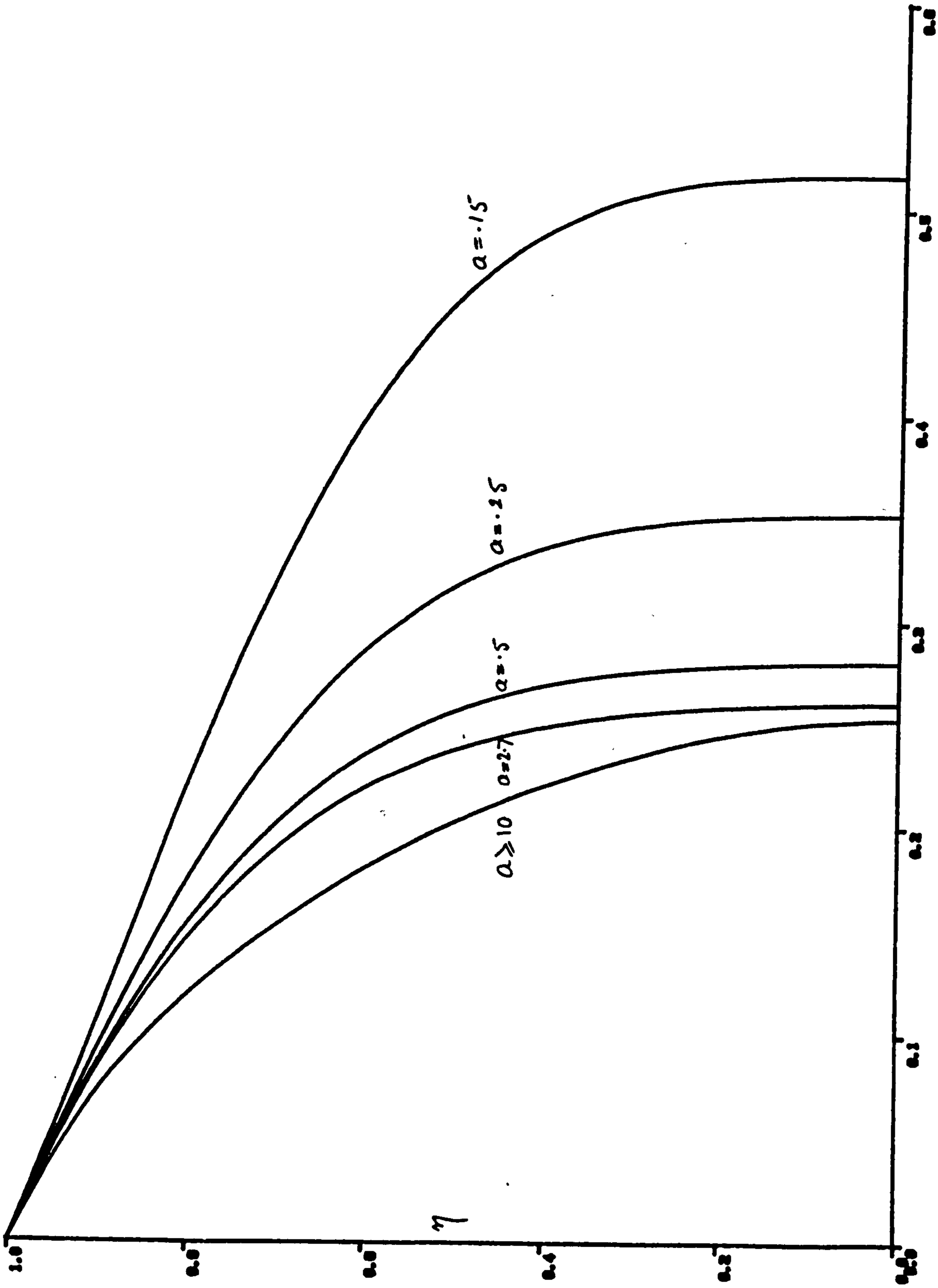

Fig. 4.3 Variation of the mean velocity (eqn. 4.82) with a, for $R=10^5$, b=8 and c=0.01 .

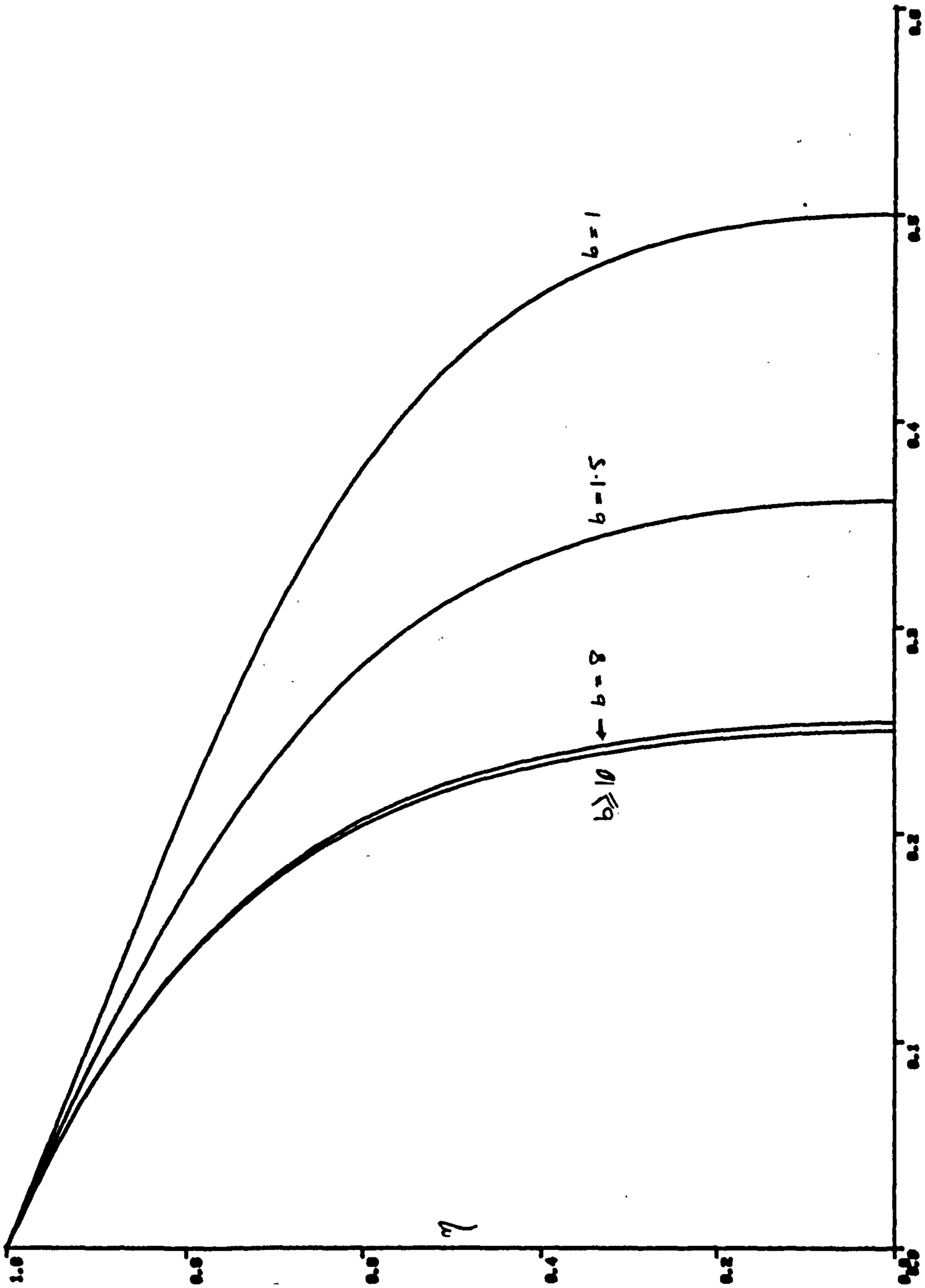

Fig. 4.4 Variation of the mean velocity (eqn. 4.82) with b, for $R=10^6$, a=2.6315 and c=0.01 .

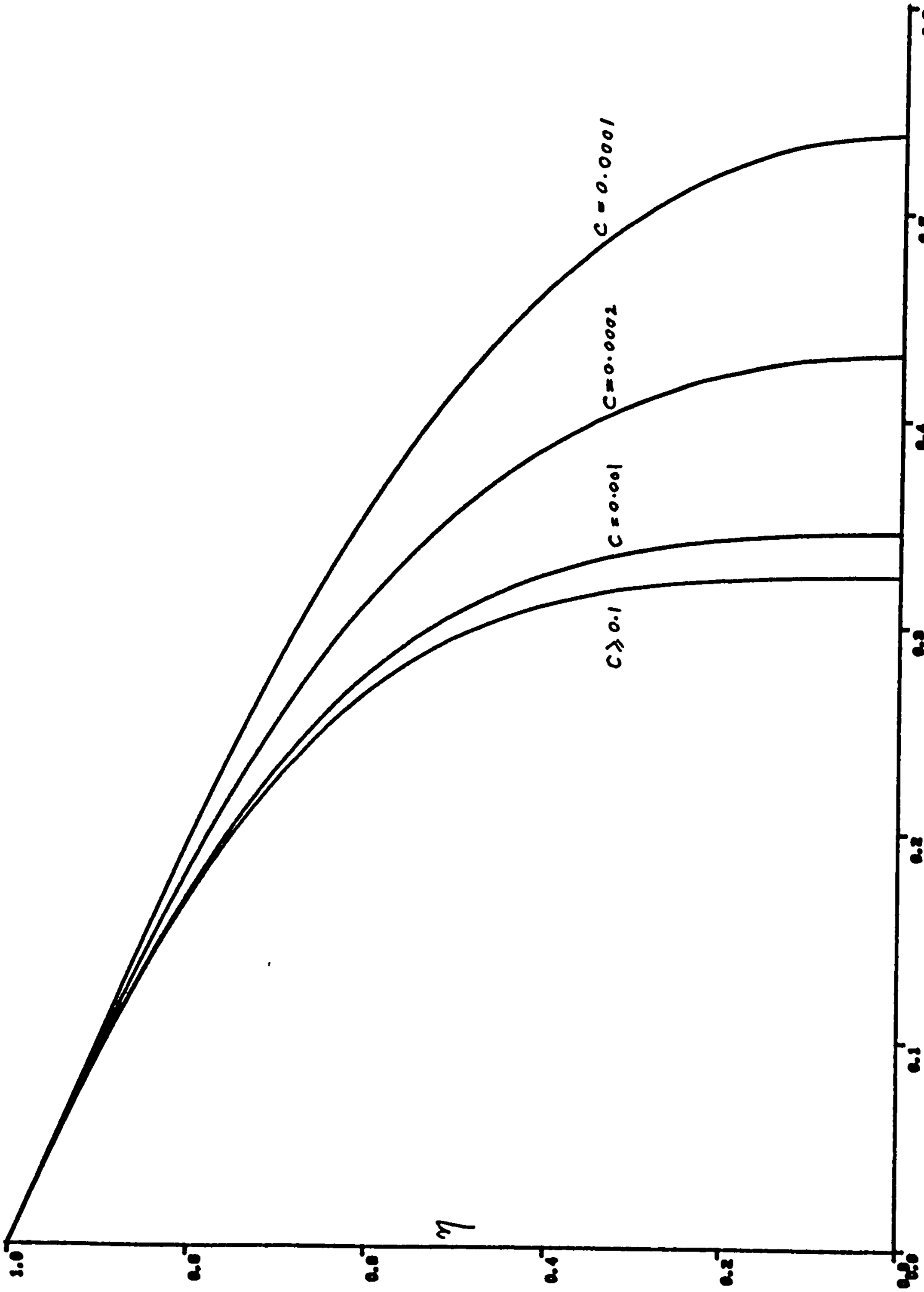

Fig. 4.5 Variation of the mean velocity (eqn. 4.82) with c, for $R=10^5$, a=0.5 and b=5.

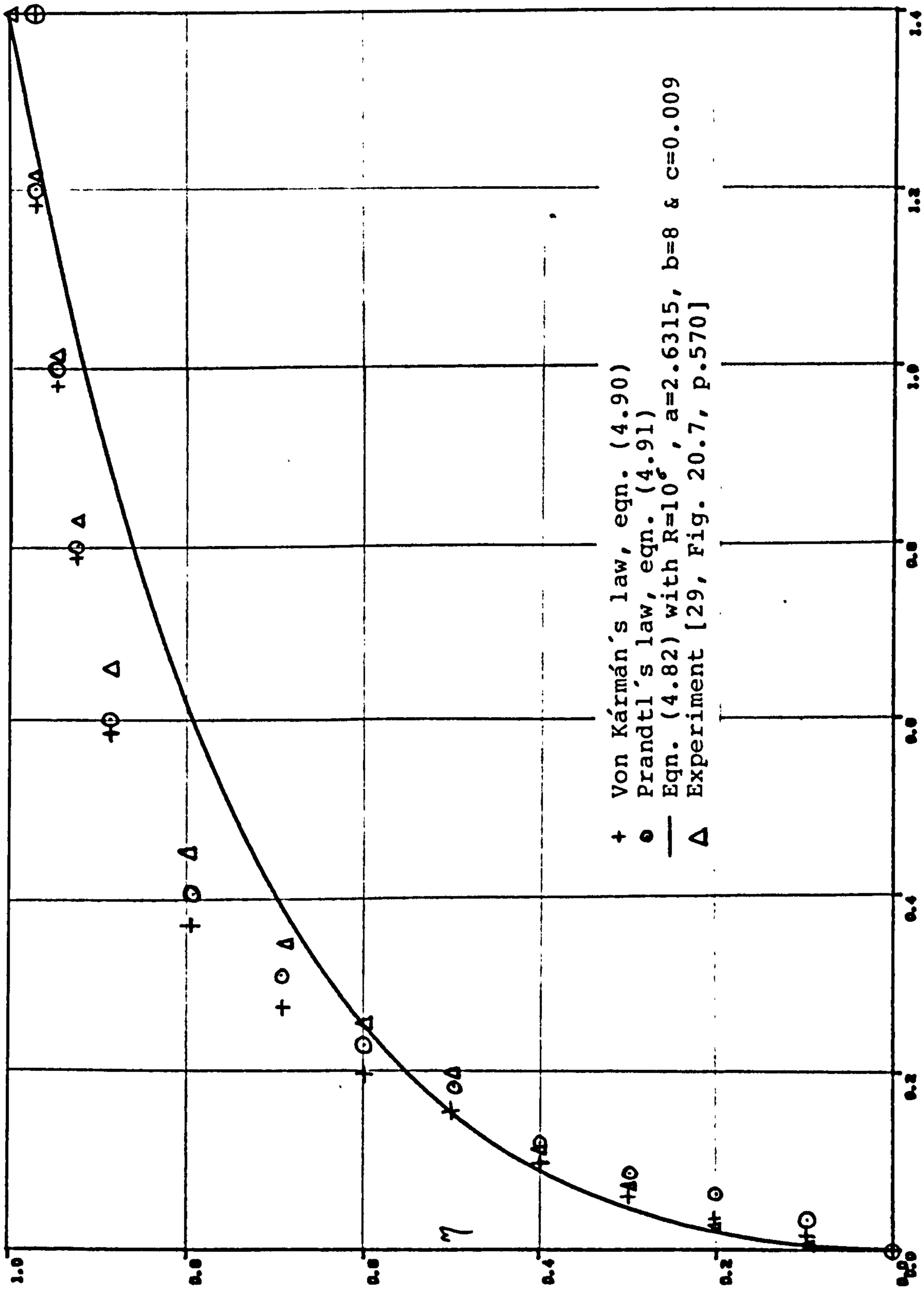

Fig. 4.6 Comparison of eqn. (4.82) with Von Kármán's and Prandtl's universal velocity distributions.

5. BOUNDARY-LAYER (B-L) THEORY.

The final problem to be examined with the aid of our model, is the steady incompressible turbulent boundary-layer flow along the surface of a solid body. This type of flow is more complex in comparison with the Poiseuille channel and pipe flows, for the equations governing the motion of a fluid in the B-L are non-linear. The non-linearity arises from the fact that in the regions close to a wall, the inertia and the viscous terms in the N-S equations are of the same order of magnitude, regardless of how small the viscosity might be.

The B-L concept was first introduced by Prandtl in 1904, when he realised that the change in the velocity from its zero value at the boundary, to its maximum in the free stream, takes place in a very thin layer close to the wall. Therefore, the space rate of change of the shearing stress is large in this layer and the viscous terms may no longer be neglected. This thin layer which is known as the boundary layer, has a thickness δ, which increases as the distance from the leading edge of the wall increases, or when the flow becomes turbulent.

The number of exact solutions to the N-S equations, where the inertia and the viscous terms are both present, are very limited, even when the flow is laminar. Examples of such solutions may be found in [9 ,ch. III]. It appears therefore, that the N-S equations need to be approximated, if the problem of boundary layers is to be treated mathematically. The method of approximation as suggested by Prandtl, is developed and described by Goldstein [9]. The resulting equations are known as the B-L equations. A number

of exact and approximate solutions to these equations in the case of laminar boundary layers are presented and described by Goldstein in the same book, and by Rosenhead [27 ,pp. 222-252]. Among them are some of the original and classic solutions given by Blasius (1908), who arrived at the similarity solutions for the B-L flow along a flat plate at zero incidence, and the more generalized solution of the Falkner-Skan equation (1930), applicable to laminar flows.

$$\text{Blasius:} \quad f'''(\eta) + 1/2\, ff'' = 0. \tag{5.1}$$

$$\text{Falkner-Skan:} \quad f'''(\eta) + ff'' + \beta(1-f'^{2}) = 0. \tag{5.2}$$

Solutions to these equations satisfy the boundary conditions

$$f = f' = 0 \quad \text{at} \quad \eta = 0 \quad \text{and} \quad f' \longrightarrow 1 \quad \text{as} \quad \eta \longrightarrow \infty \ . \tag{5.3}$$

The above well-known ordinary differential equations which were obtained by transforming the B-L equations through the similarity variables, may easily be integrated numerically. Analytic solutions to the Blasius and special cases of the Falkner-skan equations are also possible. An example of such solutions is given by Yang and Chien, who solved the Falkner-Skan equation for $\beta = -1$ [37].

More recently, Hastings and Troy derived an analytic solution for $\beta < -1$ and proved the existence of periodic solutions for $\beta > 1$ [12]. Further discussions on the existence and on the behaviour of the solutions to the Falkner-Skan equation, for both positive and negative values of β , may be found in [9, 10 and 11].

In turbulent boundary layers, two distinctive regions may be identified across the layer. An inner part, containing 10-20% of the B-L thickness, and an outer part making up the remainder. The inner part may further be divided into three layers: a very thin laminar sub-layer

next to the wall, a layer where the transition from laminar to turbulent takes place, and a fully developed turbulent layer.

Since, the fluid experiences different shear and pressure gradients in different layers, most of the existing methods of calculating the turbulent boundary layers, treat each layer separately. They assume negligible turbulent stresses in the laminar sub-layer of the inner region and negligible laminar stresses in the outer region. Only in the turbulent parts of the inner layer, are the laminar and turbulent stresses both accounted for. These methods therefore, require different closure assumptions in different regions of the boundary layer.

An example of such methods is the Cebeci-Smith differential model, in which the Reynolds stresses are related to the mean velocity through an eddy-viscosity approach which assumes different forms in the inner and outer regions. i.e. In the inner part:

$$\nu_t = (\kappa y)^2 [1 - \exp(-y/A)]^2 \, \partial u/\partial y ,$$

where $\kappa = 0.40$ and A is a constant, and in the outer part:

$$\nu_t = 0.0168 \, u_\infty \, \delta^* \gamma ,$$

where

$$\delta^* = \int_0^\infty [1 - u/u_\infty] \, dy ,$$

and

$$\gamma = [1 + 5.5 (y/\delta)^6]^{-1} \quad , [5].$$

Another example is the popular $k - \varepsilon$ model discussed in chapter one. It assumes an eddy-viscosity representation of the Reynolds stresses, in the form

$$\mu_t = c k^2/\varepsilon ,$$

where c is an empirically determined constant. An immediate

set back for this model is that the model parameters do not remain constants in the near wall regions and adjustments are required there [18 ,section 5.15].

Methods using this kind of approach can successfully be applied to certain types of flows such as the incompressible two dimensional and axisymmetric boundary layers. However, a high degree of accuracy may only be achieved if high speed computers are available.

These brief notes on the similarity solutions to the laminar B-L´s and the difficulties associated with the calculations of the turbulent B-L´s, are presented for the purpose of introduction, for our aim in this chapter is to arrive at equations similar to those of Blasius and the Falkner-Skan, which could make the calculations of turbulent B-L´s more efficient.

It should be noted that the concept of similarity solutions for turbulent flows, does not quite fit the definition given for the laminar profiles. Broadly speaking, the term ´similarity solutions´, implies that the velocity curves are similar at different stations downstream along the wall and may therefore be presented by one curve, if a suitable scaling factor is chosen. Furthermore, the solutions are independent of the Reynolds number. In the case of turbulent boundary layers therefore, we require to make the assumption that the flow is already turbulent at the leading edge of the wall. This assumption also eliminates the difficulties of describing the complex process of transition of flow from laminar to turbulent. In addition, it satisfies the requirement that the B-L thickness should be kept small for the B-L equations to

remain valid.

The equations we shall present, however, will depend on the Reynolds number, but will be independent of the space coordinate, in sections along the mean flow direction [see (5.42) and (5.45)]. We might therefore, call our solutions 'semi-similar', to avoid any possible confusions with the general definition of the similarity solutions. The presence of the Reynolds number in the equations is due to the fact that the viscous-dependent and the Reynolds stress-dependent parts of the profile require different length-scaling parameters [5].

The similarity solutions have been shown to exist in the past in the case of free shear turbulent flows. Such solutions in the similarity regions have been found by Vollmers and Rotta (1977), Wood and Leal (1983), and others, using various turbulent models.

In the following sections, we shall describe how the N-S equations may be approximated in a way analogus to that described by Goldstein. It will also be shown that the B-L equations may be transformed into an ordinary differential equation through the similarity variables.

We shall begin by considering the more general problem of B-L flow past a wedge, in which the pressure gradient is present. It will be shown that when the pressure gradient related parameter, β , is removed from the equation, the problem reduces to the special case of B-L flow along a flat plate at zero incidence, for which an equation similar to that of Blasius is obtained.

The numerical method used in solving the equations are presented in section 5.5 . In section 5.4, we describe how

an analytic solution may be obtained for the Falkner-Skan equation with additional turbulent terms, when $\beta=-1$.

5.1 Turbulent B-L flow with pressure gradient.

Consider an incompressible steady flow past a wedge of an included angle $\pi\beta$, as shown in the sketch below. Let the x-axis be parallel to the direction of mean motion and u, v and w denote the respective components of the mean velocity vector in the x, y and z directions.

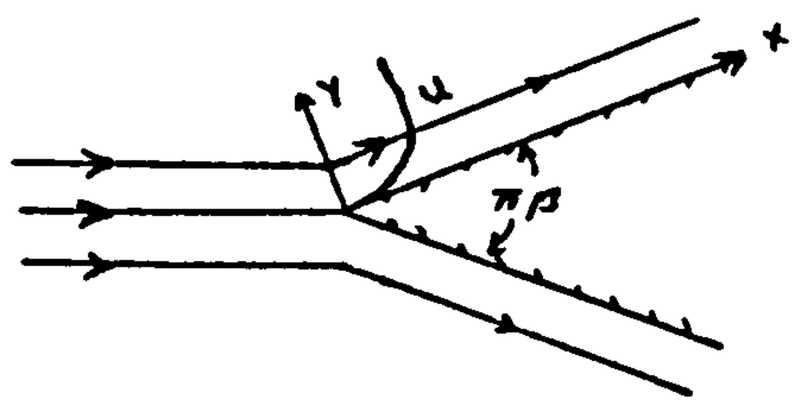

The time-averaged N-S equations in the Cartesian tensor notation, have the form

$$u_j \frac{\partial u_i}{\partial x_j} = -\frac{1}{\rho}\frac{\partial P}{\partial x_i} + \nu \frac{\partial^2 u_i}{\partial x_j \partial x_j} + \frac{1}{\rho}\frac{\partial}{\partial x_j}\tau^*_{ij}, \qquad (5.4a)$$

and

$$\partial u_i/\partial x_i = 0, \qquad (5.4b)$$

where u_i is the mean velocity in the direction denoted by i, and τ^*_{ij} represents the Reynolds stresses, defined in chapter two, by

$$\tau^*_{ij} = -\rho P_t \delta_{ij} + \rho \int_{vol} F(\underset{\sim}{X}, \underset{\sim}{X}-\underset{\sim}{X}')\, \sigma_{ij}(\underset{\sim}{X}')\, d\underset{\sim}{X}',$$

where

$$\sigma_{ij}(\underset{\sim}{X}') = \tfrac{1}{2}\left(\partial u_i/\partial x'_j + \partial u_j/\partial x'_i\right).$$

(The bars above the mean quantities are dropped for convenience.)

The z-component of the mean velocity, and the z-derivatives of all the velocity components may be neglected in the equations (5.4), since their contribution to the mean flow is quite small. This would reduce the momentum

equations (5.4a) to

$$u\frac{\partial u}{\partial x}+v\frac{\partial u}{\partial y}=-\frac{1}{\rho}\frac{\partial P}{\partial x}+\nu\left(\frac{\partial^2 u}{\partial x^2}+\frac{\partial^2 u}{\partial y^2}\right)+\frac{\partial}{\partial x}\left\{-P_t+\int_{vol} F.\frac{\partial u}{\partial x'}\,d\underset{\sim}{x}'\right\}$$

$$+\frac{\partial}{\partial y}\left\{\frac{1}{2}\int_{vol} F.\left(\frac{\partial u}{\partial y'}+\frac{\partial v}{\partial x'}\right)d\underset{\sim}{x}'\right\},$$

$$u\frac{\partial v}{\partial x}+v\frac{\partial v}{\partial y}=-\frac{1}{\rho}\frac{\partial P}{\partial y}+\nu\left(\frac{\partial^2 v}{\partial x^2}+\frac{\partial^2 v}{\partial y^2}\right)+\frac{\partial}{\partial x}\left\{\frac{1}{2}\int_{vol} F.\left(\frac{\partial v}{\partial x'}+\frac{\partial u}{\partial y'}\right)d\underset{\sim}{x}'\right\}$$

$$+\frac{\partial}{\partial y}\left\{-P_t+\int_{vol} F.\frac{\partial v}{\partial y'}\,d\underset{\sim}{x}'\right\},$$

and

$$0=-\frac{1}{\rho}\frac{\partial P}{\partial z}-\frac{\partial P_t}{\partial z},$$

and the continuity equation to

$$\frac{\partial u}{\partial x}+\frac{\partial v}{\partial y}=0,$$

where

$$u = u(x,y) \quad \text{and} \quad v = v(x,y).$$

The method of approximation we shall apply now, is based on the fact that in each of the above equations, some of the terms are of smaller order of magnitude than others and may be neglected. This method assumes the fluid has a small viscosity and the B-L thickness remains small.

To work out the order of magnitude of each term, we begin by taking u and $\partial u/\partial x$ to be O(1) and y to be $O(\delta)$. Then u=O(1) and $\partial u/\partial x$ =O(1) $\Longrightarrow$ x and $\partial^2 u/\partial x^2$ = O(1). The continuity eqn. together with $\partial u/\partial x$ =O(1) $\Rightarrow$ $\partial v/\partial y$ = O(1). $\partial v/\partial y$ = O(1) and y = $O(\delta)$ $\Longrightarrow$ v = $O(\delta)$ and $\partial^2 v/\partial y^2$ = $O(1/\delta)$.

v = $O(\delta)$ and x = O(1) $\Longrightarrow$ $\partial v/\partial x$ and $\partial^2 v/\partial x^2$ = $O(\delta)$.

u = O(1) and y = $O(\delta)$ $\Longrightarrow$ $\partial u/\partial y$ = $O(1/\delta)$ and $\partial^2 u/\partial y^2$ = $O(1/\delta^2)$.

Since the viscous and the inertia terms are of the same order of magnitude in the boundary layer, then $\nu = O(\delta^2)$. Similarly, as the laminar and the turbulent stresses are of the same order here, we have F = $O(\delta)$. It then follows that

$$\frac{\partial}{\partial x}(P/\rho+P_t)=O(1) \quad \text{and} \quad \frac{\partial}{\partial y}(P/\rho+P_t)=O(\delta).$$

It can now be seen that the x-momentum equation is O(1)

and the terms of $O(\delta^2)$, may be neglected in this equation. The y-momentum equation is $O(\delta)$ and terms of $O(\delta^3)$ may be neglected here. Hence, we obtain

$$\frac{\partial}{\partial x}(P/\rho + P_t) = -u\frac{\partial u}{\partial x} - v\frac{\partial u}{\partial y} + \nu\frac{\partial^2 u}{\partial y^2} + \frac{1}{2}\frac{\partial}{\partial y}\int_{vol} F.\frac{\partial u}{\partial y'}\, d\underset{\sim}{x}',$$

$$\frac{\partial}{\partial y}(P/\rho + P_t) = -u\frac{\partial v}{\partial x} - v\frac{\partial v}{\partial y} + \nu\frac{\partial^2 v}{\partial y^2} + \frac{1}{2}\frac{\partial}{\partial x}\int_{vol} F.\frac{\partial u}{\partial y'}\, d\underset{\sim}{x}'$$

$$+ \frac{\partial}{\partial y}\int_{vol} F.\frac{\partial v}{\partial y'}\, d\underset{\sim}{x}',$$

and (5.5)

$$\frac{\partial}{\partial z}(P/\rho + P_t) = 0.$$

Since $\frac{\partial}{\partial y}(P/\rho + P_t) = O(\delta)$, then the total change of pressure throughout the boundary layer normal to the wall is $O(\delta^2)$ and may be neglected. Hence, the pressure may be taken as constant along such normal and equal to its value just outside the boundary layer. We can therefore put

$$\frac{\partial}{\partial y}(P/\rho + P_t) = 0,$$

and from the potential flow theory

$$\frac{\partial}{\partial x}(P/\rho + P_t) = -u_\infty\frac{du_\infty}{dx}, \qquad (5.6)$$

where u_∞ is the velocity of the main flow outside the boundary layer. However, if the velocity of the potential flow is constant (as in the flow along a flat plate at zero incidence), then

$$\frac{\partial}{\partial x}(P/\rho + P_t) = 0.$$

In the neighbourhood of the leading edge of a flow past a wedge, the potential flow velocity is proportional to a power of the distance, measured from the stagnation point along the wall and can be presented by

$$u_\infty(x) = m\,x^n,$$

where m and n are constants. The pressure gradient along the wall therefore, is given by

$$\frac{\partial}{\partial x}\left(P/\rho + P_t\right) = -U_\infty \frac{dU_\infty}{dx} = -n m^2 x^{2n-1}, \qquad (5.7)$$

and the equations (5.5), reduce to

$$-n m^2 x^{2n-1} + u\frac{\partial u}{\partial x} + v\frac{\partial u}{\partial y} = \nu\frac{\partial^2 u}{\partial y^2} + \frac{1}{2}\frac{\partial}{\partial y}\int_{vol} F\cdot\frac{\partial u}{\partial y'}\, d\underset{\sim}{X}', \qquad (5.8)$$

with the boundary conditions

$$u = v = 0 \quad \text{at } y = 0 \quad \text{and} \quad u = U_\infty \quad \text{at } y = \infty .$$

The correlation function F, has the usual form

$$F = c_0 F_1(y)\; F_2(|\underset{\sim}{X} - \underset{\sim}{X}'|) \quad \text{[see ch. 2]}, \qquad (5.9)$$

where the position function F_2 is given by the Gaussian distribution function, (2.12). The expression representing F_1, will be presented later on.

Next, we shall present the equations in dimensionless forms.

5.2 The B-L equations in non-dimensional form.

Define the dimensionless variables $\hat{u}$, $\hat{v}$, $\hat{\underset{\sim}{X}}$, $\hat{\underset{\sim}{X}}'$, b and c, by

$$u = u_* \hat{u} \quad , \quad v = u_* \hat{v} \quad ,$$

$$x = d\,\hat{x} \quad , \quad y = d\,\hat{y} \quad , \quad z = d\,\hat{z} \quad ,$$

$$x' = d\,\hat{x}' \quad , \quad y' = d\,\hat{y}' \quad , \quad z' = d\,\hat{z}' \quad ,$$

$$\sigma = d\,b \quad , \quad c = \frac{d^2 c_0}{2 u_*} \text{ and } R = \frac{d u_*}{\nu} , \qquad (5.10)$$

where u_* and d are characteristic velocity and length scales, respectively.

Inserting (5.9) into (5.8) and combining the resulting equation plus the continuity equation with the above, we obtain the dimensionless B-L equation, in the form

$$-n m^2 x^{2n-1} + u\frac{\partial u}{\partial x} + v\frac{\partial u}{\partial y} = \frac{1}{R}\frac{\partial^2 u}{\partial y^2} + c\frac{\partial}{\partial y}F_1\int_{vol} F_2\frac{\partial u}{\partial y'}\, d\underset{\sim}{X}', \qquad (5.11)$$

and

$$\frac{\partial u}{\partial x} + \frac{\partial v}{\partial y} = 0 ,$$

with the boundary conditions

$$u = v = 0 \quad \text{at} \quad y = 0 \quad \text{and} \quad u = u_\infty \text{ at } y = \infty . \qquad (5.12)$$

The position function, with the dimensionless variables, becomes

$$F_2(|\underset{\sim}{X}-\underset{\sim}{X}'|) = \exp\{-\tfrac{1}{2b^2}[(x-x')^2+(y-y')^2+(z-z')^2]\}. \qquad (5.13)$$

The circumflexes representing the dimensionless quantities, are removed for convenience.

Now the question is, can we obtain similarity solutions to the above system of equations. To answer this, we shall adapt a technique similar to that pioneered by Blasius and introduce similarity variables.

5.3 The similarity variables.

The idea behind the transformation of the equations through the similarity variables, is to reduce the number of independent variables to one, so that the partial differential equations can be transformed into an ordinary differential equation.

Let us introduce the similarity variables η and ζ and define them by

$$\eta = A y x^{\lambda} \quad \text{and} \quad \zeta = x , \qquad (5.14)$$

and look for the solutions of the forms

$$u = \phi(\zeta) U(\eta) \quad \text{and} \quad v = \psi(\zeta) V(\eta). \qquad (5.15)$$

The z variable remains unchanged and the constants A and λ will be determined in the process. From (5.14), we can write

$$\frac{\partial u}{\partial x} = \frac{\partial u}{\partial \zeta} + \frac{\lambda}{\zeta}\eta\frac{\partial u}{\partial \eta} \quad , \quad \frac{\partial u}{\partial y} = A\zeta^{\lambda}\frac{\partial u}{\partial \eta} ,$$

and

$$\frac{\partial^2 u}{\partial y^2} = A^2\zeta^{2\lambda}\frac{\partial^2 u}{\partial \eta^2} . \qquad (5.16)$$

Equations (5.14) and (5.16), transform the equations

(5.11), to

$$-nm^2\zeta^{2n-1}+u\frac{\partial u}{\partial \zeta}+\lambda\zeta^{-1}\eta u\frac{\partial u}{\partial \eta}+A\zeta^{\lambda}v\frac{\partial u}{\partial \eta}$$

$$=\frac{1}{R}A^2\zeta^{2\lambda}\frac{\partial^2 u}{\partial \eta^2}+cA\zeta^{\lambda}\frac{\partial}{\partial \eta}F_1\int_{vol}F_2\,A\zeta'^{\lambda}\frac{\partial u}{\partial \eta'}\,J\,d\zeta'd\eta'dz', \tag{5.17}$$

and

$$\frac{\partial u}{\partial \zeta}+\lambda\zeta^{-1}\eta\frac{\partial u}{\partial \eta}+A\zeta^{\lambda}\frac{\partial v}{\partial \eta}=0,$$

where J is the Jacobian of the transformation, given by

$$J=\frac{\partial(x',y')}{\partial(\zeta',\eta')}=\left\{\frac{\partial(\zeta',\eta')}{\partial(x',y')}\right\}^{-1}$$

$$=\begin{vmatrix}\partial\zeta'/\partial x' & \partial\zeta'/\partial y'\\ \partial\eta'/\partial x' & \partial\eta'/\partial y'\end{vmatrix}^{-1}=\begin{vmatrix}1 & 0\\ \partial\eta'/\partial x' & Ax'^{\lambda}\end{vmatrix}^{-1}=\{Ax'^{\lambda}\}^{-1}. \tag{5.18}$$

Under the similarity transformation, the position function, becomes

$$F_2=\exp\left\{-\frac{1}{2b^2}\left[(\zeta-\zeta')^2+\frac{1}{A^2}(\eta\zeta^{-\lambda}-\eta'\zeta'^{-\lambda})^2+(z-z')^2\right]\right\}. \tag{5.19}$$

From (5.15), we can write

$$\frac{\partial u}{\partial \zeta}=U\frac{d\phi}{d\zeta},\quad \frac{\partial u}{\partial \eta}=\phi\frac{dU}{d\eta},\quad \frac{\partial^2 u}{\partial \eta^2}=\phi\frac{d^2U}{d\eta^2},$$

$$\frac{\partial v}{\partial \zeta}=V\frac{d\alpha}{d\zeta}\quad\text{and}\quad \frac{\partial v}{\partial \eta}=\alpha\frac{dV}{d\eta}. \tag{5.20}$$

Combining the above with (5.17), we obtain

$$-nm^2\zeta^{2n-1}+\phi U^2\frac{d\phi}{d\zeta}+\lambda\zeta^{-1}\eta\phi^2U\frac{dU}{d\eta}+A\zeta^{\lambda}\alpha V\phi\frac{dU}{d\eta}$$

$$=\frac{1}{R}A^2\zeta^{2\lambda}\phi\frac{d^2U}{d\eta^2}+cA\zeta^{\lambda}\frac{\partial}{\partial \eta}F_1\int_{vol}F_2\,\phi(\zeta')\frac{dU}{d\eta'}\,d\tau', \tag{5.21a}$$

and

$$U\frac{d\phi}{d\zeta}+\lambda\zeta^{-1}\eta\phi\frac{dU}{d\eta}+A\zeta^{\lambda}\alpha\frac{dV}{d\eta}=0, \tag{5.21b}$$

where $d\tau'=d\zeta'\,d\eta'dz'$.

If we assume $\phi(\zeta)$ is a regular function and divide

throughout the continuity equation (5.21b) by $\phi'(\zeta)$, we find

$$U + \lambda \zeta^{-1} \eta \frac{\phi}{\phi'} \frac{dU}{d\eta} + A \zeta^{\lambda} \frac{\nu}{\phi'} \frac{dV}{d\eta} = 0, \qquad (5.22)$$

where $\phi' = d\phi/d\zeta$.

Choosing $\phi(\zeta)$, such that

$$\zeta^{-1} \phi/\phi' = \text{constant},$$

and integrating the above w.r.t. ζ, we obtain

$$\phi(\zeta) = \zeta^{\alpha}, \qquad (5.23)$$

where α is a constant.

On the other hand, differentiating (5.22) w.r.t. ζ, gives

$$\frac{\partial}{\partial \zeta} \{ \zeta^{\lambda} \nu/\phi' \} = 0,$$

which implies

$$\zeta^{\lambda} \nu/\phi' = \text{constant}.$$

Substituting for ϕ' in the above from (5.23) and rearranging, yields

$$\nu(\zeta) = \gamma \zeta^{\alpha - \lambda - 1}, \qquad (5.24)$$

where γ is a constant.

The equations (5.21), together with (5.23) and the above, become

$$-n m^2 \zeta^{2n-1} + \alpha U^2 \zeta^{2\alpha-1} + \lambda \eta \zeta^{2\alpha-1} U \frac{dU}{d\eta} + A \gamma \zeta^{2\alpha-1} V \frac{dU}{d\eta}$$

$$= \frac{1}{R} A^2 \zeta^{2\lambda+\alpha} \frac{d^2U}{d\eta^2} + c A \zeta^{\lambda} \frac{\partial}{\partial \eta} F_1 \int_{Vol} F_2 \zeta'^{\alpha} \frac{dU}{d\eta'} d\tau', \qquad (5.25)$$

and

$$\alpha \zeta^{\alpha-1} U + \lambda \eta \zeta^{\alpha-1} \frac{dU}{d\eta} + A \gamma \zeta^{\alpha-1} \frac{dV}{d\eta} = 0.$$

At this stage, we need to evaluate the volume integral in the above, so that the equations can be simplified further.

Let

$$I = \int_{Vol} F_2 \zeta'^{\alpha} \frac{dU}{d\eta'} d\zeta' d\eta' dz'.$$

Substituting for F_2 from (5.19), yields

$$I = \int_0^\infty \int_0^\infty \int_{-\infty}^{\infty} \exp\left\{-\frac{1}{2b^2}\left[(\zeta-\zeta')^2 + \frac{1}{A^2}(\eta\zeta^{-\lambda} - \eta'\zeta'^{-\lambda})^2 + (z-z')^2\right]\right\} \zeta'^{\alpha} \frac{dU}{d\eta'}\, d\tau'.$$

The z'-integral can easily be evaluated and reduces to $b\sqrt{(2\pi)}$. The remaning double integral, however, can only be evaluated approximately. We shall estimate its value, by making a series of transformations and using power series expansions. This method is described below.

Under the transformation

$$\zeta' = \zeta(1+s) \quad \text{and} \quad \eta' = \eta(1+t), \tag{5.26}$$

we have $\quad d\zeta' = \zeta\, ds \quad , \quad d\eta' = \eta\, dt \ ,$

and

$$I = b\sqrt{(2\pi)}\,\zeta^{\alpha+1} \int_{-1}^{\infty}\int_{-1}^{\infty} \exp\left\{-\frac{1}{2b^2}\left[\zeta^2 s^2 + \frac{1}{A^2}\eta^2\zeta^{-2\lambda}\left(1-\frac{1+t}{(1+s)^\lambda}\right)^2\right]\right\}$$

$$\cdot(1+s)^{\alpha}\frac{d}{dt}U(\eta+\eta t)\, ds\, dt. \tag{5.27}$$

Assuming $t<<1$, the term $d/dt\{U(\eta + \eta t)\}$ in the above, can be presented by its Taylor expansion

$$\frac{d}{dt}U(\eta+\eta t) = \frac{d}{dt}\sum_{k=0}^{\infty}\frac{\eta^k t^k}{k!}\frac{d^k U(\eta)}{d\eta^k} = \sum_{k=1}^{\infty}\frac{\eta^k t^{k-1}}{(k-1)!}\frac{d^k U(\eta)}{d\eta^k}.$$

Substituting this expression back into the integrand, we get

$$I = b\sqrt{(2\pi)}\,\zeta^{\alpha+1}\sum_{k=1}^{\infty}\frac{\eta^k}{(k-1)!}\frac{d^k U(\eta)}{d\eta^k}$$

$$\cdot\int_{-1}^{\infty}\int_{-1}^{\infty}\exp\left\{-\frac{1}{2b^2}\left[\zeta^2 s^2 + \frac{1}{A^2}\eta^2\zeta^{-2\lambda}\left(1-\frac{1+t}{(1+s)^\lambda}\right)^2\right]\right\}(1+s)^{\alpha} t^{k-1} \tag{5.28}$$

$$\cdot\, ds\, dt.$$

If we further put

$$\chi = a_1 s \quad \text{and} \quad \gamma = a_2\left[1-\frac{1+t}{(1+s)^\lambda}\right], \tag{5.29}$$

where

$$a_1 = \zeta \ , \ a_2 = \frac{1}{A}\eta\zeta^{-\lambda} \quad \text{and} \quad \lambda < 0,$$

then

$$s = \chi/a_1 \ , \ t = (1-\gamma/a_2)(1+\chi/a_1)^{\lambda} - 1 \ ,$$

and $ds\,dt = J\,dx\,dY$.

The Jacobian of transformation J, is

$$J = \left\{\frac{\partial(X,Y)}{\partial(s,t)}\right\}^{-1} = -\frac{1}{a_1 a_2}(1+s)^{\lambda} = -\frac{1}{a_1 a_2}(1+X/a_1)^{\lambda}.$$

Under the above transformation, we obtain

$$I = b/(2\pi)\,\xi^{\alpha+1}\left(\frac{-1}{a_1 a_2}\right)\sum_{k=1}^{\infty}\frac{\eta^k}{(k-1)!}\frac{d^k U(\eta)}{d\eta^k}$$
$$\cdot\int_{-a_1}^{\infty}\int_{a_2}^{-\infty} g(X,-Y)\,\exp\{-\tfrac{1}{2b^2}(X^2+Y^2)\}\,dx\,dY\ , \qquad (5.30)$$

where

$$g(X,-Y) = (1+X/a_1)^{\lambda+\alpha}\cdot[(1-Y/a_2)(1+X/a_1)^{\lambda}-1]^{k-1}. \qquad (5.31)$$

The equation (5.30) can also be written as

$$I = b\sqrt{(2\pi)}\,A\,\xi^{\lambda+\alpha}\,\eta^{-1}\sum_{k=1}^{\infty}\frac{\eta^k}{(k-1)!}\frac{d^k U}{d\eta^k}$$
$$\cdot\int_{-a_1}^{\infty}\int_{-a_2}^{\infty} g(x,Y)\,\exp\{-\tfrac{1}{2b^2}(X^2+Y^2)\}\,dx\,dY\ . \qquad (5.32)$$

If we assume b to be small, so that $1/2b^2 >> 1$, then the double integral in the above may be regarded as of the Laplace type. The major contribution to the integrals therefore, arise from the neighbourhood of the origin, where g(X,Y), may be approximated by

$$g(X,Y) \approx (-1)^{k-1}\left[1+(\lambda+\alpha)X/a_1+\cdots\right]\left[1-(k-1)(1+Y/a_2)(1+X/a_1)^{\lambda}+\cdots\right].$$

The leading term in the above expansion (when k=1) is unity. Thus, to the first order we have

$$g(X,Y) \approx 1 + \text{higher powers of X and Y.}$$

Hence, (5.32), approximated to the same order, becomes

$$I \approx b\sqrt{(2\pi)}\,A\,\xi^{\lambda+\alpha}\,\frac{dU}{d\eta}\,I^{+}$$

where

$$I^{+} = \int_{-a_1}^{\infty}\int_{-a_2}^{\infty}\exp\{-\tfrac{1}{2b^2}(X^2+Y^2)\}\,dx\,dY\ .$$

We may now put

$$X = r\cos\phi \qquad \text{and} \qquad Y = r\sin\phi.$$

Assuming $|a_2| < |a_1|$, then

$$I^{+} = \int_0^{a_2}\int_{-\pi}^{\pi} e^{-r^2/2b^2}\, r\,dr\,d\phi = -b^2\int_0^{a_2}\frac{d}{dr}e^{-r^2/2b^2}\,dr\int_{-\pi}^{\pi}d\phi$$

$$= -2\pi b^2\left[e^{-a_2^2/2b^2}-1\right] \approx 2\pi b^2 ,$$

with an error of $O(b^2 e^{-a_2^2/2b^2})$, which is asymptotically small as $1/2b^2 >> 1$. Hence, the volume integral, to the first order is given by

$$I \approx (2\pi)^{3/2} b^3 A\,\zeta^{\lambda+\alpha}\, dU/d\eta . \qquad (5.33)$$

From the physical point of view, since we have taken b to be small, then the points $\underset{\sim}{X}'(\zeta',\eta',z')$, whose effects on the point $\underset{\sim}{X}(\zeta,\eta,z)$ we are averaging, are located fairly close to $\underset{\sim}{X}$. So in effect, it is the small scale eddies formed at these points which influence the behaviour of the flow at the point in question in this case. It is after all, eddies of small scale which determine the characteristic of a turbulent flow in the boundary layer.

Recalling the equations (5.25) and replacing the volume integral by the above expression, yields

$$-n m^2 \zeta^{2n-1} + \alpha U^2 \zeta^{2\alpha-1} + \lambda\eta\,\zeta^{2\alpha-1}\, U\, dU/d\eta + A\gamma\,\zeta^{2\alpha-1}\, V\, dU/d\eta$$

$$= \frac{1}{R} A^2 \zeta^{2\lambda+\alpha}\, d^2U/d\eta^2 + C_2 A^2 b^3 \zeta^{2\lambda+\alpha}\,\frac{d}{d\eta}\{F_1\, dU/d\eta\},$$

and (5.34a)

$$\alpha U + \lambda\eta\, dU/d\eta + A\gamma\, dV/d\eta = 0 , \qquad (5.34b)$$

where $C_2 = (2\pi)^{3/2} C$.

In order to make the above equation independent of ζ, we choose n, α and λ, such that

$$2n-1 = 2\alpha-1 = 2\lambda+\alpha ,$$

which implies

$$n = \alpha = 2\lambda + 1 . \tag{5.35}$$

Hence, the equations reduce to

$$-(2\lambda+1)m^2 + (2\lambda+1)U^2 + \lambda\eta U\, dU/d\eta + A\gamma V\, dU/d\eta$$

$$= \frac{1}{R} A^2\, d^2U/d\eta^2 + c_2 A^2 b^3 \frac{d}{d\eta}\{F_1\, dU/d\eta\}, \tag{5.36a}$$

and

$$(2\lambda+1)U + \lambda\eta\, dU/d\eta + A\gamma\, dV/d\eta = 0 . \tag{5.36b}$$

To eliminate V from these equations, we put

$$f(\eta) = \int U(\eta)\, d\eta,$$

so that

$$f' = U , \quad f'' = dU/d\eta , \text{ etc.},$$

where f is the stream function, f' is the velocity and $\alpha f''$ represents the shearing stress.

On integrating the continuity equation (5.36b), we find

$$A\gamma V = -\lambda\eta f' - (\lambda+1) f + K ,$$

where the no-slip conditions at the wall, make the constant K zero.

Combining the above with (5.36a), yields

$$\frac{1}{R} A^2 f''' + (\lambda+1) f f'' + (2\lambda+1)(m^2 - f'^2) + c_2 A^2 b^3 \frac{d}{d\eta}\{F_1 f''\} = 0.$$

If we choose A, such that $A^2 = R$, and put $m = 1$, then the above equation reduces to

$$f''' + (\lambda+1) f f'' + (2\lambda+1)(1 - f'^2) + \varepsilon \frac{d}{d\eta}\{F_1 f''\} = 0, \tag{5.37}$$

where $\varepsilon = R\, c_2 b^3$.

Since

$$u = \phi(\zeta)\, U(\eta) = \zeta^{\alpha} f'(\eta),$$

then for negative values of α, both u and u_- become infinite at $\zeta = 0$, and the solution is artificial [9 ,p.141].

If we put

$$W(Y) = (\lambda+1)^{1/2} f(\eta) \quad , \quad Y = (\lambda+1)^{1/2} \eta \, ,$$

and $\beta = (2\lambda+1)/(\lambda+1)$, (5.38)

then (5.37) becomes

$$\frac{d^3W}{dY^3} + W\frac{d^2W}{dY^2} + \beta\left[1 - \left(\frac{dW}{dY}\right)^2\right] + \varepsilon \frac{d}{dY}\left\{F_1 \frac{d^2W}{dY^2}\right\} = 0. \quad (5.39)$$

An appropriate form for the shape function F_1, is all that required now to enable us to solve the above equation. Let us try

$$F_1(\eta) = 1 - e^{-a\eta} \, , \quad (5.40)$$

where the scaling coefficient a, determines how fast the profiles fall in with the free stream flow.

The shape function with the Y variable, has the form

$$F_1(Y) = 1 - e^{-a(\lambda+1)^{-1/2} Y} \, . \quad (5.41)$$

It is convenient to make a change in the notation and rewrite (5.39), with W replaced by f, and Y by η, so that it can be presented in the standard form

$$f''' + ff'' + \beta(1 - f'^2) + \varepsilon \frac{d}{d\eta}\{F_1 f''\} = 0, \quad (5.42)$$

where

$$F_1 = 1 - e^{-a(\lambda+1)^{-1/2}\eta} \, . \quad (5.43)$$

The boundary conditions to be satisfied by the solutions of (5.42), are

$$f = f' = 0, \quad F_1 = 0 \qquad \text{at } \eta = 0,$$

and $$f' \longrightarrow 1 \quad \text{as} \quad \eta \longrightarrow \infty \, . \quad (5.44)$$

We note that the equation (5.42) is identical to the Falkner-Skan equation, except for the presence the terms representing turbulent effects. Furthermore, if we choose $\lambda = -1/2$, so that (from 5.38) $\beta = 0$, then the equation (5.37), reduces to

$$f''' + \tfrac{1}{2} ff'' + \varepsilon \frac{d}{d\eta}\{F_1 f''\} = 0 \, , \quad (5.45)$$

where

$$F_1 = 1 - e^{-a\eta}, \tag{5.46}$$

which is the Blasius equation, with additional turbulent terms, applicable to B-L flow along a flat plate with zero pressure gradient.

It is worth pointing out that in order to arrive at (5.45) from the original equations (5.21), we choose ϕ to be a constant, rather than a regular function of ξ, since we require that the free-stream velocity be independent of the space coordinate along the wall.

Numerical solutions to the equations (5.42) and (5.45), with the boundary conditions (5.44), are presented in section 5.5 . In the following section, we show how an analytic solution to the equation (5.42) may be obtained for the special case $\beta = -1$.

5.4 An analytic solution when $\beta = -1$.

At the beginning of this chapter, it was pointed out that analytic solutions to the Falkner-Skan equation have been found in the past. Yang and Chien for example, presented two types of solutions when $\beta = -1$ [37]. The boundary conditions they used were

$$f(0) = \gamma, \quad f'(0) = 0 \quad \text{and} \quad f'(\infty) = 1,$$

where γ is the suction velocity.

For $\gamma \geq \sqrt{2}$, $f''(0) = \sqrt{(\gamma^2 - 2)}$, their solution is in terms of exponential and error functions, with $f'(\eta)$ in a dominantly exponential asymptotic approach to unity. When $0 < \gamma < \sqrt{2}$, then $f''(0) = 0$, and the solution is given in terms of confluent hypergeometric functions, with an algebraic approach from above.

Since the equation (5.42) is an extended version of the Falkner-Skan, it is worth investigating how solutions to the latter may be extended in connection with finding a solution to (5.42).

If we take $\beta = -1$, then from (5.38), $\lambda = -2/3$, and (5.42) becomes

$$f''' + ff'' - 1 + f'^{2} + \varepsilon \frac{d}{d\eta}\{F_1 f''\} = 0, \qquad (5.47)$$

where

$$F_1 = 1 - e^{-\sqrt{3}a\eta}. \qquad (5.48)$$

On integrating (5.47) once and using the no-slip conditions at the wall to find the integration constant, we obtain

$$f'' + ff' - \eta - f''(0) + \varepsilon F_1 f' = 0. \qquad (5.49)$$

Since $\varepsilon = Rc_1 b^3$ and $b<<1$, then for moderate values of the Reynolds number $\varepsilon <<1$ and we may assume a straightforward expansion for f, in the form

$$f = f_0 + \varepsilon f_1 + O(\varepsilon^2), \qquad [26]. \qquad (5.50)$$

Combining (5.49) with the above, we get

$$f_0'' + \varepsilon f_1'' + (f_0 + \varepsilon f_1)(f_0' + \varepsilon f_1') - \eta - [f_0''(0) + \varepsilon f_1'(0)] + \varepsilon F_1 (f_0' + \varepsilon f_1') = 0.$$

Equating the coefficients of equal powers of ε, gives

$$f_0'' + f_0 f_0' - \eta - f_0'(0) = 0, \qquad (5.51)$$

and

$$f_1' + f_0 f_1' + f_0' f_1 + F_1 f_0'' = 0. \qquad (5.52)$$

The boundary conditions for (5.52) are

$$f_1(0) = f_1'(0) = f_1''(0) = f_1'(\infty) = 0. \qquad (5.53)$$

Equation (5.51) can be integrated once to give a Riccati equation

$$f_0' + \tfrac{1}{2}(f_0^2 - \eta^2) - f_0''(0)\eta = \tfrac{1}{2} f_0^2(0). \qquad (5.54)$$

Solutions to this equation are given by Yang and Chien.

Equations (3.10) and (3.11) in their paper represent the confluent hypergeometric function solution for $0 < \gamma \leq \sqrt{2}$. The exponential and error function solution for $\gamma \geq \sqrt{2}$, is given by equations (4.5) and (4.6) in the same paper. From either of these solutions we can substitute for f_0 and f_0' in (5.52). First, let us simplify this equation further.

Substituting for F_1 from (5.48) into (5.52) and integrating the resulting equation, we obtain

$$f_1' + f_0 f_1 + (1 - e^{-\sqrt{3}a\eta}) f_0' - \sqrt{3}\, a \int_0^\eta e^{-\sqrt{3}a\eta'} f_0'(\eta')\, d\eta' = K_1 ,$$

where η' is a dummy variable and K_1 is a constant.

Multiplying throughout the above by the integrating factor

$$\psi(\eta) = \exp\{ \int f_0\, d\eta \} ,$$

and integrating once, we have

$$f_1 \psi = \int_0^\eta \{ -(1 - e^{-\sqrt{3}a\eta^+}) f_0' + \sqrt{3}a \int_0^{\eta^+} e^{-\sqrt{3}a\eta'} f_0'(\eta')\, d\eta' + K_1 \} \psi(\eta')\, d\eta^+ , \quad (5.55)$$

where η^+ is a dummy variable.

If for example, f_0 is given by the exponential and error functions [eqn. (4.5) Yang and Chien], then

$$\psi(\eta) = \left[\frac{\sqrt{\pi}}{2} \operatorname{erf}\left(\frac{\eta + \sqrt{(\gamma^2 - 2)}}{\sqrt{2}} \right) - \theta \right]^2 \exp\{ \eta^2/2 + \sqrt{(\gamma^2 - 2)}\, \eta \} , \quad (5.56)$$

where

$$\theta = \frac{\sqrt{\pi}}{2} \operatorname{erf}\left(\frac{\sqrt{(\gamma^2 - 2)}}{\sqrt{2}} \right) - \frac{\gamma + \sqrt{(\gamma^2 - 2)}}{\sqrt{2}}\, e^{-\frac{1}{2}(\gamma^2 - 2)} .$$

The solution (5.55) is presented in an integral form, which together with (5.50) constitutes an approximate analytic solution for (5.47). We make no attempt to evaluate the integrals in the above, for there are efficient numerical techniques which can solve (5.47) easily. Such numerical solutions for different values of β and ε , are presented below.

5.5 RESULTS AND DISCUSSION.

To solve the equations (5.42) and (5.45), which are non-linear ordinary differential equations (O.D.E.) of order three, we represent them by sets of first order O.D.E.'s, which may be solved numerically. To this end, we rewrite (5.45) as

$$(1+\varepsilon F_1) f''' + (\tfrac{1}{2} f + \varepsilon F_1') f'' = 0, \qquad (5.57)$$

which may be reduced to the following system of first order O.D.E.'s.

$$(f)' = f',$$

$$(f')' = f'',$$

and (5.58)

$$(f'')' = -\left(\frac{\frac{1}{2} f + \varepsilon F_1'}{1+\varepsilon F_1}\right)(f''),$$

where

$$F_1 = 1 - e^{-a\eta}.$$

Similarly, (5.42) reduces to

$$(f)' = f',$$

$$(f')' = f'',$$

and (5.59)

$$(f'')' = -\left(\frac{f+\varepsilon F_1'}{1+\varepsilon F_1}\right)(f'') - \left(\frac{\beta}{1+\varepsilon F_1}\right)(1-f'^2),$$

where

$$F_1 = 1 - \exp\{-a(2-\beta)^{1/2}\eta\}.$$

The above systems are solved by the NAG Fortran library routine (D02HAF), which solves the two-point boundary-value problem for a system of N ordinary differential equations in an specified range (A,B), using Merson's integration method and a Newton iteration in a shooting and matching technique [38]. This routine requires that the N known boundary values and an estimate of the remaining N boundary values for the dependent variables at A and B are specified initially.

By using the actual and the estimated values at A, the routine integrates the equations from A to B, and compares the values from integration with those specified at B. The differences (usually known as residuals) should be zero for the true solution. The generalised Newton method is used to reduce these residuals to zero (or near zero, depending on the size of the acceptable error), by calculating the corrections to the estimated boundary values. This process is repeated iteratively until convergence is obtained.

The order of error we specified for the residuals was 10^{-5}. In most cases the convergence was achieved after a few iterations. The results were checked by varying the order of error and also by reproducing the solutions of the Blasius and the Falkner-Skan equations, i.e. putting $\varepsilon = 0$.

One difficulty we experienced was that since the range of integration goes from zero to infinity, we had to approximate the endpoint at infinity by a finite value, where the solution was expected to reach its asymptotic state. After many trials, it was found that for an upper range of integration of about $\eta = 8$, rapid convergence was achieved in most cases.

Let us first present the solutions to the simpler system (5.58), with the boundary conditions (5.44). This system represents the turbulent boundary layer flow along a flat plate at zero incidence, and contains two parameters, namely a and ε . The former, as mentioned before, determines the rate at which the profiles fall in with the free-stream flow. The parameter ε can be thought of as a measure of the level of turbulence present in the flow. When ε or a are zero, the problem reduces to the laminar flow (Blasius Eqn. Fig. 5.1).

Since $\mathcal{E} = Rc_1 b^3$, we note that while the parameter b was assumed small, R may take large values. Hence, if c_1 is of moderate size, then $\mathcal{E}$ is not expected to be of very large or very small magnitudes.

In the following pages, the effects of $\mathcal{E}$ and a on the solution are illustrated. Figure 5.1, shows the laminar flow solutions, in which the stream function f, the mean velocity f', and the shear stress (per unit of viscosity) f'', are plotted against the distance from the boundary. Figures 5.1, together with 5.2 and 5.3, show the variations of f and its derivatives with $\mathcal{E}$, for a fixed value of a. The effects of the variations in a, while $\mathcal{E}$ is kept fixed, is shown by figures 5.3, 5.4 and 5.5.

It can be seen that as $\mathcal{E}$ increases, it does not bring about a great change in the stream function, f. But the f" variable which represents the sum of the laminar and turbulent stresses, appears to be increasing with $\mathcal{E}$ near the boundary and diminishing at greater distances away from the wall. This confirms the fact that in the vicinity of a wall the laminar and turbulent stresses are both contributing, and hence the increase, whereas in the outer regions where the laminar stresses have diminished, the turbulent stresses are still present and decaying at a slower rate. The effects of $\mathcal{E}$ and a on the mean velocity, are better illustrated by figures 5.6 and 5.7, respectively. It is observed that for larger values of $\mathcal{E}$ and a, the velocity approaches its asymptotic state at greater heights, which implies that the boundary layer thickness becomes larger in turbulent flows.

The variation of the turbulent shear-stress τ^*, which is given by

$$\sqrt{R}\,\tau^{*} = \zeta^{-1/2}\,\varepsilon\,(1-e^{-\alpha\eta})\,f', \tag{5.60}$$

where ζ is the distance along the wall, measured from the leading edge of the plate, is presented by figure 5.8. As expected , the turbulent shear-stress rises sharply near the wall, and gradually decays as the free-stream region of the flow is approached.

The expression (5.60) is obtained by taking the second term on the r.h.s. of (5.25), (which represents the gradient of the turbulent shear-stress), and replacing the volume integral by its estimate (5.33). We note that for this special case α =0.

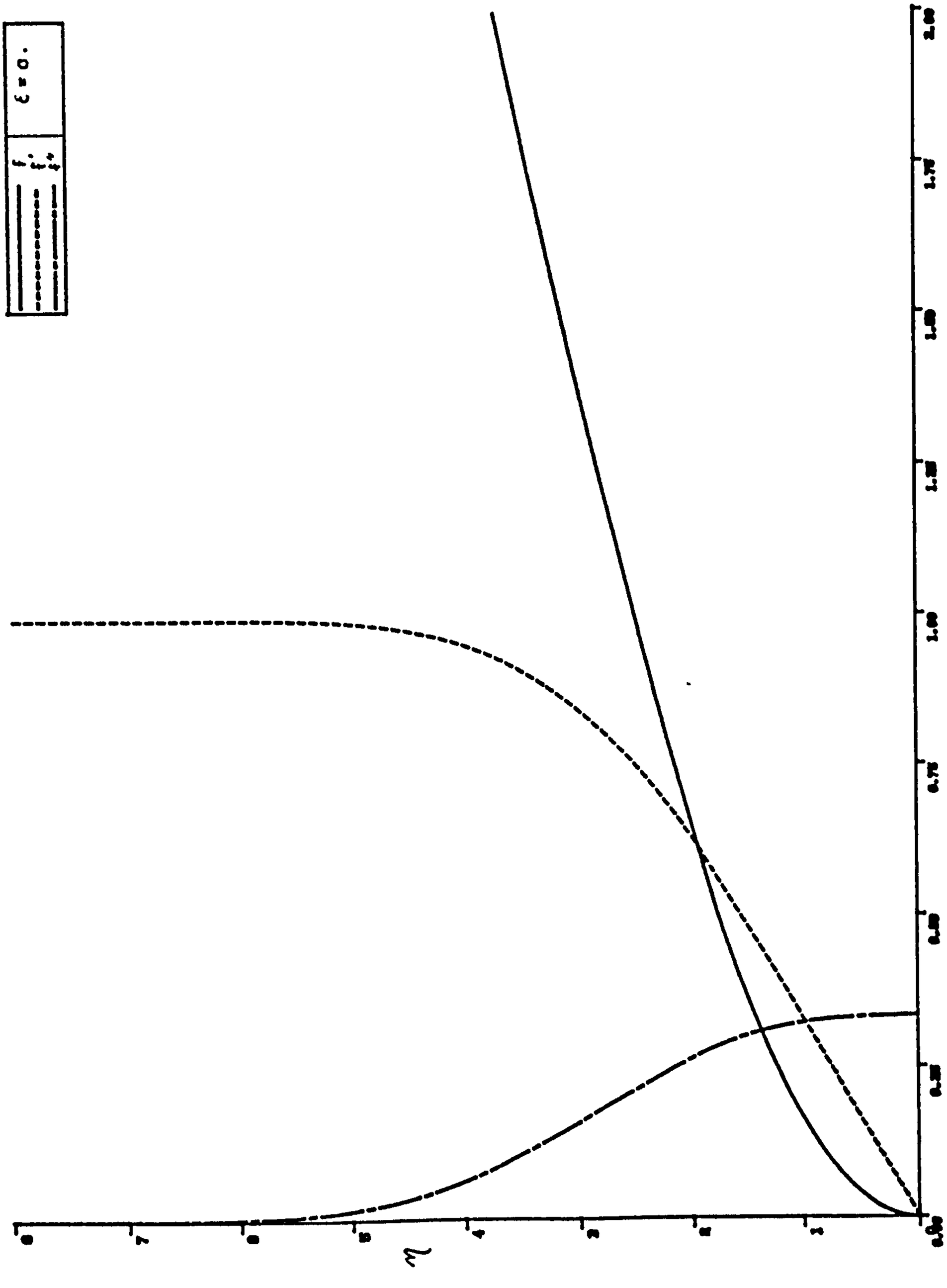

Fig. 5.1 The laminar solution as given by the Blasius eqn. $f'''+1/2ff''=0$.

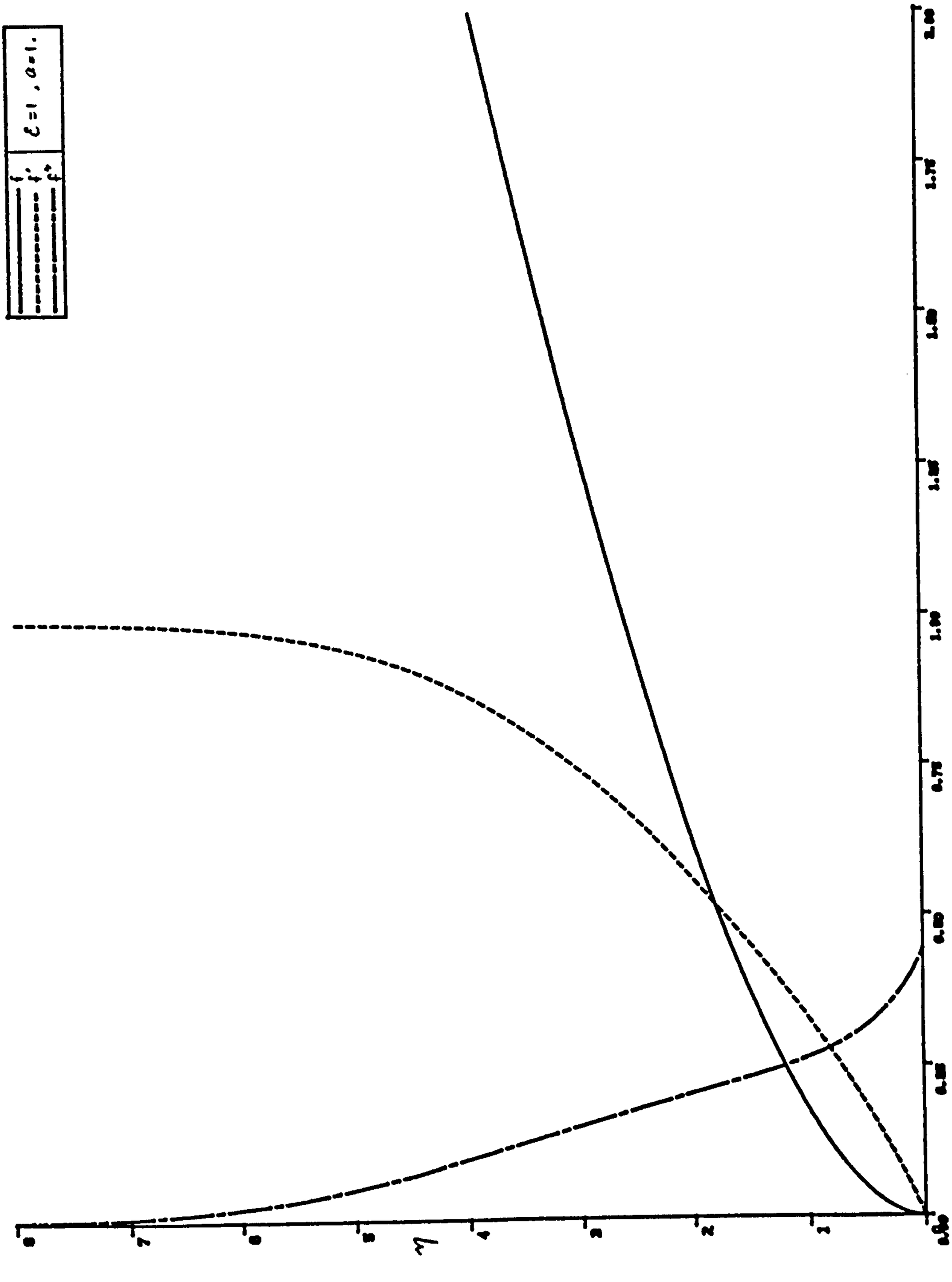

Fig. 5.2 Plots of f and its derivatives, eqn. (5.45), for $\varepsilon = 1$, $a = 1$.

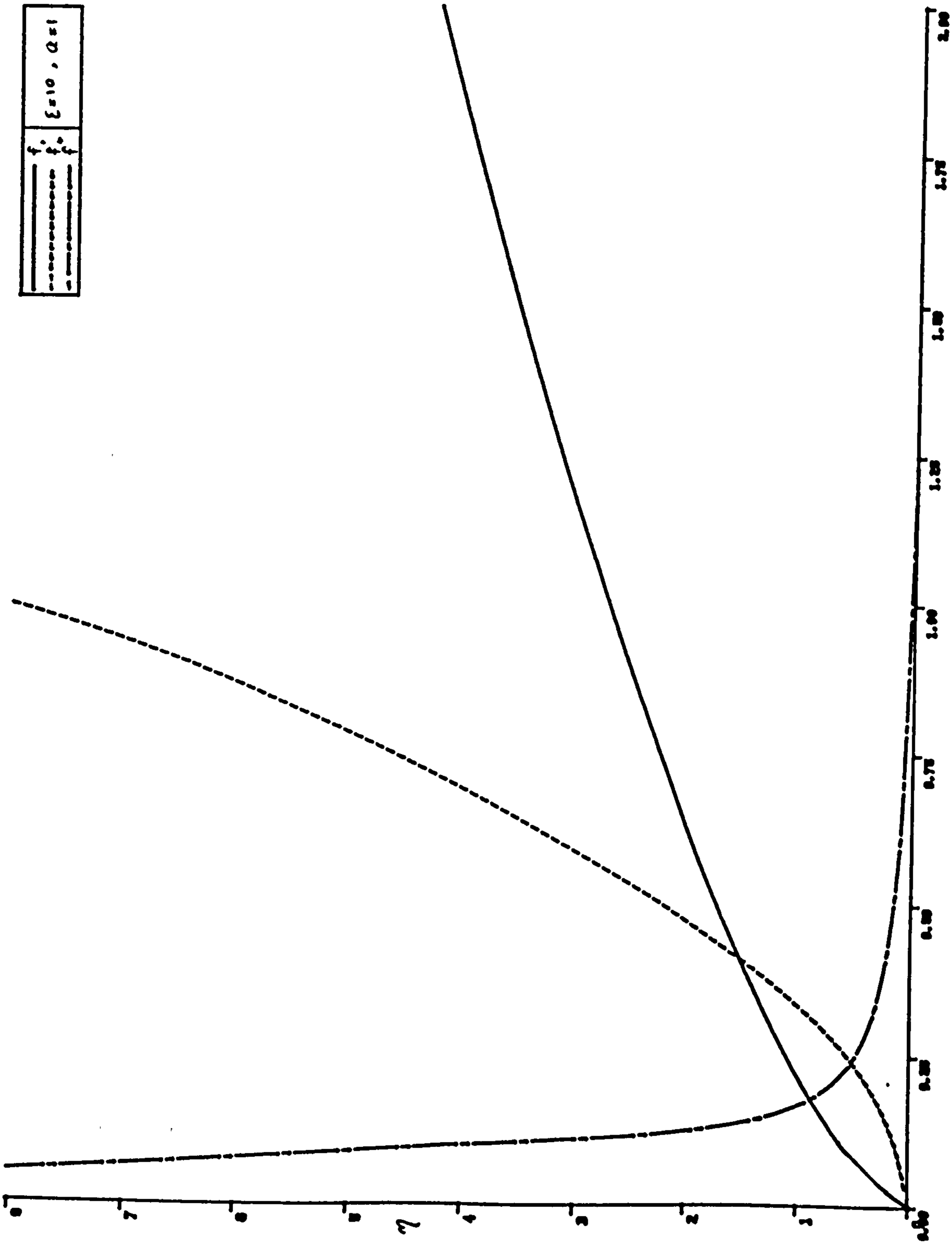

Fig. 5.3 Plots of f and its derivatives, eqn. (5.45), for $\varepsilon = 10$, $a = 1$.

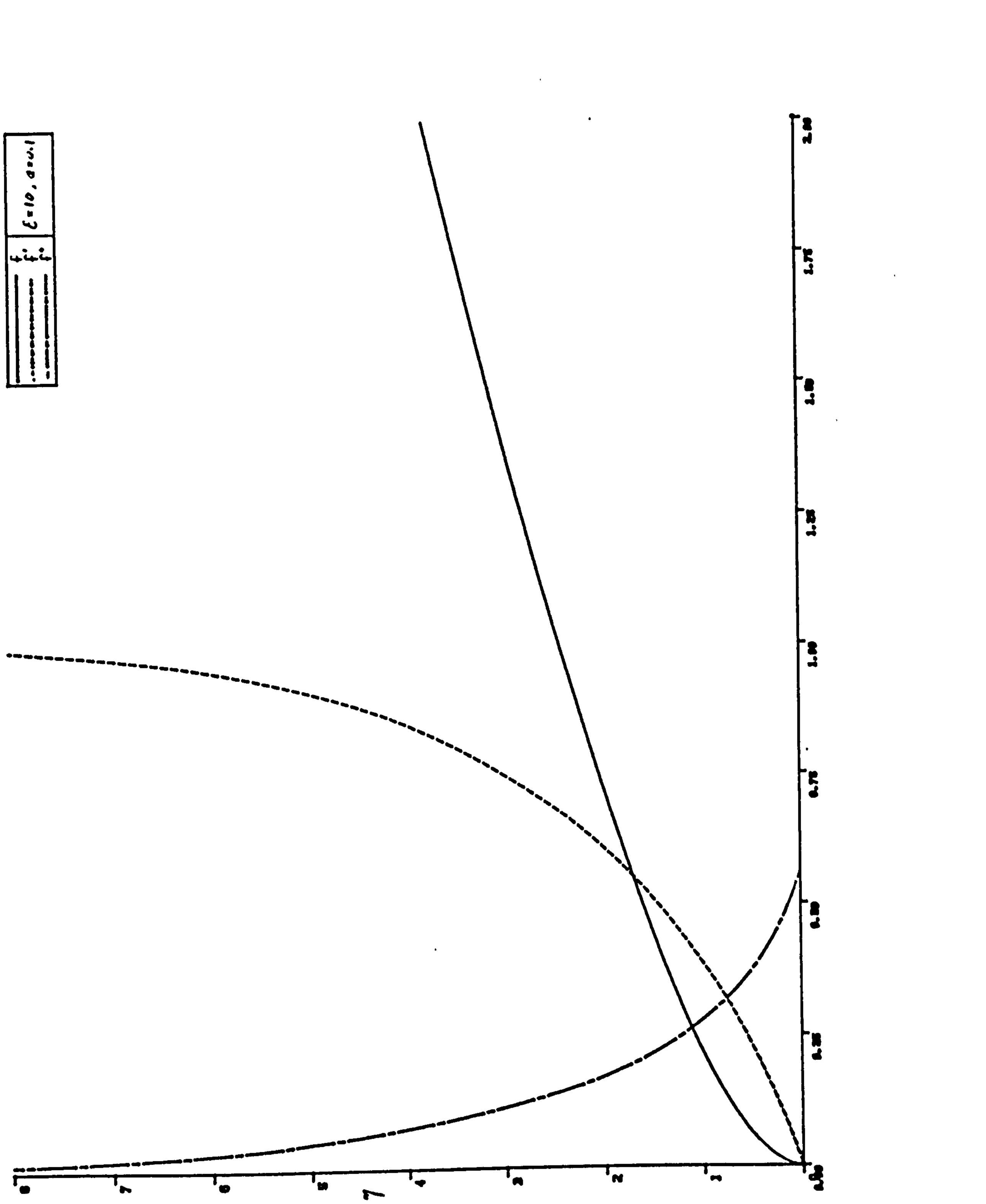

Fig. 5.4 Plots of f and its derivatives, eqn. (5.45), for $\varepsilon = 10$, $\alpha = 0.1$.

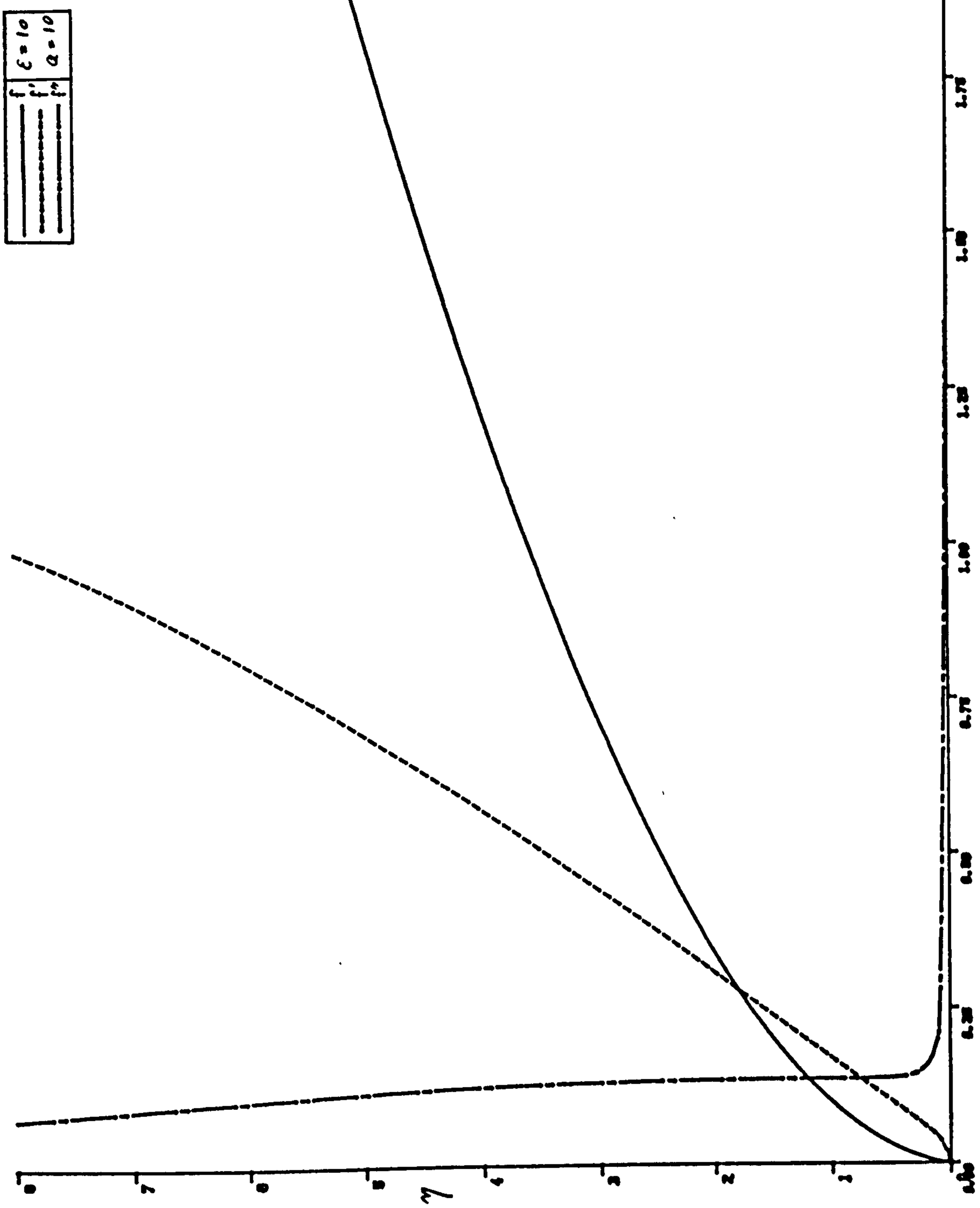

Fig. 5.5 Plots of f and its derivatives, eqn. (5.45), for $\varepsilon = 10$, $\alpha = 10$.

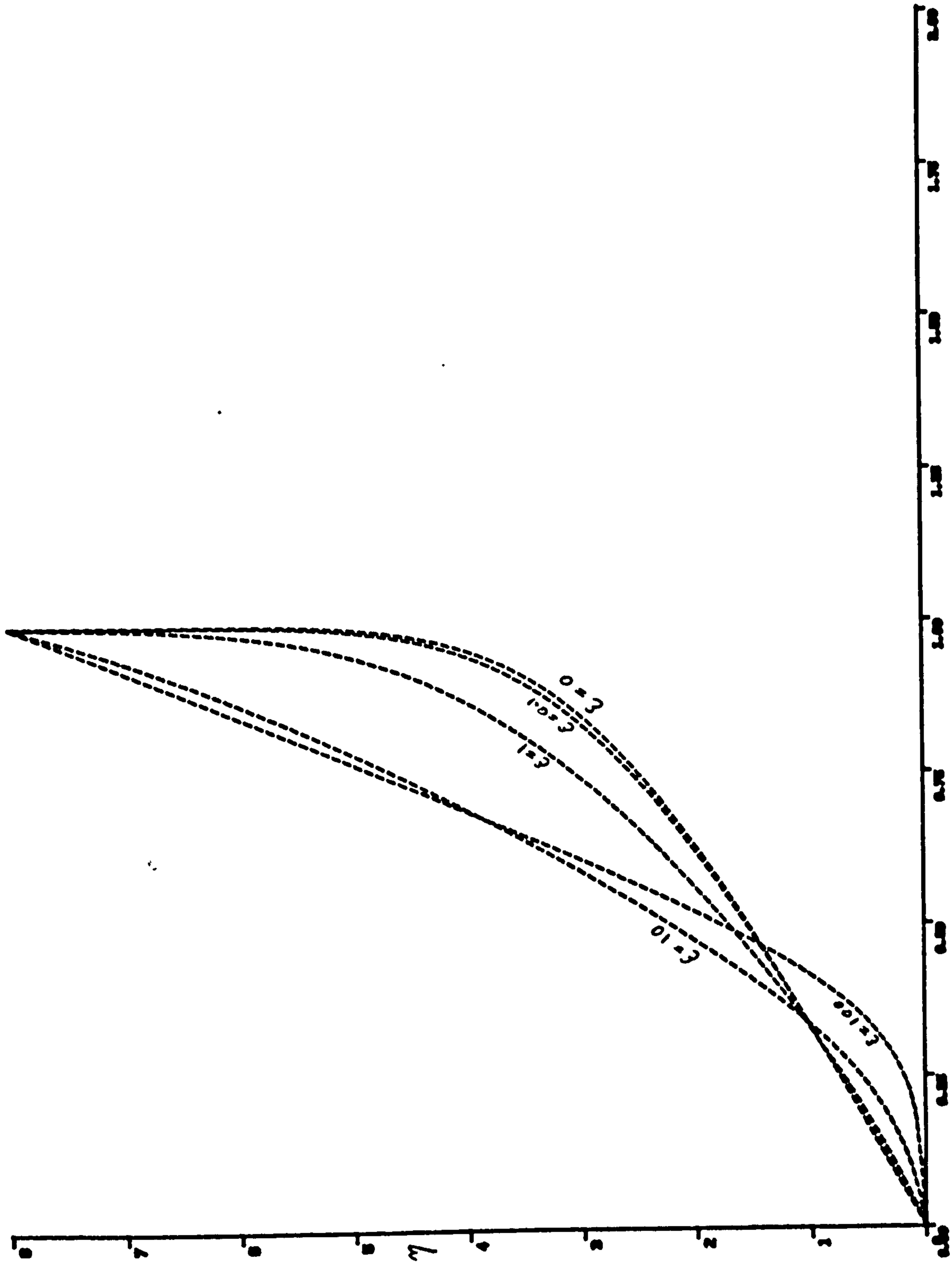

Fig. 5.6 Variation of the mean velocity (f′) with ε , for $a=1$.

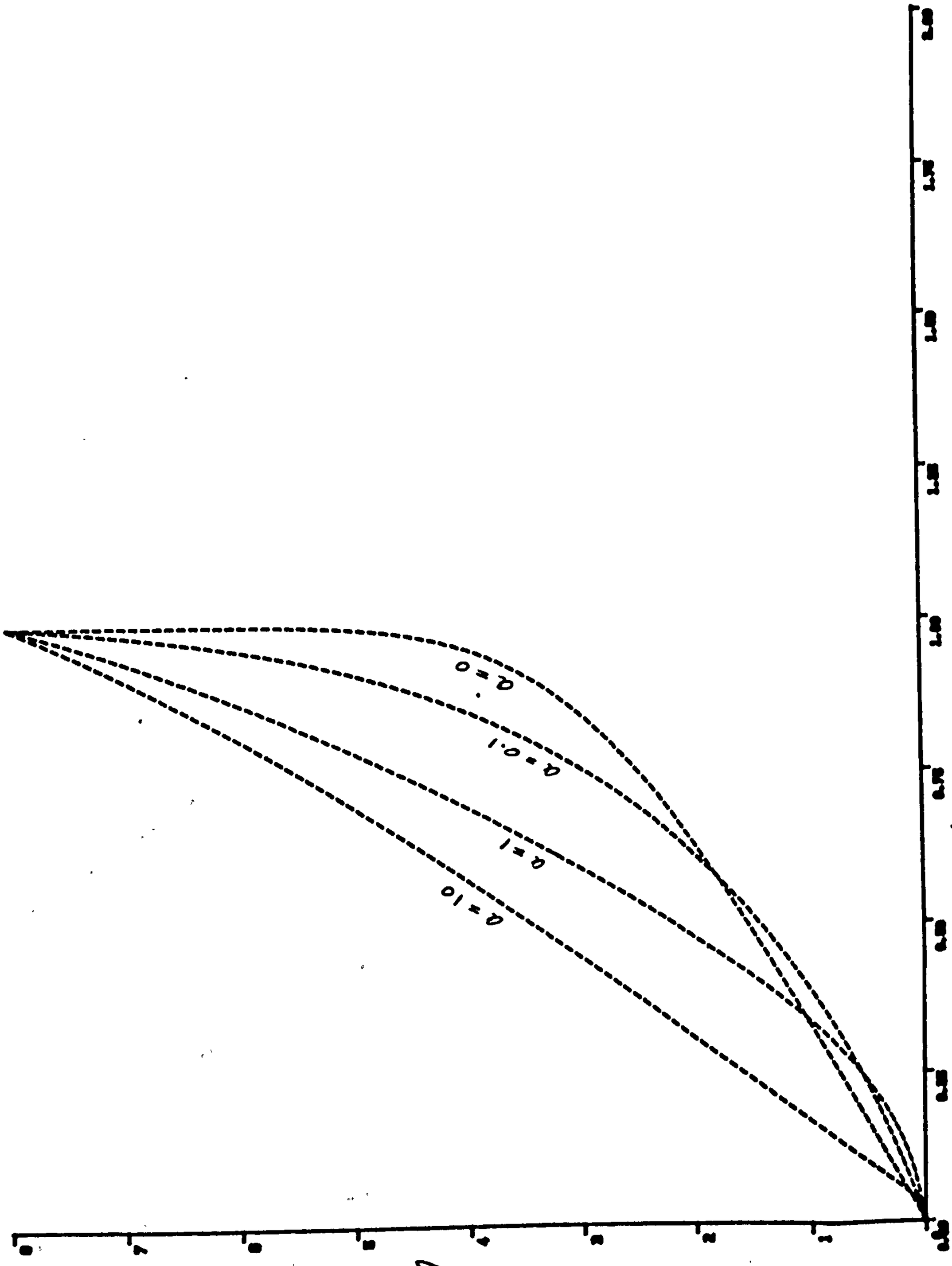

Fig. 5.7 Variation of the mean velocity (f') with α, for $\mathcal{E}=10$.

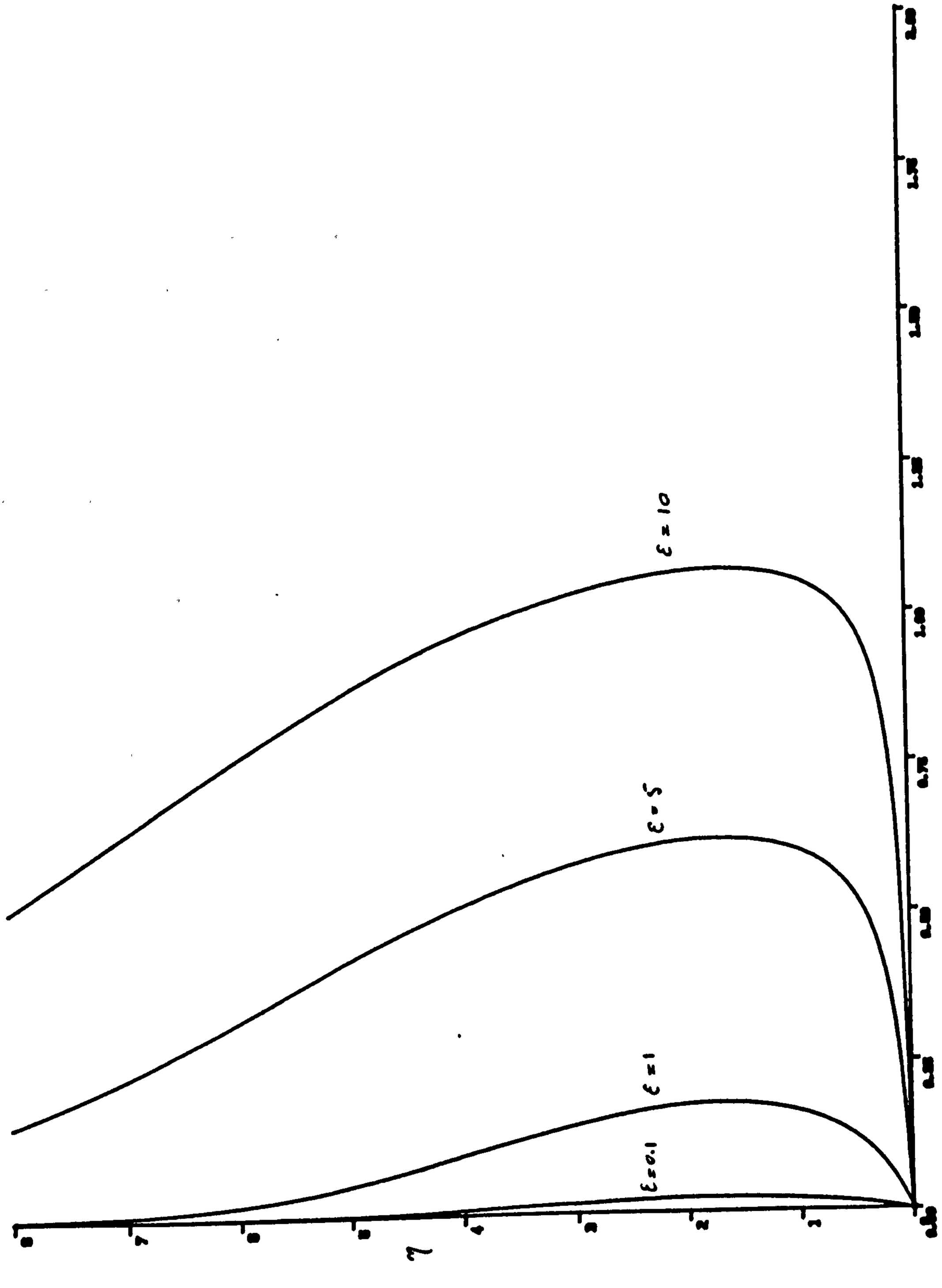

Fig. 5.8 Variation of the turbulent shear-stress with ε, for $a=1$, $\sigma=1$.

The system (5.59), corresponding to the equation (5.42), describes the turbulent boundary layer flow past a wedge. The solutions to this system satisfy he boundary conditions (5.44).

In addition to the parameters α and ε , the solutions in this case, are also dependent on the choice of β . This parameter varies with the angle of the wedge, and hence with the pressure gradient along the direction of the mean flow. It may take both positive and negative values, depending on whether the flow is accelerating ($\beta>0$) or decelerating ($\beta<0$). For β <-0.1988, separation occurs in laminar boundary layers, and a point of inflexion appears in the velocity profiles [29].

To demonstrate the effects of the parameters, we shall again present the solutions by a number of plots, in which the values of the parameters are varied. To avoid having page after page of curves, only a selection of different values of β are included, and they appear in figures 5.9 to 5.13 in decreasing order, ranging from 1 to -1.5 . The parameters α and ε are kept fixed at α =1 and ε =10.

As β decreases, it can be seen that up to β =-1, while the stream functions grow in amplitude, the velocity profiles' approach to unity becomes slower, and the shear-stresses which decrease at the wall, decay at greater heights away from the boundary.

When β =-1.5, the whole pattern of the solution changes, and the velocity profile overshoots. For the same values of β and α , no such overshoot occurs, when ε is raised to about 50, and the profiles we get in this case are almost identical to those presented in figure 5.12 .

The effects of a and ε are similar to those observed in the previous case. As an example, the variation of the profiles with ε , for fixed values of β =-0.1 and a =1, may be seen by comparing figures 5.14 and 5.15, in which ε is chosen to be 0.1 and 10, respectively. Figures 5.16 and 5.17 show the effects of a, when β and ε are unchanged.

in figure 5.18, the behaviour of the velocity profiles with the variations in ε is compared. The effects of the variations of β on the velocity are illustrated in figure 5.19 . As can be seen, when β =-0.2, the corresponding profile exhibits a point of inflexion, which indicates the occurence of the boundary layer separation.

The influence of the parameters on the turbulent shear-stress τ^*, are shown by figures 5.20, 5.21 and 5.22. The expression for the shear-stress, at any distance ζ ,from the forward stagnation point, is

$$\sqrt{R}\,\tau^* = \frac{\varepsilon}{(2-\beta)}\left[\,1 - e^{-a\eta(2-\beta)^{1/2}}\,\right]\zeta^{\frac{1-2\beta}{\beta-2}} f'' . \qquad (5.61)$$

It is noted that an increase in β , causes the turbulent shear-stress to rise near the wall, and the rate of decay becomes slightly faster.

The above expression is again obtained from the second term on the r.h.s. of (5.25).

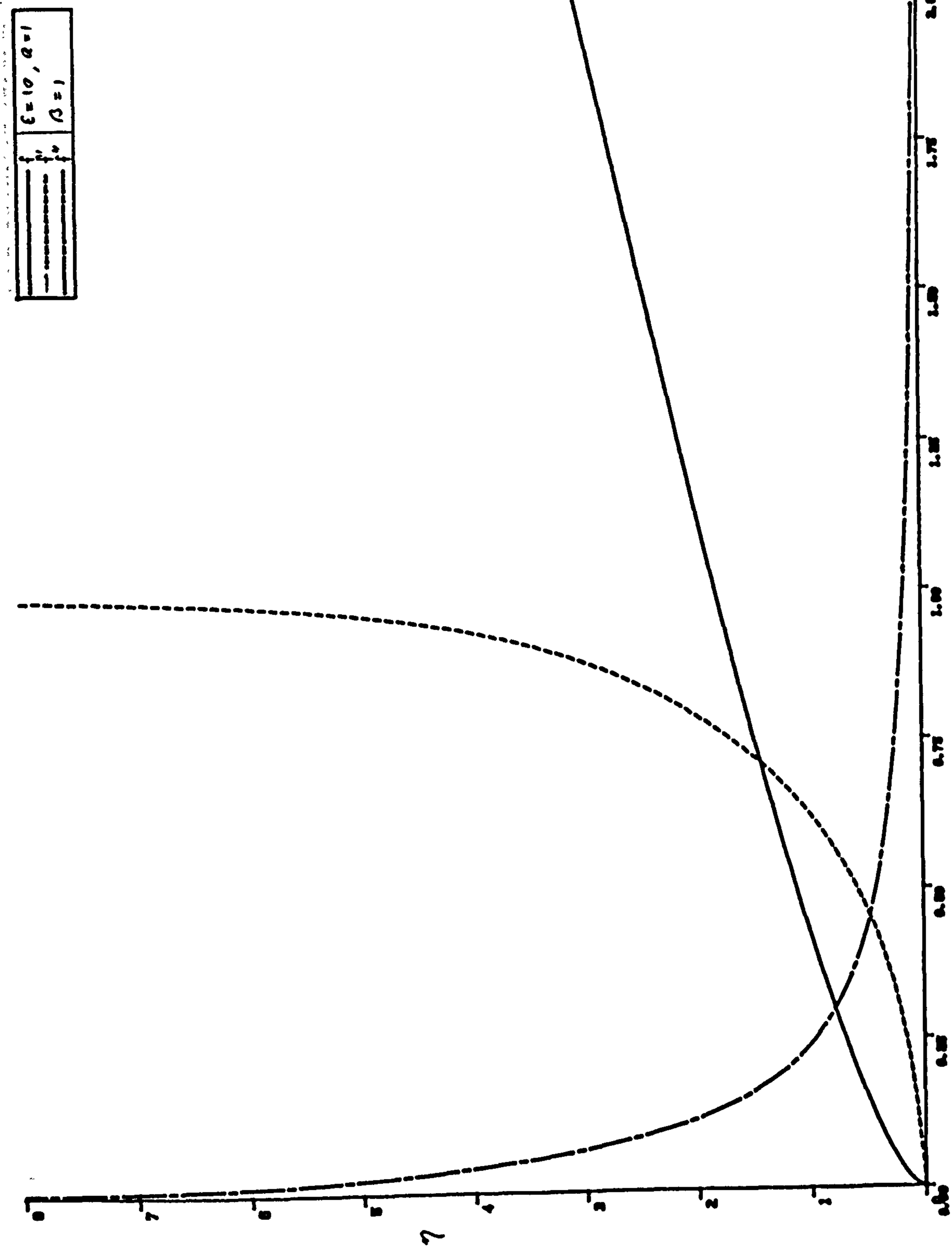

Fig. 5.9 Plots of f and its derivatives, eqn. (5.42), for $\varepsilon = 10$, $\alpha = 1$ and $\beta = 1$.

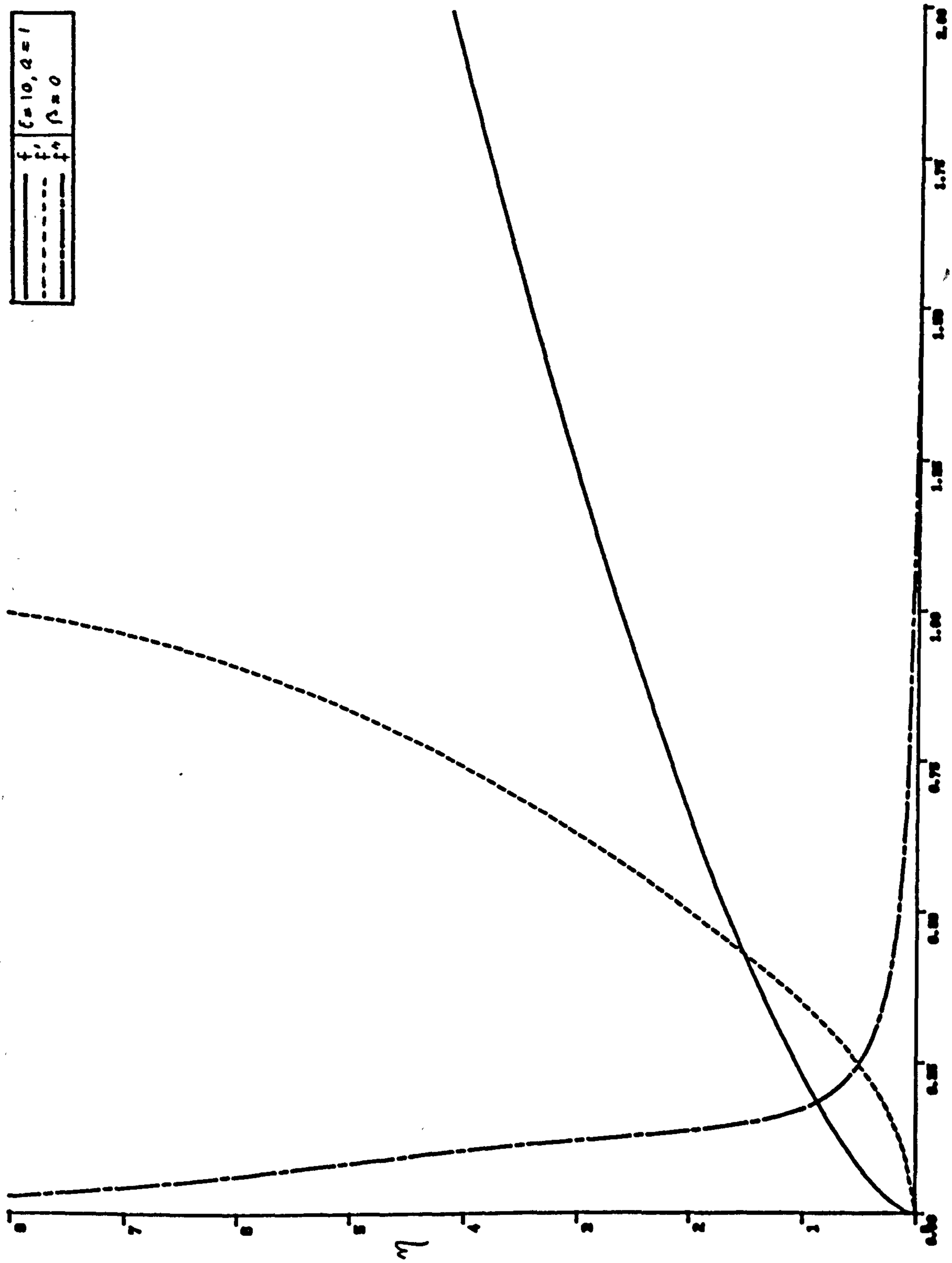

Fig. 5.10 Plots of f and its derivatives, eqn. (5.42), for $\varepsilon = 10$, $\alpha = 1$ and $\beta = 0$.

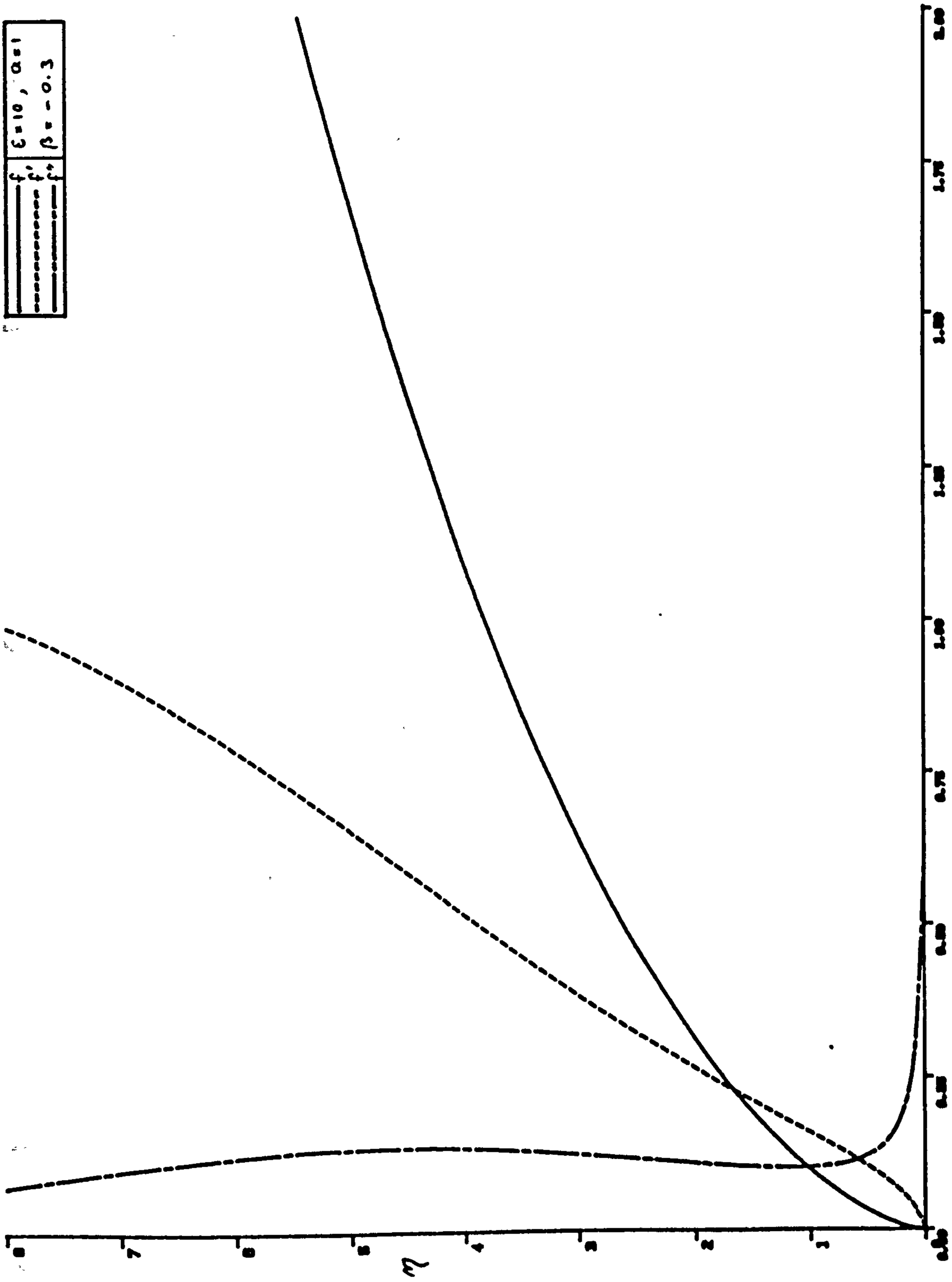

Fig. 5.11 Plots of f and its derivatives, eqn. (5.42), for $\varepsilon = 10$, $\alpha = 1$ and $\beta = -0.3$.

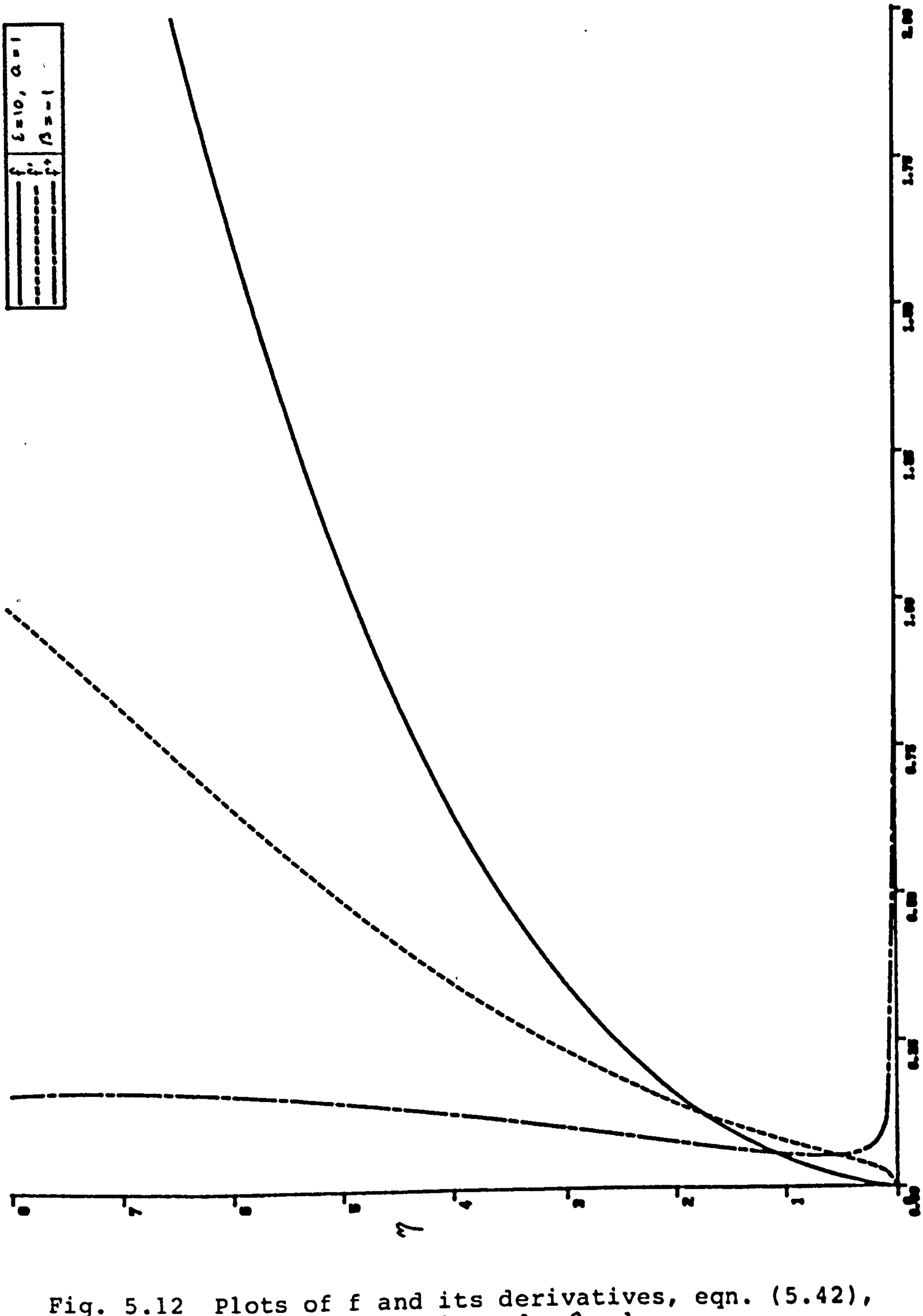

Fig. 5.12 Plots of f and its derivatives, eqn. (5.42), for $\varepsilon = 10$, $a = 1$ and $\beta = -1$.

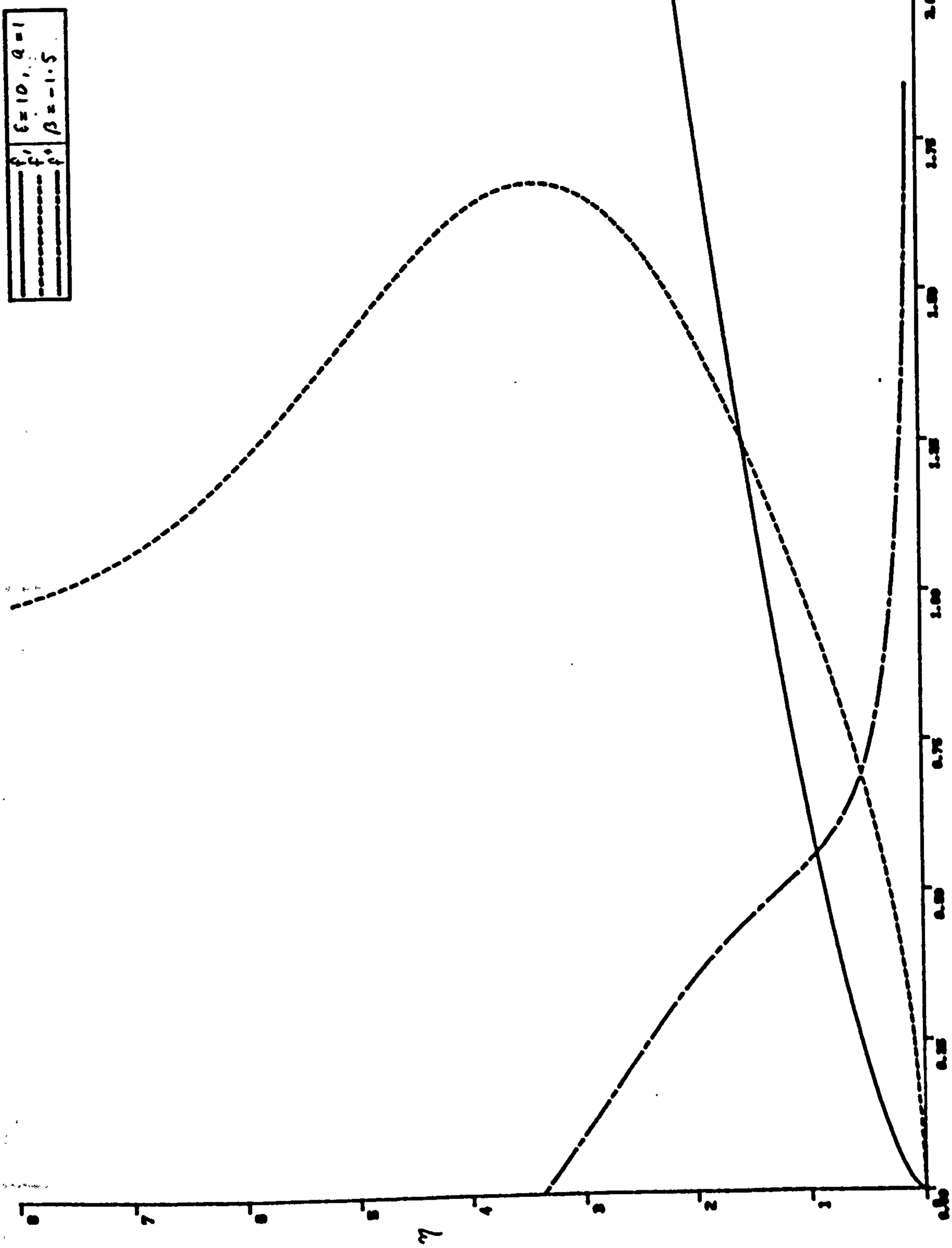

Fig. 5.13 Plots of f and its derivatives, eqn. (5.42), for $\varepsilon = 10$, $a = 1$ and $\beta = -1.5$.

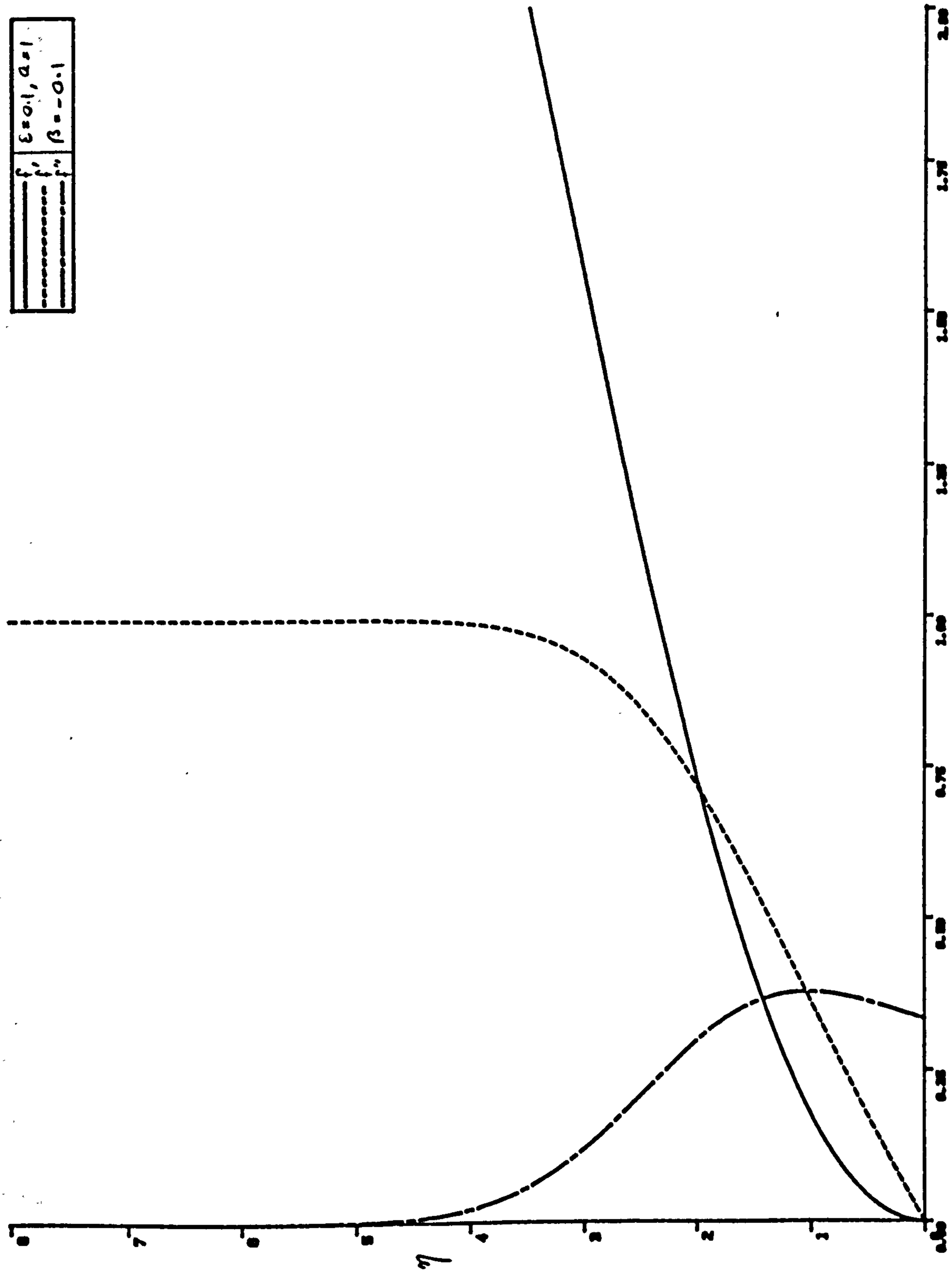

Fig. 5.14 Plots of f and its derivatives, eqn. (5.42), for $\varepsilon = 0.1$, $a = 1$ and $\beta = -0.1$.

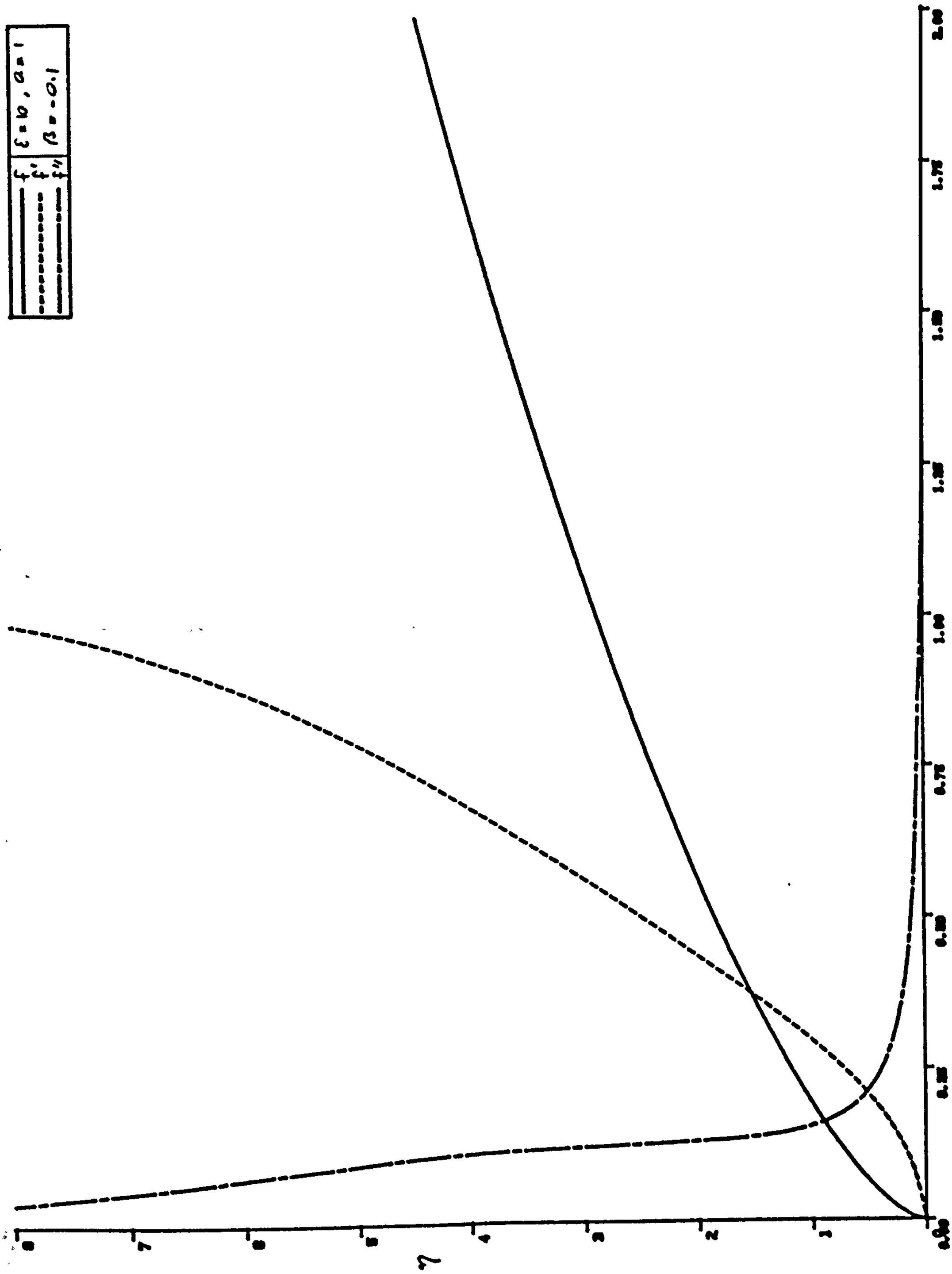

Fig. 5.15 Plots of f and its derivatives, eqn. (5.42), for $\varepsilon = 10$, $\alpha = 1$ and $\beta = -0.1$.

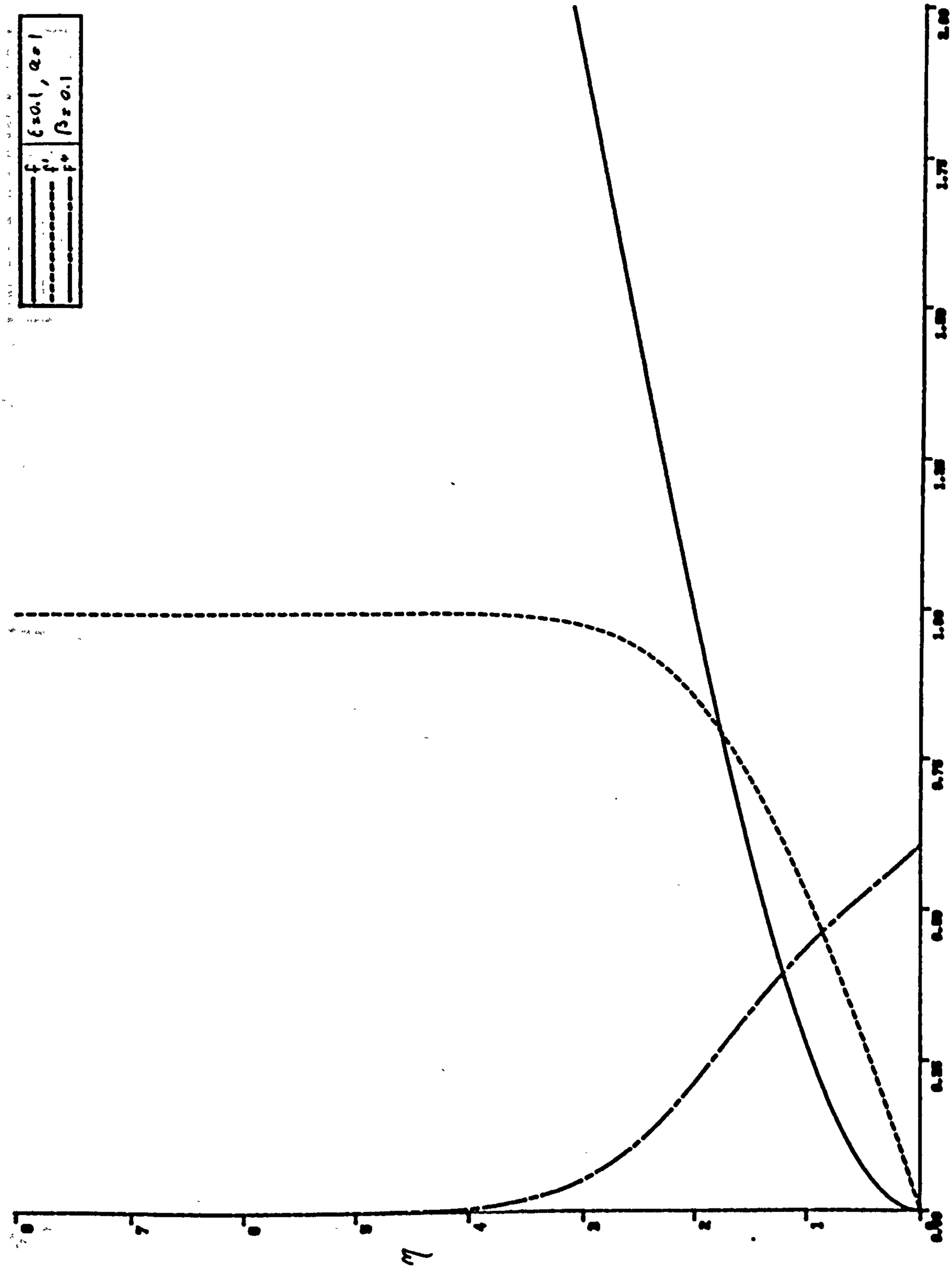

Fig. 5.16 Plots of f and its derivatives, eqn. (5.42), for $\varepsilon = 0.1$, $\alpha = 1$ and $\beta = 0.1$.

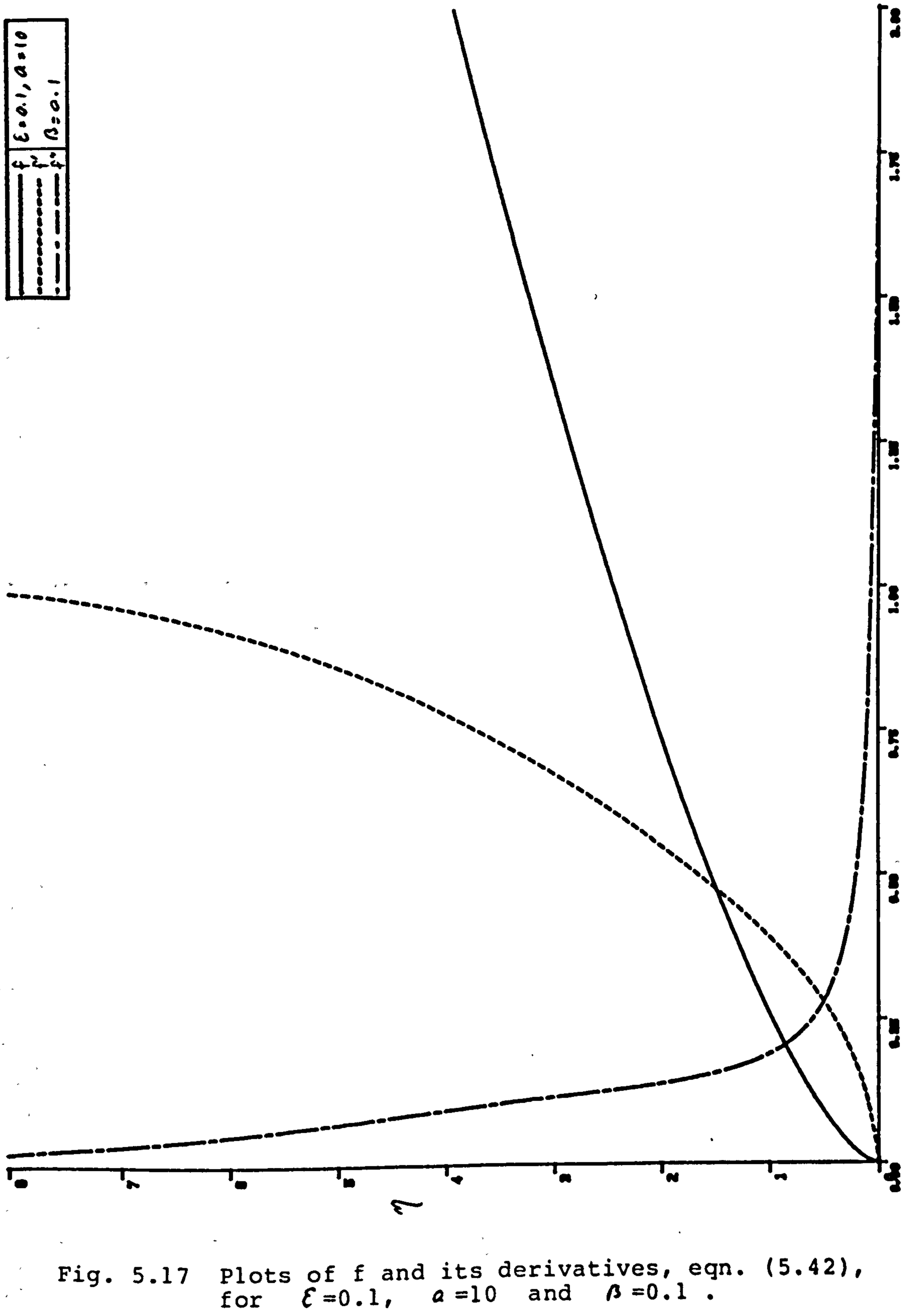

Fig. 5.17 Plots of f and its derivatives, eqn. (5.42), for $\varepsilon = 0.1$, $a = 10$ and $\beta = 0.1$.

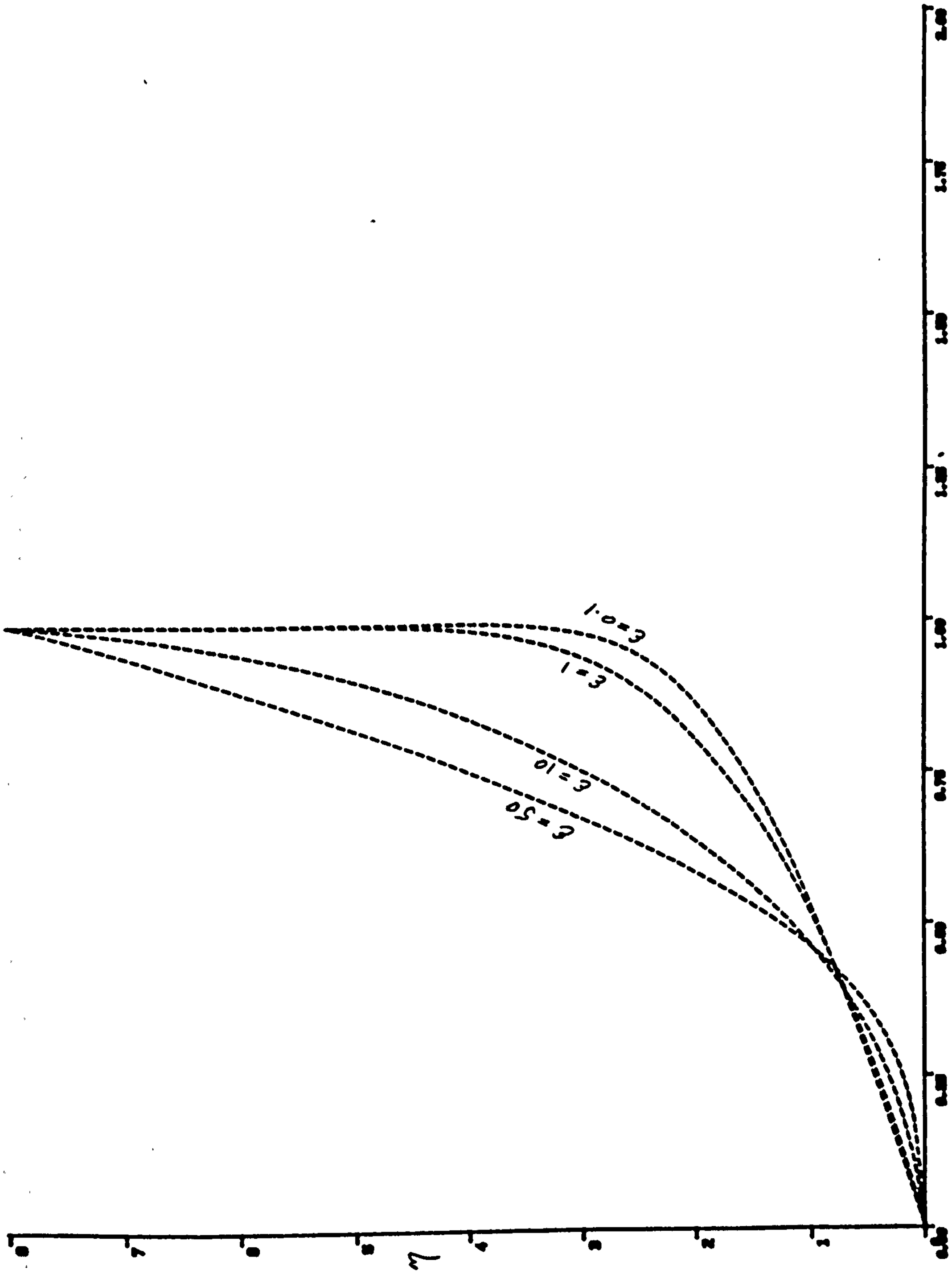

Fig. 5.18 Variation of the mean velocity (f') with η, for α =0.5 and β =0.1 .

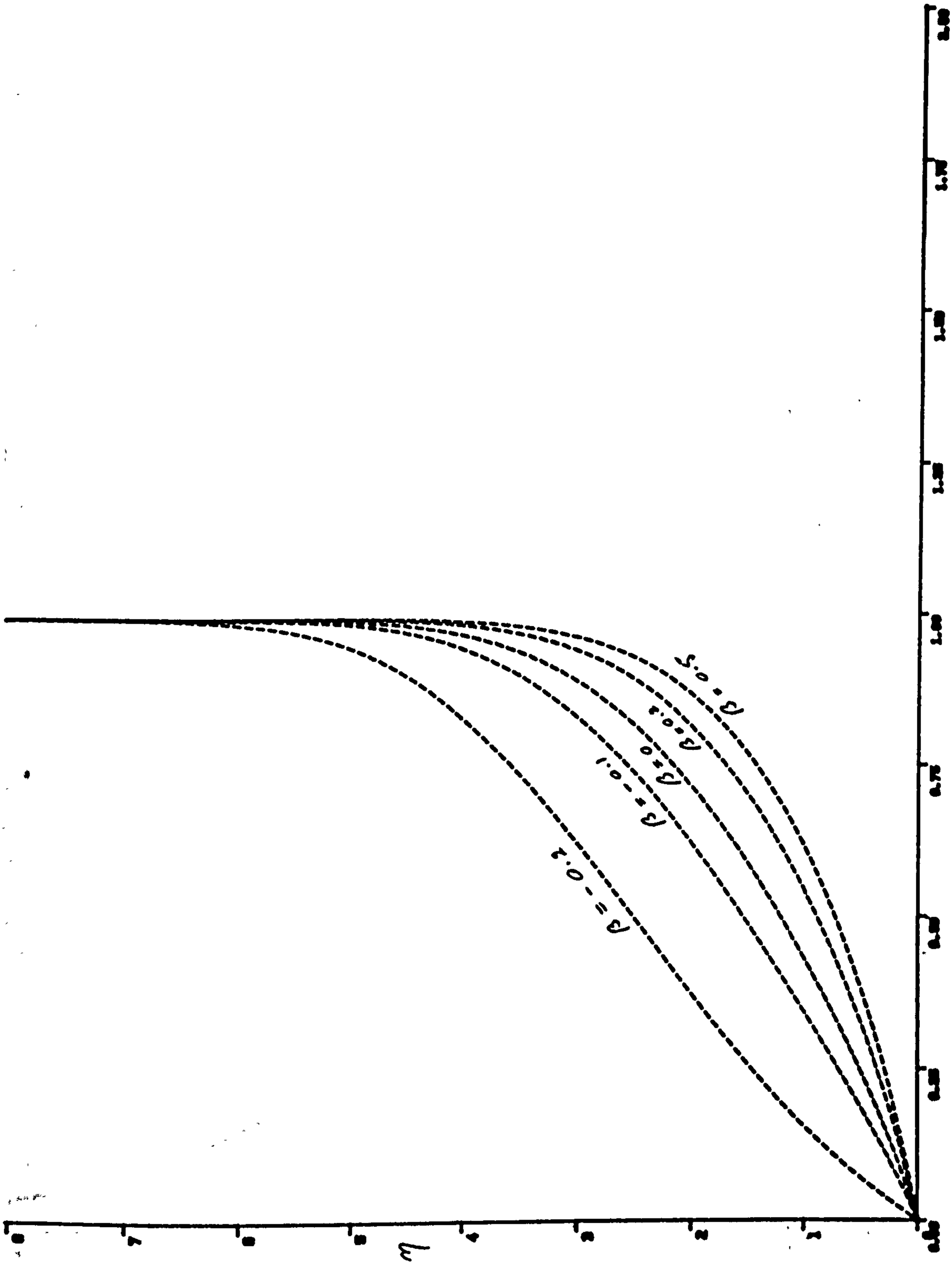

Fig. 5.19 Variation of the mean velocity (f') with β, for $\xi = 1$ and $\alpha = 1$.

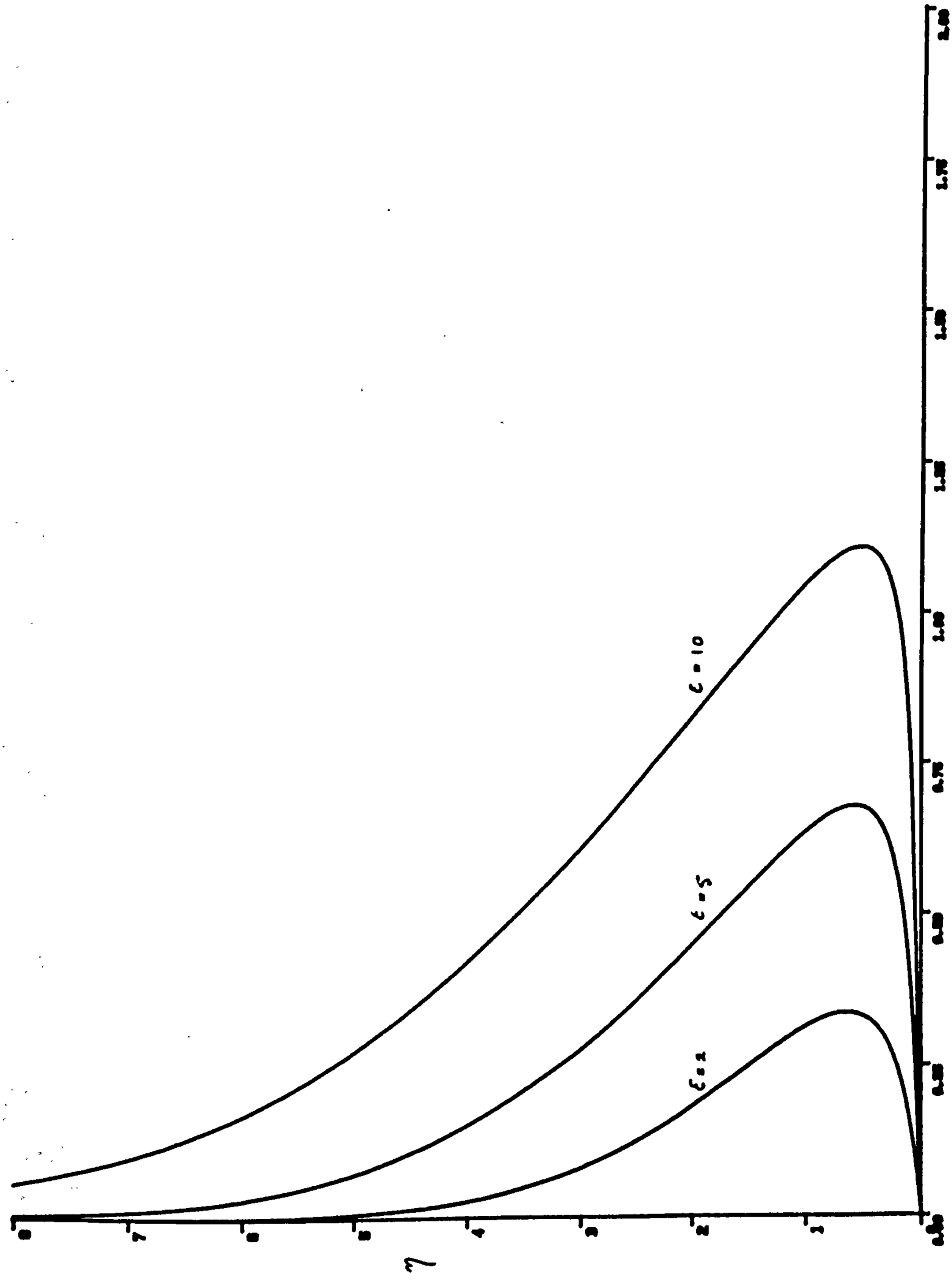

Fig. 5.20 Variation of the turbulent shear-stress with ε, for $\alpha = 1$, $\beta = 0.5$ and $\zeta = 1$.

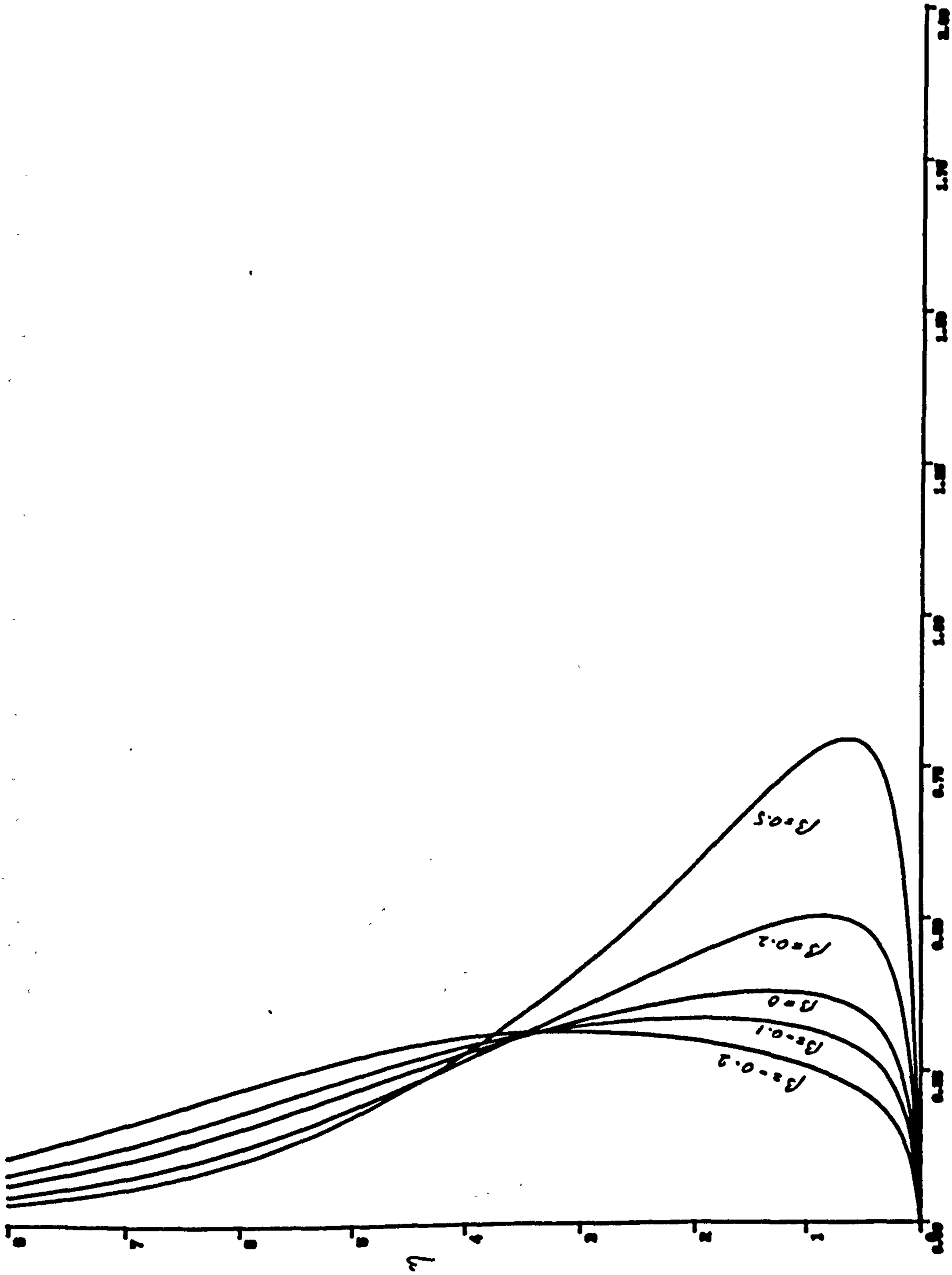

Fig. 5.21 Variation of the turbulent shear-stress with β, for $\alpha = 0.5$, $\mathcal{E} = 10$ and $\zeta = 2$.

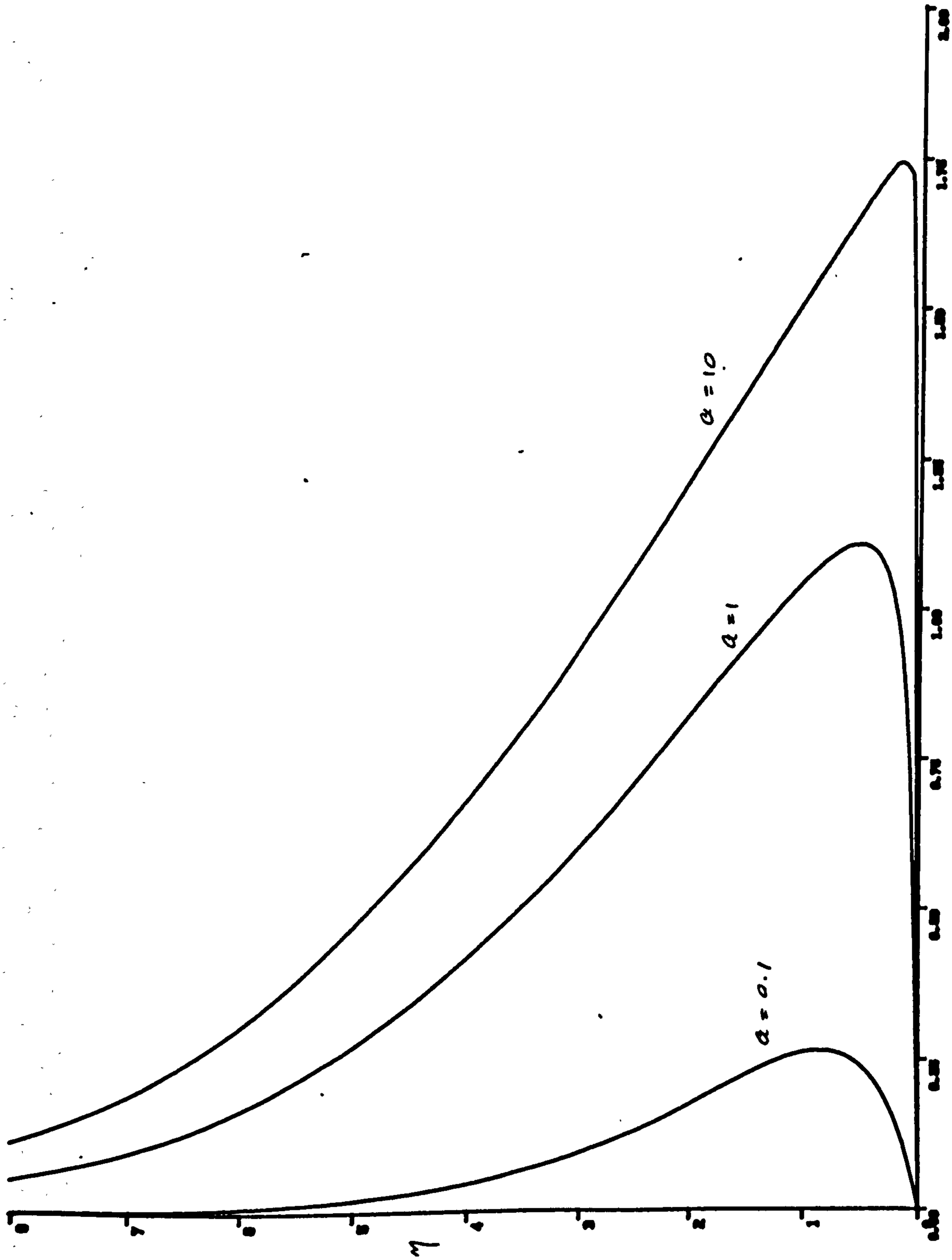

Fig. 5.22 Variation of the turbulent shear-stress with α, for $\mathcal{E}=10$, $\beta=0.5$ and $\zeta=1$.

6. CONCLUSION.

In this final chapter various aspects of the work presented in this report are summarised.

In chapter one, areas of difficulties associated with turbulence were identified and some of the most popular turbulence models and various approaches to the problem, (from the earliest models to the recent computer simulation methods), were briefly discussed. It was noted that the non-local effects of turbulence play an important role in determining the structure of the phenomenon. Since, such effects are only catered for in the more elaborate and complex models, we proposed a relatively simple mathematical model in which the structure of turbulence is described by averaging the effects of the eddies of various scales over the whole volume of flow. The model assumes that the turbulent stresses can be represented in a form analogous to the laminar stresses and the correlations between the point in question with those at other locations in the flow, follow a distribution which is assumed Gaussian.

The correlation function which in steady flows varies with the space and position, was presented by the products of a shape function and a position function. The rate at which turbulence is drawn into the free-stream region of the flow was presented by the shape function which assumed various forms, depending on the type of flow under consideration. The variation of the correlations with respect to the position in the flow was assumed isotropic with rapid decay and hence presented by the Gaussian distribution function.

The model was introduced in chapter two, where the

properties of the shape and the position functions were listed. In the same chapter the basic assumptions and the equations governing the motion of a viscous Newtonian fluid, together with some of their important properties were presented.

The application of the model to the fully developed steady Poiseuille flows between parallel plates and through circular pipes was investigated in chapters three and four, respectively. Having transformed the N-S equations into cylindrical polar coordinates in the case of the pipe flow, we showed how the equations may be simplified in each case. The chosen method of solving the equations of motion for both problems were similar and appeared to be dependent on the size of a flow parameter, ε . For sufficiently small values of ε , we showed how a solution could be obtained in the form of a Neumann series. The more interesting case of large ε , was studied in detail and approximate analytical solutions for the mean velocities were obtained for each problem. The technique we employed was to transform the equations via the integral transform methods and look for the solutions in the form of asymptotic series. Since the equations were in the integral form, we made the assumption that b>>1, (where b is the dimensionless standard deviation parameter in the Gaussian distribution function), and employed Watson's lemma to find estimates for the integrals.

Watson's Lemma has been frequently used in estimating the integrals in both chapters three and four. Closer inspection of such integrals at later stages of the work revealed that the estimates given by Watson's lemma were in fact exact solutions, provided the power series in the

integrands converged. As an example, the convergence of one such series is considered in the appendix A5.

The terms in the asymptotic series solutions were determined by successive approximations, and since $1/b<<1$, only the first few terms were retained in the final solutions.

Having obtained approximate analytic solutions for the mean velocities, the method of determining the model constants were described. In the case of the pipe flow problem, we showed how the comparison of the frictional resistance (deduced from our solution) with the Prandtl's universal law could be used in this respect.

With the appropriate numerical values for the model constants, the mean velocity profiles predicted by the model were compared with those given by the universal laws of Von Kármán and Prandtl. The agreement appeared to be quite good, in particular for the case of the flow between parallel flat plates. In the pipe flow problem however, deviation from the universal laws and from experiment were observed as the profiles approached the boundary. But at the boundary itself where the universal laws showed indefinite values, our predictions were found capable of describing the velocity, and finite values were obtained there.

The effects of the variations in the Reynolds number on the velocity profiles were examined and in both problems it was observed that the profiles became fuller with the increase in the Reynolds number. By comparing the behaviour of the profiles when the model constants were varied, we were able to study the sensitivity of the solutions and in most cases it was possible to establish a range within which

the constants could vary.

As the model appeared capable of producing satisfactory results for the relatively simple problems of Poiseuille channel and pipe flows, we chose the more complex problem of turbulent boundary layer flow along the surface of a solid body, to test the model further.

In chapter five, following a brief discussion on the similarity solutions of the laminar boundary layers, we outlined the usual methods of calculating the turbulent boundary layers. Noting the complications associated with such methods, namely, having to use different closure assumptions in different regions of the boundary layer, we proposed to derive equations similar to the Blasius and the Falkner-Skan, which could efficiently calculate every region of a turbulent boundry layer.

Beginning with the more general problem of turbulent B-L flow past a wedge, we described how the N-S equations may be approximated in a way analogous to the laminar flows, to give the B-L equations. Representing the equations in dimensionless forms, we introduced the similarity variables and showed how the B-L equations could be reduced to give an ordinary differential equation of order three, similar to that of the Falkner-Skan equation. The volume integral was evaluated approximately, by making a series of transformations and using power series expansions. On the assumption that $b<<1$, it was showm that the volume integral, if approximated to the first order, would make the equations independent of the space coordinate along the wall and hence form the basis for obtaining similar solutions. It was also shown that if the pressure gradient was absent, the problem

would reduce to the special case of B-L flow along a flat plate at zero incidence, for which an equation similar to that of Blasius was obtained.

Reducing these equations to a set of first order O.D.E's and applying the appropriate boundary conditions, enabled us to solve them numerically, by using a Nag Fortran library routine.

For the special case of $\beta = -1$, it was shown how an approximate analytic solution could be obtained by extending the existing solutions of the Falkner-Skan equation.

The numerical solutions were presented in the form of graphs for different values of the flow parameters. The effects of the variations in the parameters on the solutions and on the turbulent stresses, were also demonstrated and discussed for both equations.

The significance of these solutions lies in the fact that we have firstly shown that approximate similarity solutions to the turbulent boundary layers are possible, and secondly, such solutions can successfully predict the important features of a turbulent boundary layer (both in the inner and in the outer parts), for a variety of the flow parameters.

On the whole the model appears capable of describing the effects of the fluctuations on the mean motion adequately. Furthermore, the simplicity of the model, as was shown, makes approximate analytic solutions to the equations possible, and hence allowing a better insight into the problem of turbulence as a whole.

Another advantage of the model is its ability to describe an averaged picture of the structure of turbulence,

and hence better representing the three-dimensional character of the phenomenon.

On the disadvantages of the model, it may be argued that when the geometry of a flow becomes more complex, complications could develop when it comes to formulating a suitable shape function and when constructing the volume integral over which the correlations could be averaged. Further research in this connection, we believe, could improve the model and its range of applicability, and hence open up a whole new range of problems to which the model could be applied.

The predictions made for the mean velocity in the Poiseuille pipe flow problem, may also be improved by further investigating the expression representing the shape function. An increase in the rate of decay of this function near the boundaries, seems a possible area for further improvements.

It should also be mentioned that the determination of some of the integrals, leading to the asymptotic solutions for the Poiseuille channel and pipe flows, and the approximation of the volume integral in the boundary layer flow analysis, were based on the assumptions concerning the size of the model parameter b. Although, these assumptions were justified on the physical grounds, the question still remains over the validity and the accuracy of the results for the intermediate values of b. This aspect of the work is also worth some further investigation. Comparison with numerical solutions perhaps, could clarify some doubts.

APPENDIX A1

To evaluate

$$\bar{F}_1(s) = \int_{-\infty}^{\infty} e^{is\eta} F_1(\eta)\, d\eta .$$

Since $F_1 = 0$ for $|\eta| > 1$, we can write the above as

$$\bar{F}_1(s) = \int_{-1}^{1} e^{is\eta} F_1(\eta)\, d\eta .$$

Substituting for F_1 from (3.12), we obtain

$$\bar{F}_1(s) = e^{-a}\{\cosh a \int_{-1}^{1} e^{is\eta}\, d\eta - \int_{-1}^{1} e^{is\eta} \cosh a\eta\, d\eta\}.$$

The first integral in the above reduces to $2/s \sin s$. If I denotes the second integral, then integrating by parts gives

$$I = \frac{2}{s} \cosh a \sin s + \frac{2a}{s^2} \sinh a \cos s - \frac{a^2}{s^2} I .$$

Therefore

$$I = \frac{2}{a^2 + s^2} (s \cosh a \sin s + a \sinh a \cos s) .$$

Hence

$$\bar{F}(s) = e^{-a}\{ \frac{2}{s} \cosh a \sin s - \frac{2}{a^2 + s^2} (s \cosh a \sin s + a \sinh a \cos s)\}$$

$$= \frac{2a\, e^{-a}}{s(a^2 + s^2)} \{ a \cosh a \sin s - s \sinh a \cos s \}.$$

APPENDIX A2

To show the convergence of

$$g(b\sqrt{2}\,x) = \frac{2}{\sqrt{2}\,b}\, e^{-x^2} \sum_{m=0}^{\infty} \frac{H_{2m+1}(x)}{(2m+3)(2m+1)!} \left(\tfrac{1}{2}b^2\right)^m . \qquad \text{(A2.1)}$$

Let M be the maximum of

$$y = e^{-x^2} H_{2m+1}(x) \quad \text{on} \quad 0 \leqslant x \leqslant \infty .$$

The expansion for g certainly converges, as long as b is large enough to ensure the convergence of

$$\sum_{m=0}^{\infty} \frac{M}{(2m+3)(2m+1)!} \left(\tfrac{1}{2}b^2\right)^m . \qquad \text{(A2.2)}$$

If we put $Y = H_{2m+1}(x)$, then Y satisfies the Hermite differential equation

$$Y'' - 2xY' + 2(2m+1)Y = 0 , \qquad \text{[31], (A2.3)}$$

and $y = e^{-x^2}Y$, satisfies

$$y'' + 2xy' + 4(m+1)\,y = 0 . \qquad \text{(A2.4)}$$

Multiplying through by $y' e^{2x^2}$, gives

$$y''y'\,e^{2x^2} + 2x y'^2 e^{2x^2} + 4(m+1) yy' e^{2x^2} = 0,$$

The above equation may be written as

$$\frac{d}{dx}\left\{\tfrac{1}{2}y'^2 e^{2x^2}\right\} + 2(m+1)\frac{d}{dx}\left\{y^2 e^{2x^2}\right\} - 8(m+1)\,x\,e^{2x^2}y^2 = 0,$$

Which can be integrated once to give

$$\left[\tfrac{1}{2}y'^2 e^{2x^2} + 2(m+1)y^2 e^{2x^2}\right]_{x_0}^{x_1} - 8(m+1)\int_{x_0}^{x_1} x\,e^{2x^2}y^2\,dx = 0.$$

Hence

$$\left\{\tfrac{1}{2}y'^2(x_1)\,e^{2x_1^2} + 2(m+1)y^2(x_1)e^{2x_1^2}\right\} - \left\{\tfrac{1}{2}y'^2(x_0)\,e^{2x_0^2} + 2(m+1)y^2(x_0)e^{2x_0^2}\right\}$$

$$= 8(m+1)\int_{x_0}^{x_1} x\,e^{2x^2}y^2\,dx . \qquad \text{(A2.5)}$$

If we let x_0 and x_1 be consecutive maxima of y, so that

$$y'(x_0) = y'(x_1) = 0 \quad ; \quad (x_1 > x_0 \geq 0) , \tag{A2.6}$$

then (A2.5) reduces to

$$2(m+1)\left\{ y^2(x_1)\, e^{2x_1^2} - y^2(x_0)\, e^{2x_0^2} \right\} = 8(m+1)\int_{x_0}^{x_1} x\, e^{2x^2} y^2 \, dx . \tag{A2.7}$$

Since, the integral on the r.h.s. of the above is positive, it follows that

$$\left| y(x_1)\, e^{x_1^2} \right| > \left| y(x_0)\, e^{x_0^2} \right|$$

and therefore

$$\left| y(x_1) \right| > \left| y(x_0) \right| . \tag{A2.8}$$

If on the other hand, (A2.4) is multiplied throughout by y' and integrated once, we have

$$\int_{x_0}^{x_1} \left\{ y'y'' + 2x\, y'^2 + 4(m+1)\, y y' \right\} dx = 0 ,$$

which is equivalent to

$$\int_{x_0}^{x_1} \left\{ \frac{d}{dx}\left(\tfrac{1}{2} y'^2\right) + 2x y'^2 + 4(m+1)\frac{d}{dx}\left(\tfrac{1}{2} y^2\right) \right\} dx = 0 .$$

The first term in the above vanishes due to (A2.6), and from the remaining terms, we can write

$$(m+1)\left\{ y^2(x_1) - y^2(x_0) \right\} = -\int_{x_0}^{x_1} x y'^2 \, dx .$$

Once again, the integral on the r.h.s. of the above equation is positive, and we conclude that

$$\left| y(x_1) \right| < \left| y(x_0) \right| . \tag{A2.9}$$

Since $y(0)=0$, then the greatest value of $|y|$ is its first maximum to the right of $x=0$. To find this maximum, put

$$y' = -e^{-x^2} H_{2m+1}(x) = 0 ,$$

and it follows that the maximum values of y, occur at zeros of $H_{2m+1}(x)$, where

$$H_{2m+2}(x) = e^{x^2} \frac{d^{2m+2}}{dx^{2m+2}} e^{-x^2} .$$

If we further put

$$y = f(x) Z(X) ,$$

so that

$$y' = f \frac{dZ}{dX} X' + f'Z ,$$

and

$$y'' = f \frac{d^2Z}{dX^2} X'^2 + (f X'' + 2 f' X') \frac{dZ}{dX} + f''Z ,$$

then (A2.4), becomes

$$f X'^2 \frac{d^2Z}{dX^2} + (f X'' + 2 f' X' + 2 x f X') \frac{dZ}{dX} + [f'' + 2x f' + 4(m+1) f] Z = 0 . \qquad \text{(A2.10)}$$

(Dashes denote differentiation w.r.t. x).

If we choose f and X, such that

(i)- $f X'^2 = 4 f$.

(ii)- $f X'' + 2 f' X' + 2x f X' = 0$,

then (i) implies $X' = 2$, and therefore $X = 2x$,

and (ii) implies $f' + xf = 0$, and thus $f = \exp\{-x^2/2\}$.

Substituting the above expressions for X and f in (A2.10), reduces this equation to the normal form

$$\frac{d^2Z}{dX^2} + (m+1) Z = \frac{1}{16} (X^2 + 4) Z , \qquad \text{(A2.11)}$$

which has a solution of the form

$$Z = A \cos\{(m+1)^{1/2} X\} + B \sin\{(m+1)^{1/2} X\} + \frac{1}{16 (m+1)^{1/2}} \int_0^X (\zeta^2 + 4) Z(\zeta) \sin\{(m+1)^{1/2} (X - \zeta)\} \, d\zeta , \qquad \text{(A2.12)}$$

where A and B are constants [W.K.B. method, 31 pp.75-77].

Now since $y = f(x) Z(X)$,

and $f(x) = e^{-x^2/4}$,

then

$$Z = e^{-\frac{1}{2}x^2} H_{2m+1}(x) .$$

Therefore Z(0)=0, which implies A=0.

Also since

$$\left.\frac{dZ}{dx}\right|_{x=0} = \frac{1}{2}\left.\frac{dZ}{dx}\right|_{x=0} = \frac{1}{2} H'_{2m+1}(0)$$

$$= (2m+1) H_{2m}(0) \qquad [31, p.192],$$

$$= (-1)^m (2m+1)!/m! , \qquad [31, p.187],$$

and from (A2.12),

$$\left.\frac{dZ}{dx}\right|_{x=0} = B\cdot(m+1)^{1/2},$$

then

$$(-1)^m (2m+1)!/m! = B\cdot(m+1)^{1/2},$$

which implies

$$B = \frac{(-1)^m (2m+1)!}{(m+1)^{1/2}\, m!} .$$

Hence, if m is large, then Z is approximately

$$Z \approx \frac{(-1)^m (2m+1)!}{(m+1)^{1/2}\, m!} \sin\left\{(m+1)^{1/2} x\right\},$$

the first maximum of which occurs at

$$x = \frac{\pi}{2(m+1)^{1/2}} .$$

Since

$$y = Z f = Z e^{-\frac{1}{2}x^2} = Z\left(1 - \tfrac{1}{2}x^2 + \dots\right),$$

then $y \approx Z$ to the first approximation, and therefore

$$M = y_{max} \approx Z_{max} = \frac{(-1)^m (2m+1)!}{(m+1)^{1/2}\, m!} .$$

Substituting the above estimate for M in (A2.2), gives

$$\sum_{m=0}^{\infty} \frac{(-1)^m}{(m+1)^{1/2}\, m!\,(2m+3)} \left(\tfrac{1}{2b^2}\right)^m,$$

which is an entire function and certainly converges.

APPENDIX A3

To integrate

$$\gamma(J) = \frac{1}{2\pi} \int_{-\infty}^{\infty} \bar{\psi}(s)\, e^{-iJs}\, ds,$$

where $\bar{\psi}(s)$ is given by (3.66).

Combining (3.66) with the above, yields

$$\gamma(J) = -\frac{1}{2\pi} \int_{-\infty}^{\infty} \Big\{ 2\sqrt{(2\pi)}\, iRb \sum_{m=0}^{\infty} \frac{(-1)^m}{(2m+3)(2m+1)!}\, s^{2m+1}$$
$$+ i(a_0/b + a_3/b^3) \sum_{j=0}^{\infty} j(2j-1)(j-1)\gamma_j\, s^{2j-3}$$
$$+ i(a_4/b^3) \sum_{j=0}^{\infty} j(2j-1)(j-1)(2j-3)(j-2)\gamma_j\, s^{2j-5} \Big\}$$
$$\cdot \exp\{-(b^2 s^2/2 + iJs)\}\, ds.$$

Since, all the terms in the integrand are of the similar type, we shall show the method of integration, by considering the first term only.

Let

$$I = \int_{-\infty}^{\infty} \sum_{m=0}^{\infty} a_m\, s^{2m+1} \exp\{-(b^2 s^2/2 + iJs)\}\, ds,$$

where

$$a_m = \frac{(-1)^m}{(2m+3)(2m+1)!}.$$

Splitting the range of integration into a positive and a negative one, changing the order of the latter and rearranging, yields

$$I = -\int_{0}^{\infty} \sum_{m=0}^{\infty} a_m\, s^{2m+1} \left(e^{iJs} - e^{-iJs}\right) e^{-\frac{1}{2}b^2 s^2}\, ds.$$

The exponential terms within the brackets can be replaced by $\{2i \sin(Js)\}$, which in turn may be replaced by its Taylor expansion. thus

$$I = -2i \int_{0}^{\infty} \sum_{m=0}^{\infty} a_m\, s^{2m+1} \sum_{n=0}^{\infty} (-1)^n \frac{(Js)^{2n+1}}{(2n+1)!}\, e^{-\frac{1}{2}b^2 s^2}\, ds$$
$$= -2i \int_{0}^{\infty} s^2 \sum_{n=0}^{\infty} \left\{ \sum_{m=0}^{n} a_m \frac{(-1)^{n-m} J^{2n-2m+1}}{(2n-2m+1)!} \right\} s^{2n} e^{-\frac{1}{2}b^2 s^2}\, ds.$$

It is convenient to write the above as

$$I = -2i \int_0^\infty \sum_{n=0}^{\infty} A_n \, s^{2n+2} \, e^{-\frac{1}{2}b^2 s^2} \, ds ,$$

where

$$A_n = \sum_{m=0}^{n} \frac{(-1)^n \, 3^{2n-2m+1}}{(2n-2m+1)!\,(2m+1)!\,(2m+3)} .$$

Since b is large, Watson's Lemma can be employed to find

$$I \sim -2i \sum_{n=0}^{\infty} \tfrac{1}{2} A_n \, \Gamma(n+3/2)\,(1/b)^{2n+3} .$$

The remaining terms can be evaluated in a similar fashion.

APPENDIX A4

To evaluate

$$I = \int_0^1 \{1 - e^{-a(1-\eta)} - a e^{-a}(1-\eta)\}\, \eta^{2k+1}\, d\eta .$$

This integral can be written as

$$I = (1 - a e^{-a}) \int_0^1 \eta^{2k+1}\, d\eta + a e^{-a} \int_0^1 \eta^{2k+2}\, d\eta - \int_0^1 e^{-a(1-\eta)}\, \eta^{2k+1}\, d\eta$$

$$= \frac{1 - a e^{-a}}{2k+2} + \frac{a e^{-a}}{2k+3} - \int_0^1 e^{-a(1-\eta)}\, \eta^{2k+1}\, d\eta .$$

To find the integral in the above,

put

$$y = a(1-\eta),$$

so that $\eta = 1 - y/a$ and $d\eta = -\frac{1}{a}\, dy$.

Hence

$$\int_0^1 e^{-a(1-\eta)}\, \eta^{2k+1}\, d\eta = -\frac{1}{a} \int_a^0 e^{-y} (1 - \frac{y}{a})^{2k+1}\, dy$$

$$= \frac{1}{a} \int_0^a e^{-y} \sum_{r=0}^{2k+1} \frac{(2k+1)!}{(2k+1-r)!\, r!} (-\frac{y}{a})^r\, dy,$$

by the Binomial expansion. Hence

$$= \sum_{r=0}^{2k+1} \frac{(-1)^r\, (2k+1)!}{(2k+1-r)!\, r!\, a^{r+1}}\, \gamma(r+1, a),$$

where

$$\gamma(r+1, a) = \int_0^a e^{-y} y^r\, dy = \sum_{n=0}^{\infty} \frac{(-1)^n\, a^{n+r+1}}{(n+r+1)\, n!} \quad , \qquad [6, \text{p.13}]$$

Hence

$$I = \frac{1 - a e^{-a}}{2k+2} + \frac{a e^{-a}}{2k+3} - \sum_{r=0}^{2k+1} \sum_{n=0}^{\infty} \frac{(-1)^{r+n}\, (2k+1)!\, a^n}{(2k+1-r)!\, r!\, (n+r+1)\, n!} .$$

APPENDIX A5

To examine the convergence of

$$\phi_j(\eta) = \sum_{k=0}^{j} \frac{\eta^k}{\Gamma(c+k)\, k! \{(j-k)!\}^2} ,$$

where $0 \leqslant \eta \leqslant 1$, $C>0$ and j is a large positive integer.

The above series can be written as

$$\phi_j(\eta) = \frac{1}{\Gamma(c)\{j!\}^2}\left\{1 + \frac{(-j)^2\eta}{c\cdot 1!} + \frac{(-j)^2(1-j)^2\eta^2}{c\,(c+1)\,2!} + \cdots + \frac{(-j)^2(1-j)^2\cdots(-1)^2\eta^k}{c(c+1)\cdots(c+k-1)\cdot k!}\right.$$

$$= \frac{1}{\Gamma(c)\{j!\}^2}\, {}_2F_1\{-j, -j\,;\, c\,;\, \eta\}\,, \qquad \text{(A5.1)}$$

where ${}_2F_1$ is the hypergeometric function [31].

It is convenient to represent (A5.1) by an Euler integral. Thus we write

$$\phi_j(\eta) = \frac{1}{\Gamma(c)\{j!\}^2}\frac{K_j}{2\pi i}\int_C t^{-c-j}(t-1)^{c+j-1}(t-\eta)^j\, dt\,, \qquad \text{(A5.2)}$$

[31, p.108], where K_j is to be chosen so that

$$\phi_j(0) = 1/\Gamma(c)\{j!\}^2\,, \qquad \text{(A5.3)}$$

and it is sufficient to choose for c, a simple contour which has both 0 and 1 in its interior.

From (A5.2), we can write

$$\phi_j(0) = \frac{1}{\Gamma(c)\{j!\}^2}\frac{K_j}{2\pi i}\int_C t^{-c}(t-1)^{c+j-1}\, dt\,,$$

$$= \frac{1}{\Gamma(c)\{j!\}^2}\frac{K_j}{2\pi i}\int_C t^{j-1}\left(1-\frac{1}{t}\right)^{c+j-1} dt\,,$$

and from (A5.3), we have

$$1 = \frac{K_j}{2\pi i}\int_C t^{j-1}\left(1-\frac{1}{t}\right)^{c+j-1} dt\,.$$

If we expand c so that at every point $|t|>1$, we can write, using the Binomial expansion and the Residue theorem

$$1 = (-1)^j K_j\, \frac{\Gamma(c+j)}{\Gamma(c)\, j!}\,. \qquad \text{(A5.4)}$$

Using a similar idea, we have

$$\phi_j(1) = \frac{1}{\Gamma(c)\{j!\}^2}\frac{K_j}{2\pi i}\int_C t^{j-1}\left(1-\frac{1}{t}\right)^{c+2j-1} dt$$

$$= \frac{1}{\Gamma(c)\{j!\}^2}(-1)^j K_j \frac{\Gamma(c+2j)}{\Gamma(c+j)\cdot j!} .$$

Substituting for K_j from (A5.4), yields

$$\phi_j(1) = \frac{\Gamma(c+2j)}{\{\Gamma(c+j)\}^2\{j!\}^2} . \qquad \text{(A5.5)}$$

To obtain an estimate of the size of $\phi_j(1)$ for intermediate values of η, requires rather more analysis. The method of steepest descent [26], seems to offer an effective method. To that end we write

$$\phi_j(\eta) = \frac{1}{\Gamma(c)\{j!\}^2}\frac{K_j}{2\pi i}\int_C g(t)\exp\{j f(t)\} dt , \qquad \text{(A5.6)}$$

where

$$g(t) = t^{-c}(t-1)^{c-1} ,$$

and

$$f(t) = \log\{(t-1)(t-\eta)/t\} .$$

It is fairly easy to see that there are saddle points at $\pm\sqrt{\eta}$. At $+\sqrt{\eta}$, the line of steepest descent is along the real axis, while at $-\sqrt{\eta}$, it is perpendicular to this axis. Thus, we take c through $-\sqrt{\eta}$ and perpendicular to the real axis there.

In practice it is more informative to adopt a rather more elaborate approach. Put for convenience, $\eta = \zeta^2$, so that a possible form for curve c is the circle

$$|t - \tfrac{1}{2}| = \zeta + \tfrac{1}{2} .$$

Putting

$$\zeta Z = i\frac{t+\zeta}{\zeta+1-t} ,$$

so that

$$t = \zeta\cdot\frac{(\zeta+1)Z - i}{\zeta Z + i} ,$$

we can verify that taking c to be

$$t = \tfrac{1}{2} - (1+J)\,e^{i\theta} \quad , \quad -\pi < \theta \leqslant \pi \, ,$$

the image of c is then the real axis $-\omega<Z<\omega$, and we have

$$\phi_j(J') = \frac{(-1)^j}{\Gamma(c)\{j!\}^2}\,\frac{K_j}{2\pi}\int_{-\infty}^{\infty} G(Z)\,\exp\{j\,F(Z)\}\,dZ, \qquad \text{(A5.7)}$$

where

$$G(Z) = (2J+1)\,J^{1-c}\,\frac{\{J^2 Z - (1+J)\,i\}^{c-1}}{\{(1+J)Z - i\}^{c}\,(JZ+i)}$$

and

$$F(z) = \log\left\{\frac{(J+1)^2 + i\,(J+1)^2 z - J^2(1+J-J^2)z^2}{1+iz+J(J+1)z^2}\right\}$$

$$= 2\log(1+J) + \log\left[1 - \frac{J(2J+1)^2 z^2}{(1+J)^2\{1+iz+J(J+1)z^2\}}\right]$$

We now consider two cases.

(i) $jJ >> 1$,

(ii) jJ is O(1).

In case (i) we can clearly use a steepest descent method and obtain as the leading term

$$\phi_j(J) \sim \frac{(-1)^j K_j}{\Gamma(c)[j!]^2(2\pi)}\,(1+J)^{2j}\,G_{\bullet}\,\frac{1+J}{1+2J}\,(\pi/jJ)^{1/2}$$

$$= \frac{(-1)^j K_j}{2\Gamma(c)[j!]^2(\pi J j)^{1/2}}\,J^{1-c}\,(1+J)^{c+2j} \, , \qquad \text{(A5.8)}$$

and if the Stirling approximation [31] is used in (A5.5), it can be seen that these two results are consistent.

In case (ii), if we put $jJ = u$ and suppose u is O(1), then

$$\exp\{j\,F(z)\} = \left(1+\frac{u}{j}\right)^{2j}\left(1+\frac{uW}{j}\right)^{j} \, ,$$

where

$$W = \frac{(2J+1)^2 z^2}{(1+J)^2\{1+iz+J(J+1)z^2\}}$$

and if j is very large

$$\exp\{j\,F(z)\} \simeq \exp\{u(2-W)\}$$

This will decay very fast as $|z|$ increases and therefore in approximating ϕ_j we can neglect powers of products of J

and Z and hence put $\zeta = 0$ into all other terms. Thus

$$\phi_j \approx \frac{1}{\Gamma(c)\{j!\}^2} \frac{(-1)^j K_j}{2\pi} \zeta^{1-c} \int_{-\infty}^{\infty} \frac{\exp\{u(2 - \frac{z^2}{1+iz})\}}{(1+iz)^c} dz. \quad (A5.9)$$

We require a cut in the Z plane from i to $i\infty$. We can then bend the contour of integration around the cut so that on one side $Z = i + \rho e^{-3i\pi/2}$, and on the other $Z = i + \rho e^{i\pi/2}$

Then

$$\phi_j \approx \frac{1}{\Gamma(c)\{j!\}^2} \frac{(-1)^j K_j \zeta^{1-c}}{2\pi} 2 \sin c\pi \int_0^{\infty} \rho^{-a} \exp\{-u(\rho + 1/\rho)\} d\rho$$

$$= 2(-1)^j K_j \zeta^{1-c} \frac{1}{\pi} \sin c\pi \, K_{c-1}(2u),$$

where $K_{c-1}(2u)$ is the usual modified Bessel function [31, P.162].

Again using the Stirling formula, we have

$$(-1)^j K_j \approx \Gamma(c) j^{1-c},$$

and hence

$$\phi_j \approx \frac{2u^{1-c}}{\Gamma(c)\Gamma(1-c)\{j!\}^2} K_{c-1}(2u) \longrightarrow 1 \quad \text{as } u \longrightarrow 0 \quad \text{for } 0<C<1.$$

REFERENCES.

[1] Batchelor G. K.
'Homogeneous turbulence',
Cambridge University press, 1953.

[2]+ Brown S. N. & Stewartson
'On Similarity Solutions of the Boundary-layer equations with algebraic decay',
J. Fluid Mech. Vol 23, part 4, p.673, 1965.

[3]+ Cantwell B. J.
'Organized motion in turbulent flow',
Ann. Rev. Fluid Mech. 13, 457-515, 1981.

[4]+ Carlson D. R., Widnall S. E. & Peeters M. F.,
'A flow-visualization study of transition in plane Poiseuille flow',
J. Fluid Mech., vol. 121, 487-505, 1982.

[5] Cebeci T. & Smith A. M. O.
'Analysis of Turbulent Boundary Layers',
Academic press, 1974.

[6] Copson E. T.
'Asymptotic Expansions',
Cambridge University press, 1965.

[7]+ Emmons H. W.
'The laminar-turbulent transition in a boundary layer',
Part I, J. Aero. Sci. 18, 490-498.

[8]+ Goldshtic M. A., Zametalin V. V. & Shtern V. N.
'Simplified theory of the near-wall turbulent layer of Newtonian and drag-reducing fluids',
J. Fluid Mech., vol. 119, 423-441, 1982.

[9] Goldstein S.
'Modern Developments in Fluid Dynamics',
Vol. I, Dover, 1965.

[10] Hartee,
Proc. Camb. Phil. Soc., 33, 223-239, 1937.

[11] Hastings S. P.
'Reversed flow solution of the Falkner-Skan Equation',
SIAM J. Appl. Math., vol. 22, No. 2, 1972.

[12] Hastings S. P. & Troy W.
'Oscillatory solutions of the Falkner-Skan equation',
Proc. R, Soc. Lond. A 397, 415-418, 1985.

[13] Henry F. S., El Telbany M. M. & Reynolds A. J.
'Application of the κ-ε model to turbulent channel flows'
Brunel University Report, FM, 1981.

[14] Henry F. S. & Reynolds A. J.
'Analytical Solution of Two Gradient-Diffusion Models Applied to Turbulent Couette Flow',
J. of Fluids Engineering, Vol. 106, June 1984.

[15] Hunt J. N.
'Incompressible Fluid Dynamics',
Longmans, 1964.

[16] Kaneda Y. & Leslie D. C.
'Tests of subgrid models in the near-wall region using represented velocity fields',
J. Fluid Mech., vol. 132, 349-373, 1983.

[17] Lamb H.
'Hydrodynamics',
Cambridge University press, Sixth edition, 1932.

[18] Launder B. E. & Spalding D. B.
'Mathematical Models of Turbulence',
Academic press, 1972.

[19] Launder B. E., Reece G. J. & Rodi W.
'Progress in the development of a Reynolds stress turbulent closure',
J. Fluid Mech., vol. 68, 537, 1975.

[20] Leslie D. C.
'Simulation methods for turbulent flows',
Numerical Methods for Fluid Dynamics,
Edited by K.W. Morton & M.J. Baines, Academic press, 1982

[21] Lumley J. L.
'Computational modeling of turbulent flows',
Adv. Appl. Mech., 18, 123, 1978.

[22] Mellor G. L. & Herring H. J.
'A survey of the mean turbulent field closure models',
AIAA J. 11, 590, 1973.

[23] Miles J. W.
'Integral Transforms in Applied Mathematics'
Cambridge University press, 1971.

[24]+ Moffatt H. K.
'Some developments in the theory of turbulence',
J. Fluid Mech., vol. 106, 27-47, 1981.

[25] Moin P. & Kim J.
'Numerical investigation of turbulent channel flow',
J. Fluid Mech., 118, 341, 1982.

[26] Neyfeh A. H.
'Introduction to perturbation techniques',
Wiley, 1981.

[27] Rosenhead L.
'Laminar Boundary Layers',
Oxford University press, 1963.

[28] Ruelle D. & Takens F.
'On the nature of turbulence',
Comm. Math. Phys. 20, 167-192, 1971.

[29] Schlichting H.
'Boundary Layer Theory',
Mc Graw Hill, Sixth edition, 1968.

[30] Schumann U.
'Subgrid scale model for finite difference simulations
of turbulent flows in plane channels and annuli',
J. Comp. Phys. 18, 376, 1975.

[31] Spain B. & Smith M. G.
'Functions of Mathematical Physics',
Van Nostrand Reinhold, 1970.

[32] Speziale C. G.
'On nonlinear $k-\ell$ and $k-\varepsilon$ models of turbulence',
J. Fluid Mech., 178, 459-475, 1987.

[33] Vollmers H. & Rotta J. C.
'Similar Solutions of the Mean Velocity, Turbulence
Energy and Length Scale Equations',
AIAA J., Vol. 15, 714, 1977.

[34] Watson G. N.
'A Treaties on the Theory of Bessel Functions',
Cambridge University press, Second edition, 1966.

[35] Whittaker E. T. & Watson G. N.
'A course of Modern Analysis',
Cambridge University press, second edition, 1915.

[36] Wood P. E. & Leal L. G.
'Similarity solutions of free shear flows with mean
Reynolds stress turbulence models',
Numerical Heat Transfer, vol. 6, 235-244, 1983.

[37] Yang H. T. & Chien L. C.
'Analytic solutions of the Falkner-Skan equation
when $\beta = -1$ and $\gamma = 0$',
SIAM J. Appl. Math, vol. 29, No 3, Nov. 1975.

[38] HALL G. & WATT J. M.
'Modern Numerical Methods for Ordinary Differential
Equations',
Clarendon, Oxford, 1976.

+ General references, not referred to directly in the text.